

Master's thesis

Jonathan Hermansen

Combining Low-Cost 3D Printing and Vacuum forming to Create Early Stage Proof-of-Concept Prototypes

Master's thesis in Mechanical Engineering

Supervisor: Christer Westum Elverum

January 2019

NTNU
Norwegian University of Science and Technology
Faculty of Engineering
Department of Mechanical and Industrial Engineering



Norwegian University of
Science and Technology

Jonathan Hermansen

Combining Low-Cost 3D Printing and Vacuum forming to Create Early Stage Proof-of-Concept Prototypes

Master's thesis in Mechanical Engineering
Supervisor: Christer Westum Elverum
January 2019

Norwegian University of Science and Technology
Faculty of Engineering
Department of Mechanical and Industrial Engineering

Abstract

This master thesis looks at expanding the possibilities of 3D printing by creating a low cost prototyping process using 3D print and vacuum forming hybrids. This means encapsulating 3D printed parts in polymer sheets by vacuum forming, essentially making attachments without any need for additional attachment methods other than vacuum forming. A process was developed and important factors of the process were identified, tested and compared. These tests include qualitative and quantitative testing and resulted in a set of guidelines that can be used for easier application to prototypes, products and further development of the process. The main results show that the process works, although certain limitations are present. The attachment between the 3D printed and vacuum formed part are capable of withstanding forces higher than what the 3D print itself can withstand. This is however highly dependant on the test setup. More actual usage related tests, focusing on testing the attachments, show that they are capable of withstanding up to around 470N. It should be noted that this is also highly dependant on the use case. Another important factor is the limited angular orientation possible. This means that the attachments are limited to a suggested range of 30° to 90° relative to the horizontal plain. This might limit the use of this process. Possible use of the process include attachment points and structural attachment like ribs. The main focus in this thesis is on attachment points and only one test was done on structural attachments, however with good results.

Sammen drag

Denne masteroppgaven ser på mulighetene for å utvide bruksområdet til 3D printing ved å lage en billig prosess for prototyping ved hjelp av 3D print og vakuumformede hybrider. Dette innebærer innkapsling av 3D-printede deler i vakuumformede polymerark. Behovet for ytterligere operasjoner etter vakuumforming blir derfor eliminert. En prosess ble utviklet og viktige faktorer i prosessen ble identifisert, testet og sammenlignet. Disse testene inkluderer kvalitativ og kvantitativ testing og resulterte i et sett retningslinjer som vil promotere anvendelse av prosessen i prototypings-, produksjons- og utviklingsprosesser. Hovedresultatene viser at prosessen fungerer, selv om visse begrensninger er tilstedeværende. Koblingen mellom den 3D-printede og vakuumformede delen er i stand til å motstå krefter som er høyere enn det den 3D-printede delen tåler. Dette er imidlertid svært avhengig av testoppsettet. Mer bruksrelaterte tester, med fokus på å teste koblingen, viser at de er i stand til å motstå omtrent 470N. Det skal nevnes at dette også er svært avhengig av brukstilfellet. En annen viktig faktor er den begrensede vinkelorienteringen som er mulig. Dette betyr at koblingene er begrenset til et område på 30° til 90° i forhold til det horisontale planet. Dette kan begrense bruken av denne prosessen. Mulig bruk av prosessen inkluderer festepunkter og strukturelle funksjoner som ribber. Hovedfokuset i denne oppgaven er på festepunkter og bare en test ble utført på strukturelle funksjoner. Testene viste likevel gode resultater.

Preface

This is a the final thesis for the degree of Master of Science (M.Sc) at The Department of Mechanical and Industrial Engineering (MTP), Faculty of Engineering, at NTNU Gløshaugen. The work in this thesis has been under the supervision of Associate Professor Christer W. Elverum. This thesis is a continuation of the authors pre master's thesis. The work in this thesis is therefore largely based on the pre master's thesis, and a lot of work from the pre master's thesis is included in this thesis. The main idea for this thesis was developed during meetings with Associate Professor Christer W. Elverum, PhD Candidate Sigmund A. Tronvoll, Thomas H. Briedis, Ole Steen Karlsen and the author. These meetings took place during the work for the pre master's thesis. The idea was further developed through meeting with Associate Professor Christer W. Elverum and the author.

Acknowledgements

I would like to thank Associate Professor Christer W. Elverum for all the assistance, ideas and great discussions about the topics in this thesis. I would also like to thank PhD Candidate Sigmund A. Tronvoll for assistance and for letting me use his equipment. Lastly, I would like to thank Senior Engineer Carl-Magnus Midtbø for guidance and assistance during the tests performed in this thesis.

TABLE OF CONTENTS

Abstract	i
Preface	ii
Acknowledgements	ii
Table of Contents	iv
List of Figures	vii
List of Figures	ix
Chapter I	1
1 Introduction	1
1.1 Problem formulation	3
1.2 Objectives	4
Chapter II	5
2 Theory	5
2.1 Set-based	5
2.2 Vacuum forming	6
2.3 Injection molding characteristics	8
2.4 Additive manufacturing	9
2.5 Modularization	20
Chapter III	21
3 Methodology	21
3.1 mold and air vents	21
3.2 Pins	28
3.3 Ribs	30
3.4 The jigs	31
3.5 Software	34
3.6 3D printer	35
3.7 Vacuum forming	37
3.8 Test setup	38

Chapter IV	42
4 Work and Results	42
4.1 molds and air vents	42
4.2 Qualitative Testing of Attachment	45
4.3 Quantitative Testing of attachment	53
Chapter V	64
5 Discussion	64
5.1 Set-based approach	64
5.2 mold and vent hole design	64
5.3 FDM	65
5.4 Vacuum forming	68
5.5 Qualitative tests	69
5.6 Quantitative tests	74
Chapter VI	80
6 Use and Proposed guidelines	80
6.1 Guidelines	81
Chapter VII	82
7 Conclusion and further work	82
Bibliography	84
Appendix	i

LIST OF FIGURES

1.1	Section of a polymer sheet (white) vacuum formed around a pin (black) manufactured using FDM.	2
1.2	Mobile consumer flood barrier module concept [31]	3
2.1	Illustration of a vacuum forming process [23].	7
2.2	Illustration of a injection molding process [47].	8
2.3	Injection molded boss [54].	9
2.4	AM steps [26] [43].	10
2.5	Illustration of chord height [13]. The chord height describes the distance between the actual surface (red) and the STL mesh (black) [13]. The greater the distance the less accurate the approximation is [13]. It is also worth noting that the STL mesh is inside of the actual surface, which in this case results in a undersized arc, since the chord height is large compared to the arc. [13]	11
2.6	The angular deviation describes the angle that is created between the normals of adjacent triangles [13]. The approximation can be improved by decreasing the angular deviation [13]. The angular deviation is described as a tolerance which can be set to a max value to ensure sufficient STL-files [13]. [13]	12
2.7	Illustration of the different parts and functions of a FDM machine [56].	14
2.8	Illustration of stair case or stepping effect. Notice the smoother slope of the 0.1mm layers (right) compared to the 0.2mm layers (left). The layers are colored orange while the CAD model is black. [59]	16
2.9	Different amount of fill pattern ranging from 25% (left) to 75% (right) [11]. . .	16
2.10	The figure show raster angles at 0° (left), 45° (middle) and 90° (right) in relation to the x-axis (green arrow) in the horizontal plane [45].	17
2.11	Estimates of UFP(ultrafine particles)-emissions of common FDM materials [7].	19
2.12	Estimated emission rates of volatile organic compounds (VOC). Each individual VOC emission rate has an estimated uncertainty of 36% [7].	20
3.1	Vent hole designs: (1) star shaped, (2) large gaps, (3) no venting and (4) circular venting	22
3.2	Figure showing printed hole sizes compared to the measurement in the CAD software (arrows).	23
3.3	Figure showing the diameter (left) and the dimensions of one arm (right) of the <i>star shaped</i> vent holes. All measurements are in <i>mm</i> or degrees.	24
3.4	Image of the mold base with inserts.	25

3.5	Illustration of the mold used for the angled tests.	25
3.6	Illustration of the angle of the pin (a_{pin}) in relation to the horizontal plane for the angled tests.	26
3.7	Illustration of the mold inserts used for the sunken tests.	26
3.8	Illustration of the mold used for the rib tests.	27
3.9	Dimensions of the <i>nail-like</i> design (left), straight slope design (middle) and the curved design (right)	28
3.10	Undercut illustrated by Formech [23]	29
3.11	Image of the <i>medium bolt</i> pin.	30
3.12	Illustration of the rib design with dimensions.	30
3.13	Welded test jig setup	32
3.14	Drawing of the bottom 3D-printed jig with dimensions. All dimensions are in millimeters.	32
3.15	Drawing, with dimensions, of the top plate of the 3D-printed jig. All dimensions are in millimeters.	33
3.16	Drawing of the centering tool used for centering the test pieces in the 3D-printed jig. All measurements are in <i>mm</i>	34
3.17	Illustration of manually drawn (yellow) and automatically generated (green) support structure for the sideways printed pins. Not that the pin is also colored yellow.	36
3.18	Illustration of the automatically generated (green) support structure for the bottom part of the jig.	36
3.19	Formech 686 vacuum forming machine [22]	38
3.20	MTS Criterion Model 42 (left) [40] and welded test jig attached to the machine (right)	40
3.21	Image of the metal jig (left) and the 3D-printed (right) jig attached to the machine.	40
3.22	Images of spitting the test pieces (left) and the microscope used for measuring the undercuts (X_s) (right).	41
3.23	Illustration of the measurement of the overhang (X_s).	41
4.1	Mold with 8 solid top layers (left) and original mold (right), both after one test	44
4.2	Image of the increased height caused by the deformation.	44
4.3	Illustration of the increased height, $h + \Delta h$, caused by the deformation.	45
4.4	Diameter of the best pinhead (24mm) compared to the star shaped vent hole (15mm).	46
4.5	Deformation of the curved pinhead design after vacuum forming.	47
4.6	Protrusion of pinhead	47
4.7	Pictures of the attachment of <i>angle pin 2</i> (left) and <i>angle pin 5</i> (right)	48
4.8	Image of the test results of <i>sunk test 7</i> (bottom left), 8 (upper left), 9 (bottom middle), 10 (upper middle), 11 (bottom right) and 12 (upper right). Notice the large shapes, similar to air-bubbles, formed around the pins.	51
4.9	Pictures of a comparison between mold with no ribs (top) and a mold with ribs (bottom). Notice how the weight (grey) goes below the red line in the top image and stay at the red line in the bottom image. This was tested with a 22,4kg weight.	52
4.10	Pictures of test results from the rib tests.	53
4.11	Point of failure on the transition between the pinhead and the narrowest part of the pin	55

4.12	Graph of test results for the <i>test 1</i> and 2 pins.	55
4.13	Point of failure on the transition between the skim and the pinhead	56
4.14	Pin and vacuum formed part after detachment. The deformed stem of the tap is caused by the grips on the test jig.	57
4.15	Image of the broken pinhead from <i>test 6</i>	57
4.16	Image of broken pin from <i>test 14</i> and <i>test 15</i> (the numbers in the images are not relevant).	58
4.17	Image of the sections of <i>test 18</i> (top) <i>19</i> (middle) and <i>20</i> (bottom). The outer white shape is the vacuum formed sheet while the inner white rectangular shape is the pinhead.	59
4.18	Graph of test results for the <i>test 5, 6</i> and 7 pins.	60
4.19	Graph of test results for the <i>test 8</i> to 13 pins.	60
4.20	Graph of test results for the <i>test 14</i> to 17 pins.	61
4.21	Graph of test results for the <i>test 18</i> to 20 pins.	62
5.1	Picture of non-circular pinheads printed sideways.	66
5.2	Picture of thin section of convex pinhead	68
5.3	Picture of the placement of vent holes on the inside of the angled mold. Notice that all the vent holes, except 0° and -20°, are pointed downwards (or out if the image) when the mold is placed right side up.	71
5.4	Picture of the lesser quality of the 0° (left) and -20° (right) vent holes. Notice the poor quality of the left side of the 0° vent hole.	71
5.5	Images of the thin sections of the sunken tests. Notice how much more light is let through from <i>sunk test 3</i> compared to <i>sunk test 2</i>	72
5.6	Image of large uneven shapes, similar to air bubbles.	73
5.7	Image of the inside of the vacuum formed ribs.	74
5.8	Image of the flexible top plate of the 3D-printed jig. Notice the difference in the gap between <i>a</i> and <i>b</i>	76
5.9	Image of the part of the 3D print jig attached to the bottom part of the jig. Notice the lack of deformation at the hole where the bolt attaching the jig to the machine was attached.	77
5.10	Image of one of the sides of the grip used to grip the pins in the test machine.	77
6.1	Images of injection molded car bumper (left) [19] and Tool Storage Box (right) [14].	80

LIST OF TABLES

2.1	AM figures [34].	12
2.2	AM Advantages and Disadvantages [34].	13
2.3	Common FDM materials [34].	18
2.4	Thermal properties of ABS and PLA.	19
3.1	Table with details of the different vent holes. Note that the dimensions are based of the CAD model and may be slightly different for the 3D printed models.	23
3.2	Table with information about the different sunken inserts. A visualisation of the parameters are shown in figure 3.7. Note that the dimensions are based of the CAD model and may be slightly different for the 3D printed models.	27
3.3	Table with dimensions of the pin designs tested in the qualitative test.	29
3.4	Table with dimensions for the pins used in the quantitative tests. Note that the dimensions are based of the CAD model and may be slightly different for the 3D printed models.	29
3.5	Table of rib dimensions tested. Note that the dimensions are based of the CAD model and may be slightly different for the 3D printed models.	31
3.6	Table of the dimensions of the top plates used in the 3D-printed test jigs. Note that the dimensions are based of the CAD model and may be slightly different for the 3D printed models.	33
3.7	Table of the dimensions of the centering tool used for centering the test pieces in the 3D-printed jig. Note that the dimensions are based of the CAD model and may be slightly different for the 3D printed models.	34
3.8	Table with details about the printers and general settings used, according to the <i>Prusa 3D Printing handbook</i> for the <i>mk2</i> and <i>mk3</i> printers [43] [44]	35
3.9	Printer parameters for the molds.	37
3.10	Printer parameters for the jig.	37
3.11	Printer parameters for pins.	37
3.12	Description of the rating system used for qualitative testing	39
3.13	Tables with information about settings used for the tensile tests.	39
4.1	Table with results form the first vent hole test.	43
4.2	Table comparing the general trends shown through testing the different pin designs.	46
4.3	Table of angles tested.	47
4.4	Table of results from angled pin tests.	48

4.5	Table of sunken attachment tests.	49
4.6	Table of results from angled pin tests.	50
4.7	Table of results from rib tests.	51
4.8	Table with details of each tests. More detailed information about pin type, printer settings, top plates and jig type can be found in table 3.4 and 3.11, 3.11, 3.6 and figures 3.13, 3.14 and 3.15.	54
4.9	Results from the overhang measurements.	59
4.10	Results from the quantitative tests.	63

1 Introduction

Prototyping has become an important, sometimes inevitable tool in the product development process. When developing a new product, one may have to explore new areas that never have been explored before, where uncertainties and the lack of previous knowledge and documentation governs the process. To be able to overcome these uncertainties, and other possible problematic factors, one may find that prototyping can be a very useful tool. A prototype is defined as *"an approximation of the product along one or more dimensions of interest."* by Ulrich and Epping [55]. They also describe prototyping as a tool to learn, communicate, integrate and to set milestones [55]. Prototypes can therefore speed up the product development process and ensure wanted performance and reliability of a product [55]. Elverum, Welo og Tronvoll states that prototyping can be used as a proof-of-product tool [18] that can confirm your ideas and calculations as to show that they are correct and will work as a final product. Kriesi, et al. also mentions that prototypes can be looked at as a tool to make a product ready for production, in the later stages of the product development process [32]. Prototyping and prototypes can therefore be a very useful and important tool, both to yourself and your team, but possibly also to investors and user groups.

Kriesi, et al. states that prototyping often is used to get the process going and therefore as a tool to learn about possible specifications and problems that might arise [32]. Elverum, Welo og Tronvoll also discuss prototyping as a tool for design thinking, where the prototypes and the prototyping process are used to help think in the design thinking process. They note that the speed of the prototyping process is crucial here. This is because faster prototyping will result in faster learning and therefore better progression in the design thinking process [18]. It is therefore often important to use prototyping tools that can ensure rapid prototyping with results that are sufficient for testing uncertain parameters. Ulrich and Eppinger suggests that there are two main types of prototyping, physical and analytical [55]. Analytical prototypes can be mathematical models, 3D CAD(Computer aided design)-models or computer simulations. Physical prototypes, on the other hand, can be physical models with similar look and feel to the product and hardware that can validate a products functionality. Both of these types of prototypes can be useful and sometimes necessary. This thesis will however focus on the latter.

One of the technologies that has helped ensure rapid physical prototyping is Additive manufacturing (AM), or in the less formal term 3D printing [26]. AM allows easy and rapid manufacture of physical parts from CAD-models. This makes it easy for product developers to produce prototypes with certain qualities. This thesis will focus one of these AM technologies, called Fused Deposition Modeling (FDM). FDM is a readily available AM technology [26], which is quick and cost-effective [46]. The FDM process does however have certain limitations [26], which will be further discussed in section 2.4.

The goal of this thesis is to avoid some of the limitations of the FDM process by combining the FDM technology with vacuum forming. Vacuum forming is a manufacturing technology that, because of previously large tool costs, have been used for mass production [30]. Development in technology have made it possible to significantly lower the time and cost of tool manufacturing with the use of AM technologies like FDM [30] [53]. With this process FDM parts are used as mold tools and the vacuum formed part is the final product. Vacuum forming does however also have its limitations, which will be further discussed in section 2.2. This thesis will therefore look at the limitations of FDM and vacuum forming, and try to eliminate these limitations by combining parts produced using both technologies into one prototype, as shown in figure 1.1. This can in turn be used as a prototyping process for rapidly producing prototypes with qualities that would be difficult to achieve if only one of the technologies mentioned were used.



Figure 1.1: Section of a polymer sheet (white) vacuum formed around a pin (black) manufactured using FDM.

1.1 Problem formulation

Since 2015, AquaFence has worked on creating a mobile flood barrier for consumer use, shown in figure 1.2. This is a project in collaboration with The Norwegian University of Science and Technology (NTNU). AquaFence is a Norwegian company that specializes in the design and production of mobile flood barrier systems for use in emergency situations. Their products are designed to serve as alternatives to more traditional large scale flood barrier systems, such as sandbag walls and permanent structures. These systems often require heavy machinery and pre-installed attachment points in the ground to be moved and secured properly. This makes them less suitable for private use. The main goal of the flood barrier system being developed is to solve this problem and to bridge this gap in the product lineup.

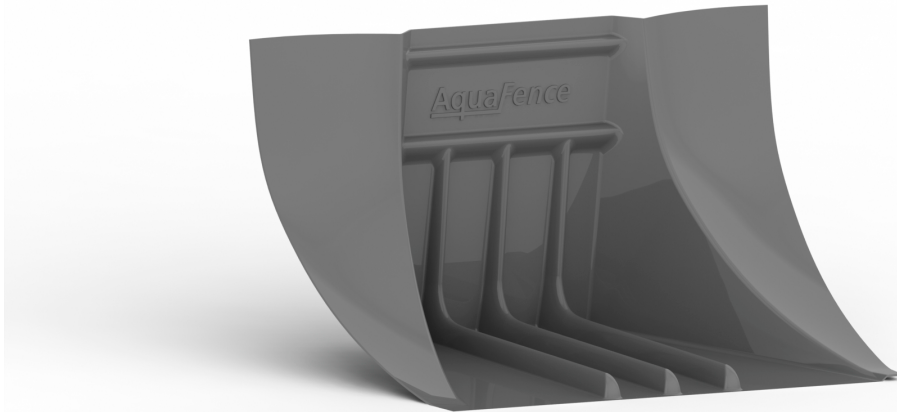


Figure 1.2: Mobile consumer flood barrier module concept [31]

Earlier work on this project has focused on the structural design and sealing solutions of the flood barrier system. The intended final production method for this system is injection molding. This production method is relatively costly [23]. Prototyping has therefore been an important part of this process. The prototyped profiles, shown in figure 1.2, are quite large. The profiles are prototypes in 1:2 scale with contained dimensions of 600x600x400mm, which means that the surface area of the product is also quite large considering the shape. The prototypes have therefore primarily been created using vacuum forming with molds manufactured using FDM. This has allowed for rapid testing of design modifications at a reasonable price, with large numbers of prototypes and design iterations.

This prototyping process did however show some limitations, which spurred the idea for the prototyping process developed in this thesis. The Structural integrity of the vacuum formed prototypes was somewhat poor. This was because of the nature of a thin sheet of material vacuum formed into a 3-dimensional object. The nature of a thin sheet of material also made it difficult to join parts or create attachment points without additional operations. Common joining methods for polymer, polymer composites or polymer-metal hybrids are adhesive bonding,

mechanical fastening or welding [2]. All of these processes requires additional steps after the vacuum forming process [2]. Producing similar prototypes only using FDM would also limit the rapid nature of the prototyping process. Manufacturing large parts using FDM takes long time, especially if good surface finish and mechanical properties are necessary [3]. Additional processes might also be necessary if a smooth surface finish is required [3].

Previously, FDM was only used to manufacture the mold tool and was therefore not a part of the final prototype. Early investigation in this thesis revealed that some of the areas where limitations of vacuum forming was present are areas where FDM had an advantage. This was true for the opposite as well. The idea therefore arose to combine vacuum formed and FDM parts into one final product, that could be used for prototyping. It would therefore be possible to utilize benefits of the vacuum forming process combined with the benefits of FDM process. This could also possibly avoid the issues caused by the limitations of each process.

Desktop 3D printers are readily available at low prices, which means that individuals can afford to have their own machines at home [26]. This also means that prototyping workshops can have access to this technology with little investment. It is therefore likely that a 3D printer is available in a prototyping situation. Although professional vacuum forming machines may be expensive, its relatively easy to make your own at home, with a vacuum cleaner and a kitchen oven [16]. This means that both technologies used in this thesis are available at a low investment cost. This thesis will therefore focus on expanding the possibilities of 3D printing by creating a low cost prototyping process by using parts that are 3D print and vacuum forming hybrids.

1.2 Objectives

A list of objectives was created to give a overview of what this thesis will achieve. These objectives are listed below:

- Investigate the possibilities of expanding the use of 3D printing and vacuum forming by combining the technologies into 3D print and vacuum forming hybrids.
- Develop a rapid, low cost product development process using 3D print and vacuum forming hybrids.
- Identify, test and compare important factors impacting the process.
- Develop guidelines for the use of the process.

2 Theory

In this section, we will look at the existing literature used as a basis for the work in this article. The process developed in this thesis is, based on the literature found, significantly different from other, already existing, processes. It was therefore difficult to find existing literature on this specific process. Doing development with little to no prior information existing on the specific topic, requires extensive research into related topics, to promote progression. A development processes might require a lot of time and money, which substantiates the importance of avoiding rework if not necessary.

2.1 Set-based

Smith [50] describes set-based developments in contrast to the more usually practiced point-based development; in point-based design the course is decided on at the beginning of the process and the focus is kept on this course, while in set-based there are many sets of possibilities or options kept open. This is further substantiated by Ghosh and Seering [25] suggesting two main principles of set-based thinking.

- "Considering sets of distinct alternatives concurrently"
- "Delaying convergent decision making"

Ghosh and Seering [25] argue for these principles with seven characteristics of set-based product development based on an extensive literature review done on the subject:

-
- "Emphasis on frequent lo-fidelity prototyping"
 - "Tolerance for under defined system specifications"
 - "More efficient communication among subsystems"
 - "Emphasis on documenting lessons learned/knowledge"
 - "Support for decentralized leadership structure and distributed, non-collocated teams"
 - "Supplier/subsystem exploration of optimality"
 - "Supports flow-up knowledge creation"

Following these characteristics will, according to Ghosh and Seering [25], help make sure that the product development process progress in a set-based manner. The first characteristic will for example aid concurrent development and enable easy differentiation of prototypes from the start. The second characteristic will allow the development process to progress without the need for concentrating on one concept. The third and fourth characteristics supports better flow of communication across prototypes, as well as allowing for well reasoned evaluation of a wider set of options. The last three points are related to product development teams, companies and suppliers. They ensure good communication while still maintaining a concurrent product development strategy and avoiding early convergent decision making.

2.2 Vacuum forming

A Vacuum Forming Guide by *Formech International Ltd* [23] has a thorough description of important factors to consider about vacuum forming. All the information in this section are gathered from *A Vacuum Forming Guide* by *Formech International Ltd* if not otherwise stated.

Kaminski and Macarrão [36] gives a good general overview of the process and possibilities of vacuum forming. The general process is based around a plastic sheet fixed to a frame with a mold placed underneath it. The plastic sheet is heated up so that it becomes moldable, and after a sufficient temperature is reached, the sheet is formed around the mold with the use of vacuum. Vacuum forming is described as an attractive process for manufacturing prototypes and parts. This is because of its low cost and short lead time, which allow for relatively quick prototyping with mechanical characteristics that might be satisfactory for static evaluation. Kaminski and Macarrão [36] points out that vacuum forming also has some limitations, which including creating certain grooves and fixing screw points. This is closely related to the main challenge in this thesis.

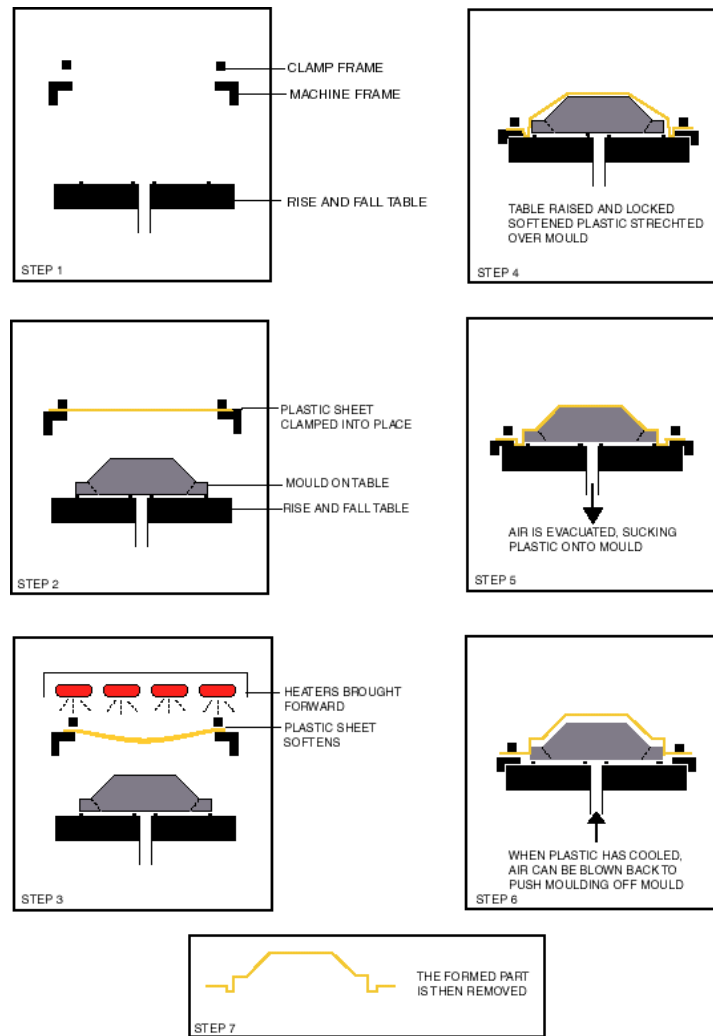


Figure 2.1: Illustration of a vacuum forming process [23].

The plastic sheets that are most commonly used in vacuum forming are thermoplastics, which become malleable when heated [41]. The temperature required to make the sheets moldable is dependant on the type of thermoplastic used. Thermoplastics are grouped into two main groups, crystalline and amorphous, with crystalline thermoplastics consisting of a ordered molecular structure and amorphous thermoplastics consisting of random molecular structure. The random nature of amorphous thermoplastics makes them generally easier to vacuum form than crystalline thermoplastics. This is because the amorphous thermoplastic can be heated to its glass transition temperature (T_g) and has a larger temperature range between T_g and the temperature for its viscous state (T_v), than crystalline thermoplastics. The vacuum forming process should preferably be operated with the plastic sheet in the temperature range between T_g and T_v , which means that amorphous thermoplastics requires less accuracy in temperature than crystalline thermoplastics. One of the most common used amorphous thermoplastics for vacuum forming is high impact polystyrene (HIPS). HIPS can be molded at low temperatures and has medium to high strength. Acrylonitrile Butadiene Styrene (ABS) is another amorphous thermoplastic which can be used for vacuum forming. ABS has somewhat higher strength than HIPS but requires a higher temperature to be molded.

The design of the mold is also a factor that has a lot of impact on how the vacuum formed product will turn out. Some of the characteristics that are important to consider when vacuum forming are draft angles, venting and undercuts. Draft angles are important to facilitate removal of the mold from the vacuum formed part. A minimum typical draft angle recommended is 5°, but greater taper angles will generally result in easier removal of the mold. Proper venting will assure that air, trapped between the plastic sheet and the mold, can escape, to prevent bubbles that might create unwanted geometries. The vent holes may affect the surface of the finished part, and therefore it is recommended to have as few vent holes as possible with a small enough diameter to minimize this effect. As a general rule, it is recommended to have vent holes that have a diameter less than half of the thickness of the sheet used for vacuum forming. As the vacuum formed part needs to be released from the mold, it is not possible with undercuts. This is also substantiated by the need for draft angles, as previously mentioned. The limitations caused by undercuts can however be used to our advantage, which will be discussed later in this thesis.

2.3 Injection molding characteristics

M. Grover [28] writes that the most commonly used molding process for thermoplastics is injection molding. The molding process starts with a polymer heated to a plastic state before pressure is applied to force the polymer into a mold cavity, where it hardens [28]. Both small and large components can be manufactured with vacuum forming, ranging from parts weighing about 50g up to about 25kg [28]. However, because of high mold manufacturing cost, the production of injection molded parts is mostly suited for large production quantities and not processes such as prototyping [28].

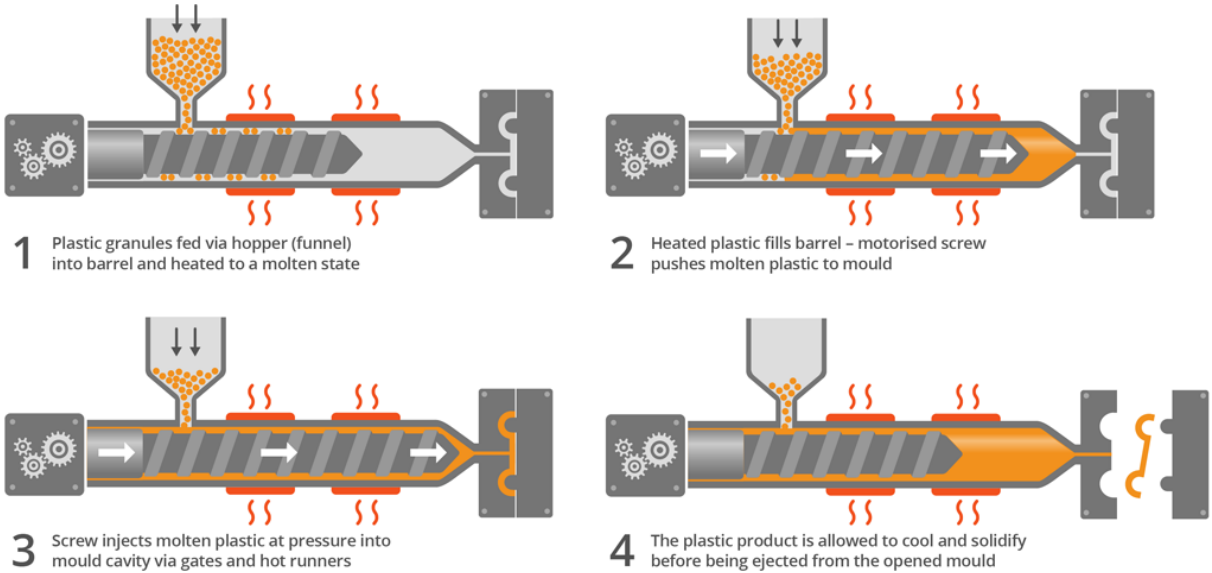


Figure 2.2: Illustration of a injection molding process [47].

Injection molding has, as mentioned above, some advantages compared to vacuum forming. Some of these advantages are discussed in *Injection Molding Design Guidelines* by Stratasys

Direct [54]. These advantages include the ability to create 3-dimensional structures with complex shapes that can go beyond what can be created by a sheet, as well as the ability to mold different types of attachment points. One type of attachment points possible to manufacture are bosses [54]. Bosses are cylindrical projections with holes for the incorporation of fastening hardware, such as screws or threaded inserts [54]. Usually, additional operations after vacuum forming are required to make comparable connecting points on a vacuum formed part.

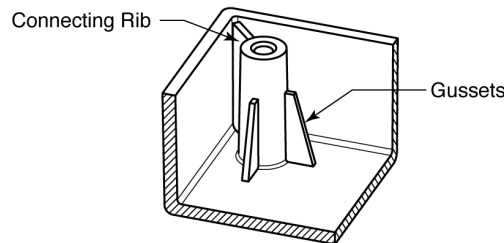


Figure 2.3: Injection molded boss [54].

2.4 Additive manufacturing

Additive manufacturing (AM) is described by I. Gibson, D. Rosen and B. Stucker [26] in *Additive Technologies Manufacturing 3D Printing, Rapid Prototyping, and Direct Digital Manufacturing*. The information provided in the next two paragraphs is gathered from *Additive Technologies Manufacturing 3D Printing, Rapid Prototyping, and Direct Digital Manufacturing* if not otherwise stated.

AM is used as a term used for a group of similar manufacturing methods and is often used in conjunction with rapid prototyping (RP) or as a formalized term of 3D printing. Rapid prototyping (RP) is the manufacture of a product or part used to visually and/or functionally represent the final product. This means that one would prefer to create a version of the final product that requires less resources to produce but still display the most important characteristics of the final product. The task of creating a prototype might involve several steps. Assuming that a CAD-drawing is created, one approach might be to do the manufacturing in several stages, which might include hand carving, molding and/or machining such as milling or turning. One might also use automated machining such as CNC machining, but all these processes will require some kind of skills, additional steps and/or expensive machines to be performed. Hand carving might introduce certain errors depending on your carving skills, moulding require the creation of molds and machining requires knowledge and machines that might be expensive. Additive manufacturing is an alternative to these processes, and might reduce the number of processes and resources required to manufacture similarly sufficient prototype and sometimes also final products. [26]

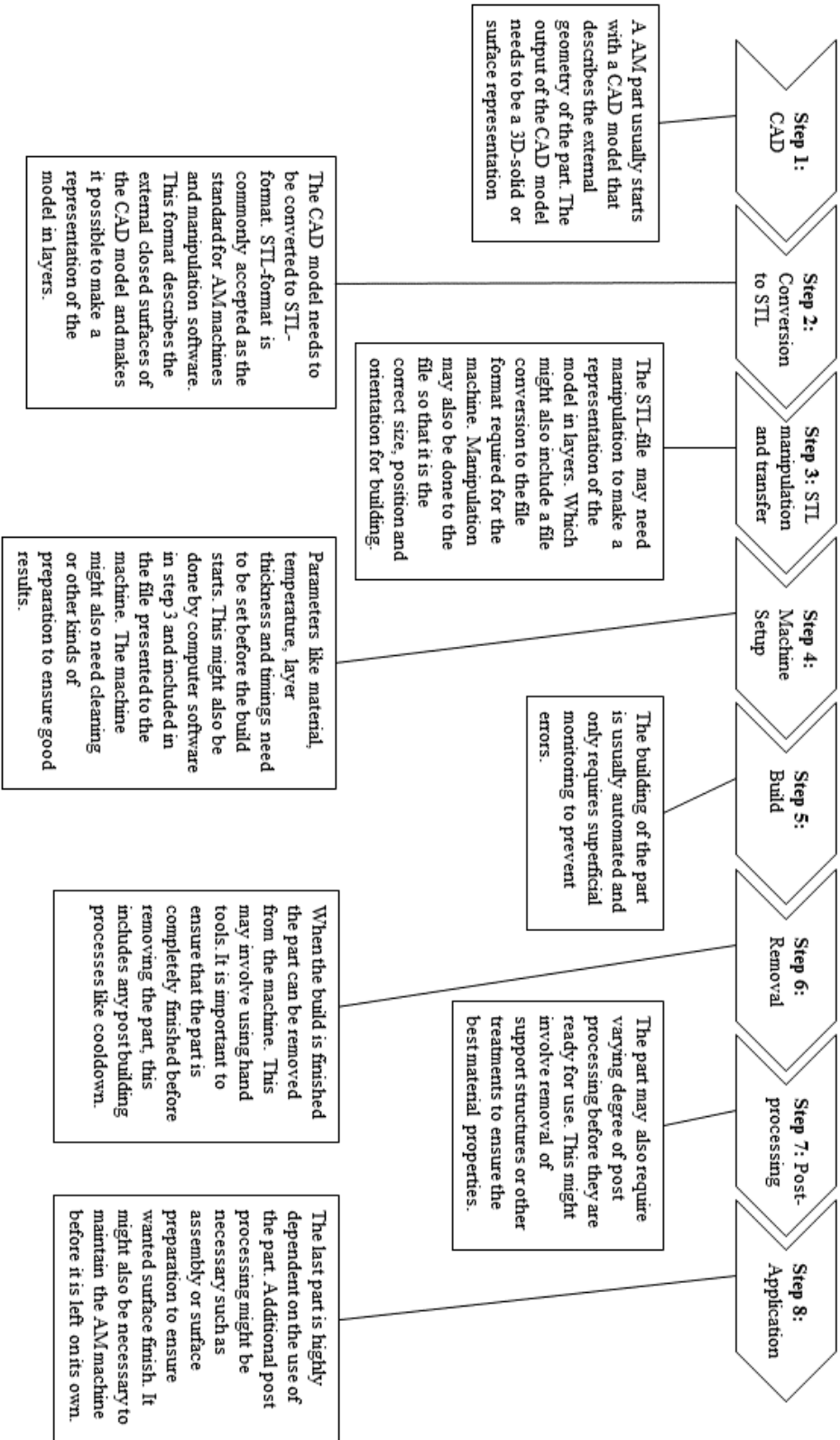


Figure 2.4: AM steps [26] [43].

Machining may involve the removal of material from a block of material similar or greater in size than the final product. The manufacturing processes associated with AM does however manufacture products by adding material. This does, in most circumstances, involve a layer-wise deposition of material on a build plate. These layers consists of thin cross-sections based on the parts CAD model. The process of making a part using AM is shown in figure 2.4. [26]

2.4.1 The STL-file

The way a part is divided into layers is usually done through manipulation of the STL-file, which can be obtained from the CAD software. STL is commonly known as an abbreviation of stereolithography and is according to Gibson, Rosen and Stucker [26] the standard output of most solid modeling CAD software. This file type describes surfaces by dividing it into triangles described by three points and a facet normal vector [10]. The normal vector indicates the outward side of the triangle [10]. This method of approximation is often called tessellation [13] which according to oxford dictionaries is defined as to "Cover (a plane surface) by repeated use of a single shape, without gaps or overlapping." [42]. Tessellation in terms of STL-files is an approximation of the CAD model [26] which introduce certain parameters that can be manipulated based on the requirements of the end result. Two of these parameters are "chord height or tolerance" and "Angular deviation or angular tolerance" [13]. These are shown in figure 2.5 and figure 2.6, respectively.

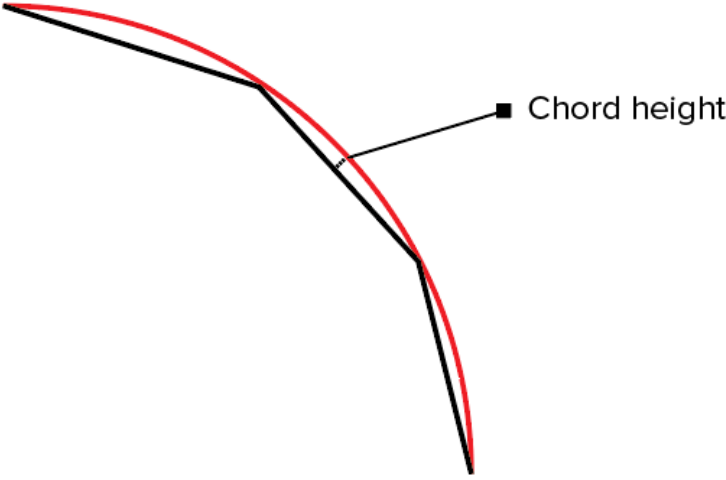


Figure 2.5: Illustration of chord height [13]. The chord height describes the distance between the actual surface (red) and the STL mesh (black) [13]. The greater the distance the less accurate the approximation is [13]. It is also worth noting that the STL mesh is inside of the actual surface, which in this case results in a undersized arc, since the chord height is large compared to the arc. [13]

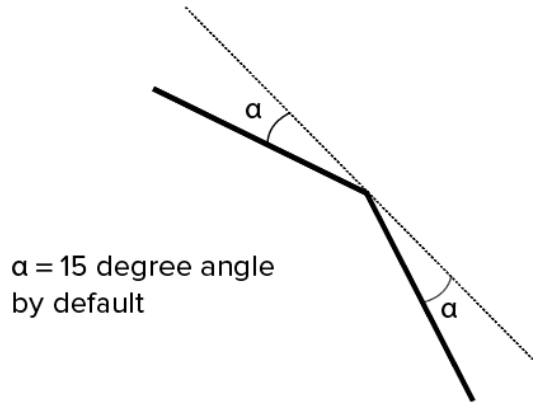


Figure 2.6: The angular deviation describes the angle that is created between the normals of adjacent triangles [13]. The approximation can be improved by decreasing the angular deviation [13]. The angular deviation is described as a tolerance which can be set to a max value to ensure sufficient STL-files [13]. [13]

2.4.2 AM technologies

Common AM technologies today are Vat Photopolymerization, Powder Bed Fusion, Material Extrusion, Material Jetting, Binder Jetting and Direct Energy Deposition [46]. The investigation into the different AM technologies is however beyond the scope of this thesis. A general description of common figures, advantages and disadvantages of the common AM technologies are summarized by J. Lee, J. An and C. Chua [34] and presented in table 2.1 and table 2.2. It is worth noting that this information is dated to January 2017, and because of a rapidly changing technology might have changed some. Several factors are involved in a AM process like the material used, and only some of the factors are presented in the figures in table 2.1. It will therefore not be sufficient to conclude that one of the technologies are superior to the other based on these figures.

AM processes	Example system	Specific energy density ($\frac{J}{cm^3}$)	Fabrication speed ($\frac{cm}{hour}$)	Resolution ($\frac{elements}{mm^3}$)
Binder Jetting	CJP	0.026	1.27-1.9	1900
Direct Energy Deposition	LENS	50,000	4.4	17
Material Extrusion	FDM	N.A.	0.05	46
Material Jetting	Polyjet	0.06	0.4	15200
Powder Bed Fusion	SLS/SLM	300	2.5	211
Sheet Lamination	LOM	336	0.45	1907
Vat Photopolymerization	DLP/SLA	0.94	1.5	3152

Table 2.1: AM figures [34].

Process	Advantages	Disadvantages
Binder Jetting	<ul style="list-style-type: none"> Large number of potential materials Able to create ceramic molds for metal casting Support structures are included automatically in layer fabrication Low-imaging specific energy High material deposition rate and high material utilization High efficiency for repair and add-on features Mainly metal and suitable for large components Deposition of thin layers wear resistant metals on components 	<ul style="list-style-type: none"> Rough or grainy appearance Poor strength Post-processing required to remove moisture or improve strength
Direct Energy Deposition	<ul style="list-style-type: none"> Low-imaging specific energy High material deposition rate and high material utilization High efficiency for repair and add-on features Mainly metal and suitable for large components Deposition of thin layers wear resistant metals on components 	<ul style="list-style-type: none"> Low to medium part complexity Poor surface finish and resolution Poor dimensional accuracy Limited materials for production purposes
Material Extrusion	<ul style="list-style-type: none"> Low cost of the entry-level machines A variety of raw materials are available Versatile and easy to customize No waste of model material High resolution and accuracy Multiple materials and multiple colors Support is not required for polymer powder Both polymer and metal powder can be recycled High part complexity and wide range of materials Good accuracy and resolution for metals High fabrication speed No support structures are needed Low warping and internal stress Multi-materials and multi-colors are possible High-resolution and accuracy, good surface finish High fabrication speed Low-imaging specific energy Wide range of materials 	<ul style="list-style-type: none"> Low level of precision and long build time Unable to build sharp external corners Anisotropic nature of a printed part Post-processing may damage thin and small features Support materials cannot be recycled thus wasted
Powder Bed Fusion	<ul style="list-style-type: none"> Support is not required for polymer powder Both polymer and metal powder can be recycled High part complexity and wide range of materials Good accuracy and resolution for metals High fabrication speed No support structures are needed Low warping and internal stress Multi-materials and multi-colors are possible High-resolution and accuracy, good surface finish High fabrication speed Low-imaging specific energy Wide range of materials 	<ul style="list-style-type: none"> Rough surface finish for polymer Relatively slow build rate Small to medium parts only Expensive machines High material waste Difficult to remove support trapped in internal cavities Thermal cutting produces noxious fumes Possible warpage of lamination as a result of heat of laser Require support Require post processing to remove support Require post curing for enhanced strength
Sheet Lamination	<ul style="list-style-type: none"> No support structures are needed Low warping and internal stress Multi-materials and multi-colors are possible High-resolution and accuracy, good surface finish High fabrication speed Low-imaging specific energy Wide range of materials 	<ul style="list-style-type: none"> Difficult to remove support trapped in internal cavities Thermal cutting produces noxious fumes Possible warpage of lamination as a result of heat of laser Require support Require post processing to remove support Require post curing for enhanced strength
Vat Photopolymerization	<ul style="list-style-type: none"> High-resolution and accuracy, good surface finish High fabrication speed Low-imaging specific energy Wide range of materials 	<ul style="list-style-type: none"> Require support Require post processing to remove support Require post curing for enhanced strength

Table 2.2: AM Advantages and Disadvantages [34].

2.4.3 Fused Deposition Modeling

Fused deposition modeling is known as a quick and cost-effective AM technology [46]. The competition in the FDM technology market has made this kind of AM technology readily available at low prices [26]. Desktop versions using FDM is common at relatively low prices, which means that individuals can afford to have their own machines at home [26]. These factors make FDM an easily available technology and possibly a good entry into the AM technology. This is probably also why this technology was chosen as the main part of NTNU's additive prototyping workshops. FDM was therefore a natural choice of AM technology to use in this thesis.

S. Ghosh and W. Seering [25] describes the FDM process like this. FDM is the process where a filament, usually a thermoplastic polymer, is extruded from a work head on to the existing parts surface in layers. The print is usually made on a build platform. The work head and/or the build platform move horizontally in x and y in order to trace the geometry of the model. After a layer is completed, the work head or the build plate moves upwards vertically in the z direction in order to trace a new layer. The filament is solid before it is pulled into the work head, which heats the filament so that it partly melts [58], and then extrudes it onto the parts surface. The extruded filament then cools and becomes cold welded to the colder part on the baseplate [25].

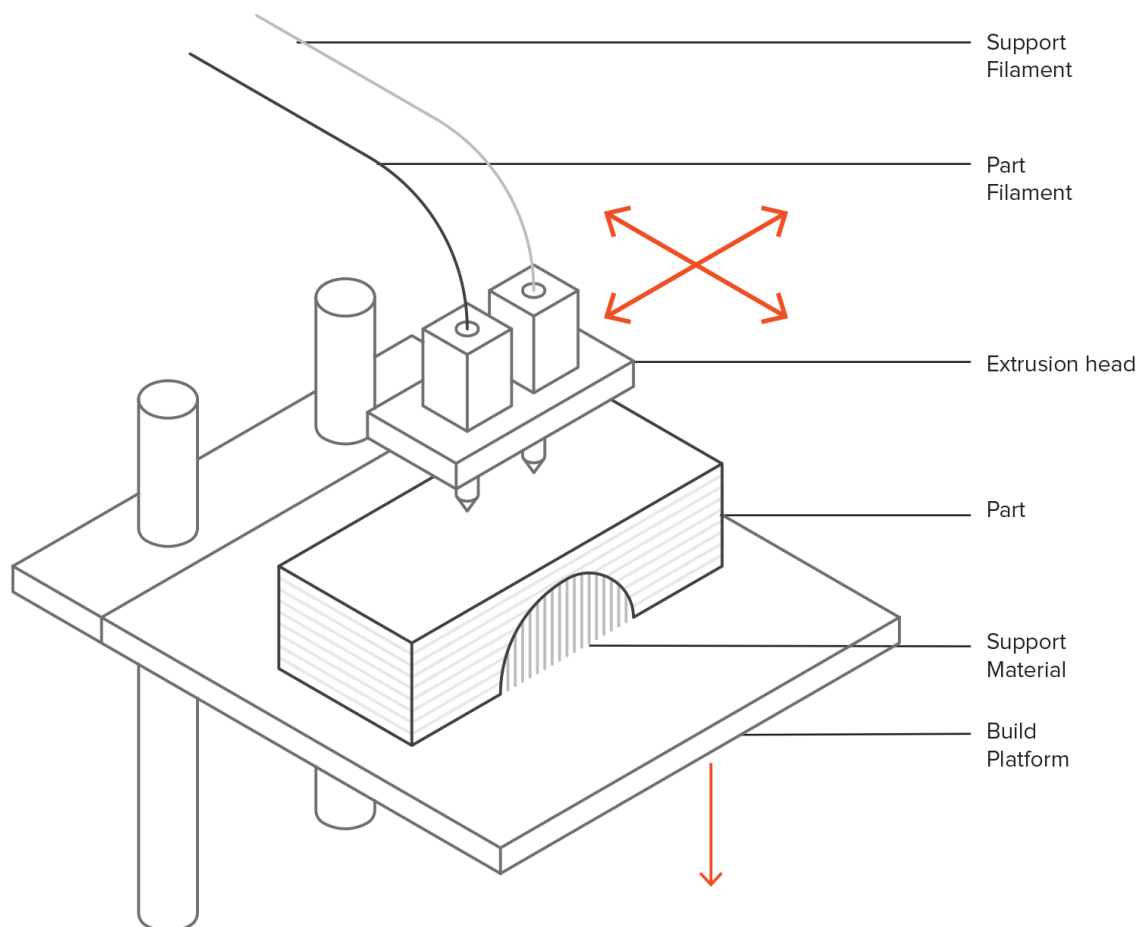


Figure 2.7: Illustration of the different parts and functions of a FDM machine [56].

Figure 2.7 shows a extrusion head with two extruders, one for part filament and one for support material. If the part has overhang features or bridges and no previous layers to deposit filament on, it might be necessary with support structures [57]. Support material can also be used if the part is supposed to be built on a base of material raised over the build plate [57]. Adding support material is mainly done in two ways, either support structures that are supposed to be broken of or support structures that are dissolvable [12]. Dissolvable support structures use two extruders, as shown in figure 2.7, where the support material is different to the part material [12]. This type of support structures is usually removed by immersing the part in water or Limonene [12]. Support structures that are not dissolvable do not require two extruders [12]. These types of support structures are made of the same material as the part material and are usually printed with lower density than the main part [12]. These kinds of support structures may also be designed to minimize the contact surface area to the main part to facilitate easy removal [12]. Removing these support structures usually involves using hand tools or machining like a knife or saw, which introduce the risk of damaging the main part [12]. The printers chosen for NTNU's additive prototyping workshops do only have one extruder and therefore only has the possibility for non dissolvable support structures.

As previously stated, making parts using FDM is done by extruding material in layers [25]. This introduce a parameter called layer thickness. Layer thickness corresponds to the vertical movement of the build plate or extruder, and can be modified depending on the detail wanted [26]. Smaller layer thickness will give finer detail, but may increase print time as the number of layers required to finish a print increases as the layer thickness decreases [26] [29]. Greater layer thickness may also increase inaccuracies like staircase effect [29] or stepping [26] which makes the outer surface less smooth, shown in figure 2.8. A study by V. Kuznetsov, A. Solonin et al. [33] also indicates that layer thickness has a great effect on the mechanical properties of a FDM printed part. In this study PLA(Polylactic acid)-filament was printed in layer thicknesses ranging from 0.06mm to 0.6mm. The extrusion of filament in a FDM process is done through a nozzle, which exists in varying nozzle diameters [26]. V. Kuznetsov, A. Solonin et al. [33] also test the effect the nozzle diameter has related to the layer thickness. Their findings indicate that part strength decreases when layer thickness is increased, which is also supported by B. Rankouhi, S. Javadpour et al [45]. However, increasing the nozzle diameter, while keeping the layer thickness constant, resulted in increased strength [33]. This effect also became more evident with greater layer thicknesses [33]. Their study therefore suggests not using layer thicknesses greater than 80% of the nozzle diameter [33].

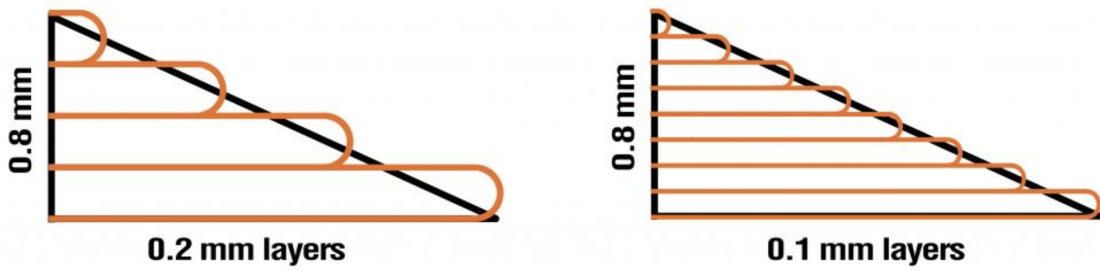


Figure 2.8: Illustration of stair case or stepping effect. Notice the smoother slope of the 0.1mm layers (right) compared to the 0.2mm layers (left). The layers are colored orange while the CAD model is black. [59]

How the layers are laid up and the pattern they are printed in might also have a large effect on the mechanical properties of the part [26]. Infill or fill patterns, as shown in figure 2.9, can be used to minimize time, material and weight of the part, but might compromise the strength of the part [26]. Other influential parameters are raster angle and counter number or external perimeter. Raster angle can be described as the angle which the raster is traced in respect to the x-axis in the horizontal plane of the print [39], as shown in figure 2.10. B. Rankouhi, S. Javadpour et al [45] finds that raster angles of 0° to the load axis has the highest ultimate tensile strength, and that the ultimate tensile strength decrease gradually as the raster angle is changed to 45° and then 90° . Counter number or external perimeter is the number of perimeters around the outside of the part [39], and can be best observed as the solid outer perimeter of the left part in figure 2.9. S. Mishra, R. Malik and S. Mahapatra [39] observes that the strength of the part increases as the number of counters is increased. They therefore suggest that parts built simply using counters, as opposed to counters and internal raster, will be the strongest [39]. All these factors does however result in a part that is highly anisotropic, and the strength of the part along the layers, in the horizontal plane might be significantly higher than across the layers, in vertical direction [33].

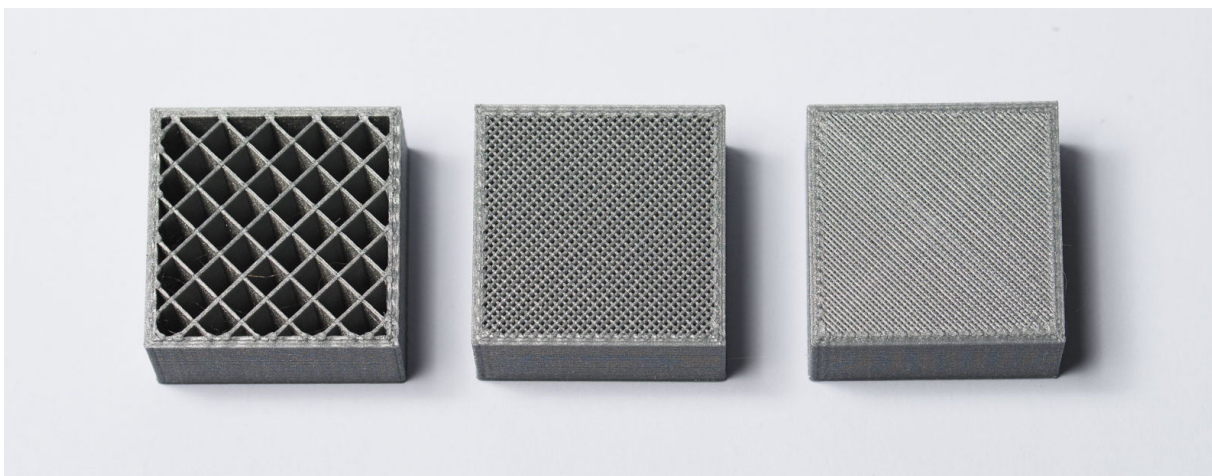


Figure 2.9: Different amount of fill pattern ranging from 25% (left) to 75% (right) [11].

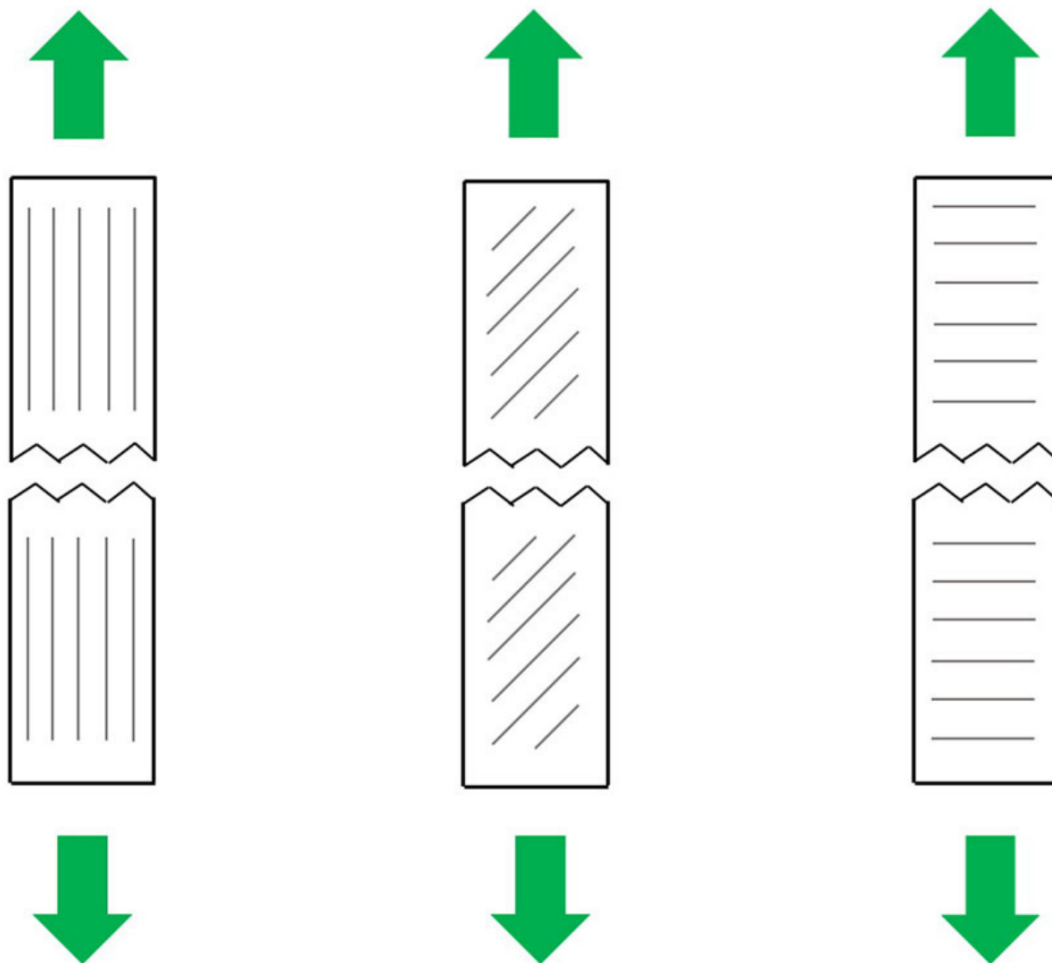


Figure 2.10: The figure show raster angles at 0° (left), 45° (middle) and 90° (right) in relation to the x-axis (green arrow) in the horizontal plane [45].

2.4.4 Common Materials used in FDM

FDM involves extrusion of material, which means that conceptually any material that can flow and then harden can be used in the FDM process [8]. However, the main focus of the FDM industry seems to be on thermoplastics [8]. S. Ore and S. Aage [41] writes that plastics can be divided into two categories, thermosets and thermoplastics. Thermosets are defined as a polymer that through a chemical reaction involving heat creates chains of the polymer bound together in a network [41]. This results in a polymer that can not become plastic again after hardening [41]. Thermoplastics, however, becomes malleable after heating, and can be reheated and reshaped again and again [41]. This makes thermoplastics ideal for use in the FDM process [8].

Some of the thermoplastics commonly used in the FDM process are Acrylonitrile Butadiene Styrene (ABS), polycarbonate (PC) and polylactic acid (PLA) [8]. There are varying qualities to each of these materials, and a study into these qualities are not in the scope of these thesis.

A table, developed by J Lee, J. An and C. Chua [34], of common FDM materials are shown in figure 2.3 to give a general overview.

Material	Properties	Applications/industries
ABS	Tough and strong	Automotive, aerospace, medical-devices
ASA	Mechanical Strength and UV stability	Functional prototyping from brackets and electrical housings to automotive prototypes and practical production parts for outdoor use under the sun
Nylon 12	Good chemical resistance, high fatigue resistance and high impact strength	Ideal material for applications that demand impact-protective components and high fatigue endurance, including antenna covers, custom production tooling, friction-fit inserts and snap fits in automotive and aerospace industries
PC	High tensile and flexural strength	Functional prototypes, tooling and fixtures, blow-molding master in automotive and aerospace industries
PPSF/PPSU	Chemical and heat resistance and mechanical strength	PPSF/PPSU can withstand various sterilization methods including ethylene oxide, autoclaving, and radiation. Sterilizable medical devices, automotive prototypes, and tooling for demanding applications in a variety of industries
PEI or ULTEM	Biocompatible, mechanical, chemical and thermal stability	Due to its high strength-to-weight ratio and existing certification, ULTEM is ideal for rapid prototyping and advanced tooling applications in aerospace, automotive, medical and food-production industries
PLA	Good tensile strength and surface quality	Ideal for model and prototypes that require aesthetic detail and environmentally-friendly for both home and office
TPU	Excellent tear and wear resistance, high impact strength and hardness	Exceptional flexibility (i.e. elongation at break) and corrosion resistance to many common industrial chemicals and oils. Highly versatile material with the both rubber and plastics properties for a variety of industrial application

Table 2.3: Common FDM materials [34].

PLA is the material most readily available at the NTNU's additive prototyping workshops, and was therefore a natural choice as a starting point for the process developed in this thesis. The glass transition temperature (T_g) and the melting temperature (T_m) of PLA compared to another common thermoplastic used in the FDM process, ABS, can be seen in table 2.4. The glass transition temperature, is the temperature where the material transitions from a hard, glassy or brittle phase to a flexible, elastomeric condition [27]. Looking at table 2.4 one can see that T_g for PLA is lower than for ABS. This means that PLA is less resistant to high temperatures than ABS [44]. The manual supplied with the printers at the NTNU's additive prototyping workshops suggests printing PLA and ABS with an extruder temperature at 215°C and 255°C respectively [44], which is above the melting point of the materials [9]. This will, according to M. Behzadnasab and A. Yousefi, result in stronger interlayer adhesion [9]. ABS does therefore require higher temperatures to print than PLA. The manual also suggests using a warm room or enclosure to avoid thermal contraction or warping of parts made of ABS [44]. This is not necessary when using PLA, which show little to no warping [44]. The low extruder temperature required to print PLA also makes it easier to print smaller parts [44]. Another possible benefit of printing PLA is that it is biodegradable [20] and release less ultra fine particles and volatile organic compounds (VOC) than other common thermoplastics used in the FDM process [7]. This can be seen in figure 2.11 and figure 2.12. It is uncertain whether the VOC emissions released from the PLA is toxic. However, comparing the VOC emissions of PLA to ABS shows that the

emissions from PLA is significantly lower [7]. It is also worth noting that a large part of the emissions from ABS is styrene, which is known as a possible human carcinogen [7]. All these factors combined makes PLA easier to use in a FDM process than other thermoplastics, which is possibly why NTNU chose PLA as their material for their additive prototyping workshops.

	ABS	PLA
Tg(°C)	105 [21]	45-60 [20]
Tm(°C)	205 ¹ [21]	150-162 [20]

Table 2.4: Thermal properties of ABS and PLA.

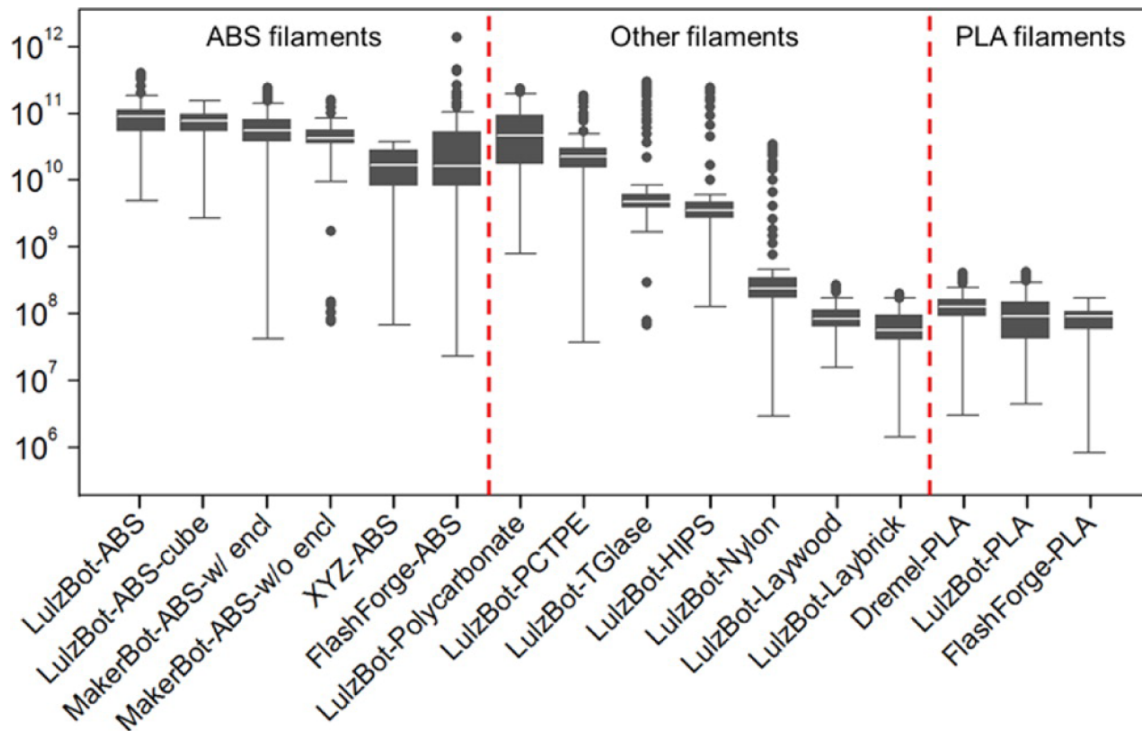


Figure 2.11: Estimates of UFP (ultrafine particles) emissions of common FDM materials [7].

¹because of the amorphous nature of ABS, it does not technically have a melting point [52].

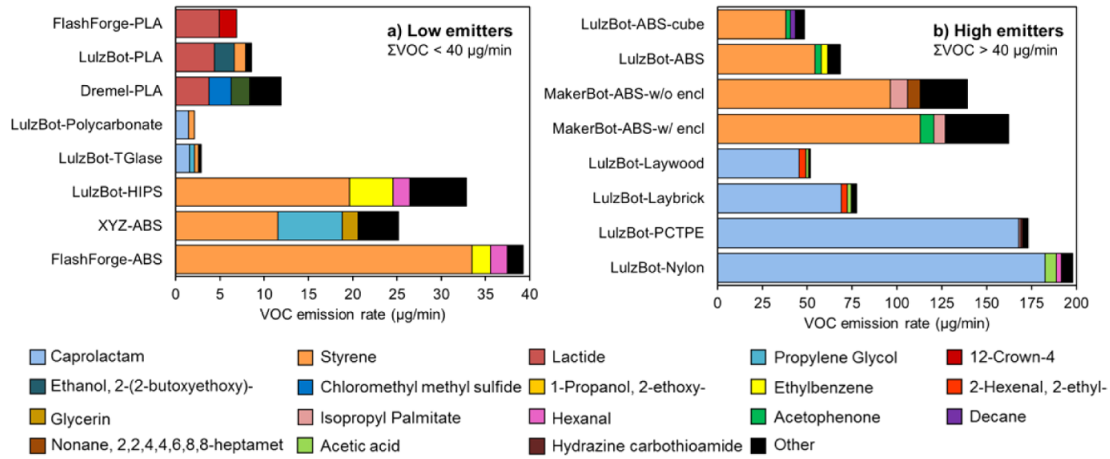


Figure 2.12: Estimated emission rates of volatile organic compounds (VOC). Each individual VOC emission rate has an estimated uncertainty of 36% [7].

2.5 Modularization

Modularization is discussed by P. Smith in *Flexible Product Development: Bring Agility for Changing Markets* [51]. All the information provided in this section is gathered from *Flexible Product Development: Bring Agility for Changing Markets*.

P. Smith [51] states that there are two main types and one related type of development architectures. The architecture most important to flexibility is modularity. Modular architecture is based on separating products into parts which connect strongly within themselves and more weakly to other parts of the product. Some parts might also be cleanly isolated. Opposite to modularity is integral architecture, where the parts interconnect heavily. Interconnected parts may cause major changes to the whole product, if one part is modified. The last architecture is based around platforms. Platforms might provide strategic flexibility in the way of allowing changes to a product, based on parts that are interchangeable for that platform. One example might be camera bodies (platform) with interchangeable lenses (part).

As modularity might increase flexibility it also creates some challenges. Modular development often requires more planning than integral architecture, to avoid making large changes which can be time consuming and expensive. Planning and good communication flow between parts are also important, to allow for the full integration of parts later in the development process. Performance might also be lowered by the use of a modular architecture, because of compromises in the design to allow for modularity.

3 Methodology

The work done in this project is largely based on a set-based development approach. At the beginning of the project, discussions were based on an idea about a product development process that might work. Further investigation into the idea, by looking at existing processes and hand sketching different idea variations, resulted in the development of different designs that had the possibility of generating the wanted results. To facilitate the testing of the different designs, it was necessary to develop a platform. The mold became this platform, and was designed to allow for a set-based approach where several different designs could be tested simultaneously. To physically realize all the concepts, an entry level 3D-printer was used, which allowed for relatively fast production of prototypes. Sets of the different designs were printed, matching the number of sets possible to test, based on how the mold was designed. The different designs were then vacuum formed, utilizing the appropriate sheet dimensions to minimize material waste. After vacuum forming, the designs were inspected and stored for possible further inspection and testing. The molds were used multiple times, until the vacuum forming process had caused significant damage to the molds, affecting the results of the prototyping tests. After several different sets of designs, and their different parameters, were qualitatively tested, one design was chosen to be further quantitatively tested. Quantitative testing was done with a tensile testing machine. The test pieces were then inspected, and the data points from the tests were later plotted in a graph to show the tensile behaviour of the attachment.

3.1 mold and air vents

The molds were developed using the guidelines for mold design, presented in *A Vacuum Forming Guide* [23]. The first mold was designed using the recommended draught angle of 5° , but after realizing that it was hard to separate the vacuum formed part from the mold, the draught angle was changed to 8° . The first mold was also designed with a set of six holes for the pins to sit in so that they could be left in the vacuum formed part after vacuum forming. The six holes are shown in figure 3.1 and described in table 3.1. Some of these holes have venting, which are inspired by the guidelines by Formech [23]. The *circular venting* holes had vents designed

according to the guidelines by Formech, meaning vent holes designed to be 1mm in diameter after printing [23]. The other three holes with venting were designed as experimental holes. These holes were designed to give a lot of air flow while still holding the pins in place. The *large gaps* holes has a lot of air flow in large gaps. This is also creating large areas where the mold is in contact with the pins, which might result in uneven attachment around the pinhead. The *star shaped* hole was designed trying to minimize the pin-to-mold contact while still maintaining good airflow similar to the *large gaps* holes has. The *star shaped* vent holes was chosen for further testing, which is discussed in section 5. The details of the *star shaped* vent holes are shown in figure 3.3

The holes with a diameter of 1mm, designed according to the guidelines by Formech [23], where drawn at 2mm in the CAD model. This was done after printing a set of hole sizes, and comparing them to the measurements from the drawing in the CAD software, as can be seen in figure 3.2. This test showed that small holes become smaller than shown in the CAD drawing when printed.

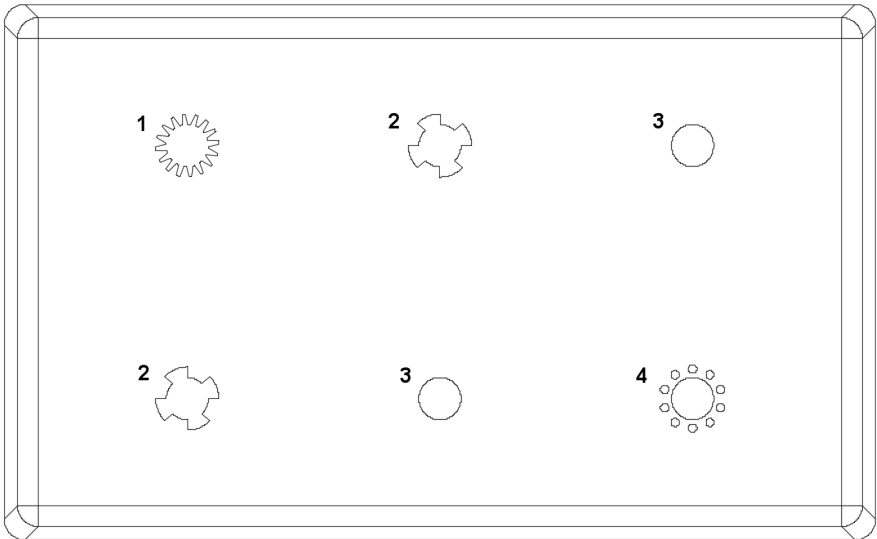


Figure 3.1: Vent hole designs: (1) star shaped, (2) large gaps, (3) no venting and (4) circular venting

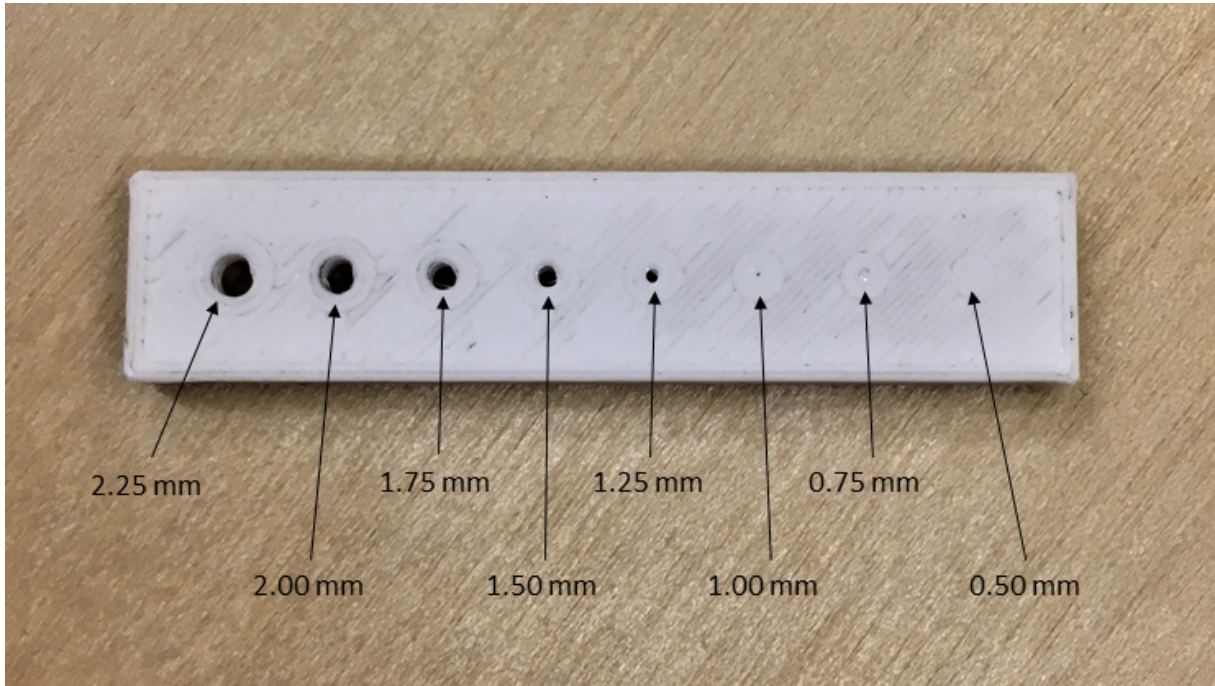


Figure 3.2: Figure showing printed hole sizes compared to the measurement in the CAD software (arrows).

Table 3.1: Table with details of the different vent holes. Note that the dimensions are based of the CAD model and may be slightly different for the 3D printed models.

Vent hole type	Venting	Inner diameter [mm]	Outer diameter [mm]	Number of vent gaps
Star shaped (1)	YES	10	15	16
Large gaps (2)	YES	10	15	4
No venting (3)	NO	10	–	–
Circular venting (4)	YES	10	15	10

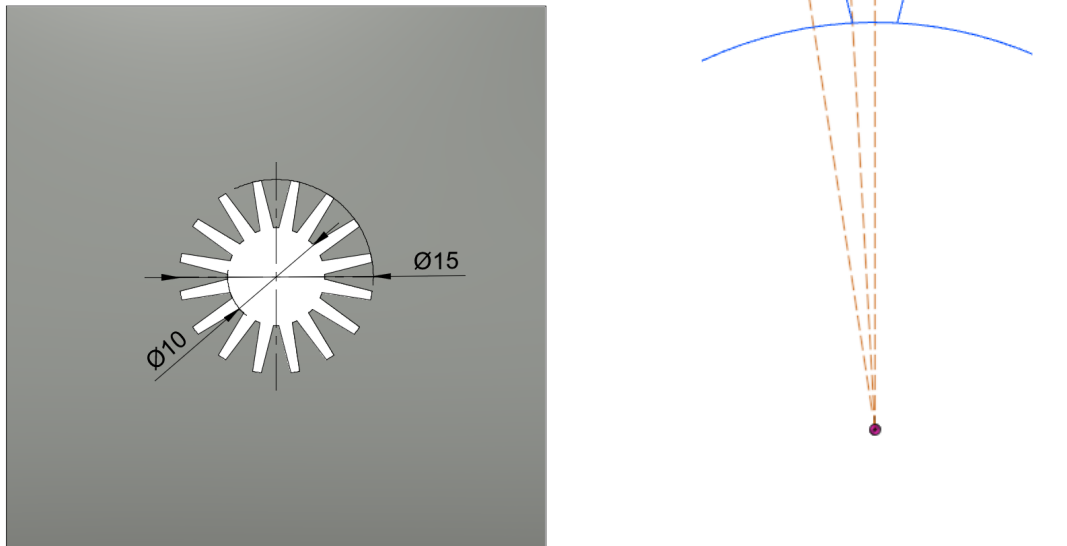


Figure 3.3: Figure showing the diameter (left) and the dimensions of one arm (right) of the *star shaped* vent holes. All measurements are in *mm* or degrees.

A mold base with inserts was later developed to allow for rapid change in vent hole and mold design, which can be seen in figure 3.4. The printing time of six modules was reduced to an estimated 8 hours compared to the previous molds which printed at an estimated 19 hours. The printer settings used for this comparison is the *Slic3r PE* software settings, shown in table 3.9. The times given are the time estimates shown in the *Slic3r PE* software.

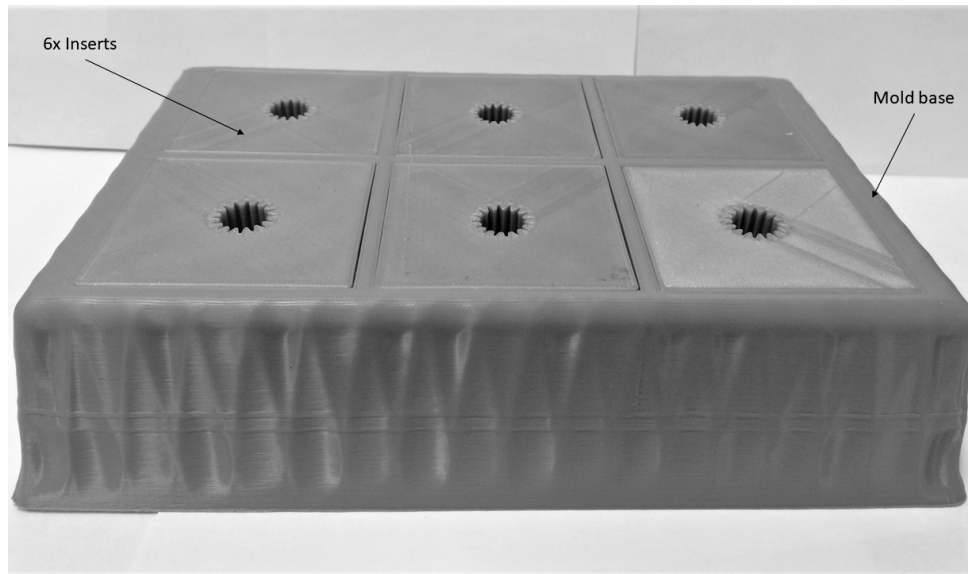


Figure 3.4: Image of the mold base with inserts.

3.1.1 Mold for angled tests

The molds used for the angled tests were inspired by the regular mold and *star shaped* vent hole design. The angle mold and its details are shown in figure 3.5. The -20° angle created an undercut which could complicate removal of the vacuum formed sheet form the mold, as discussed in the section 2.2. This was solved using the guidelines from *A Vacuum Forming Guide* [23], placing the 45° angle at the opposite side of the undercut.

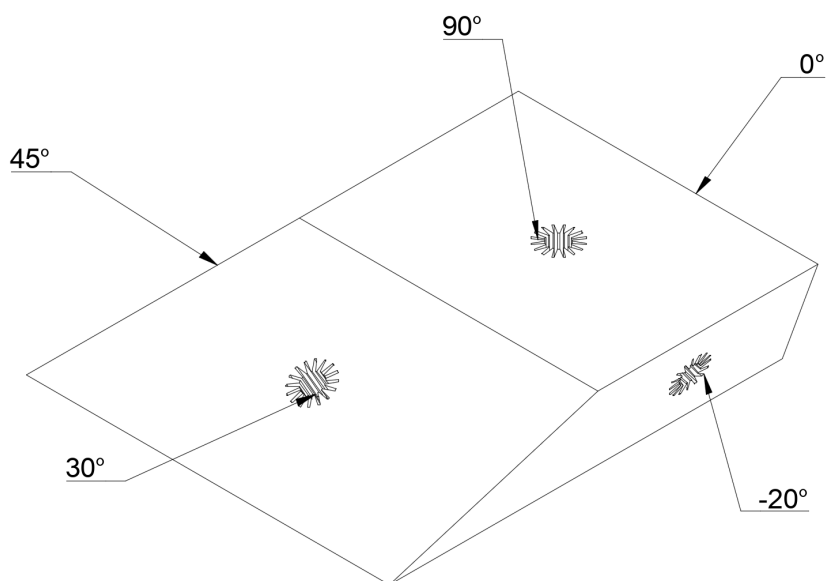


Figure 3.5: Illustration of the mold used for the angled tests.

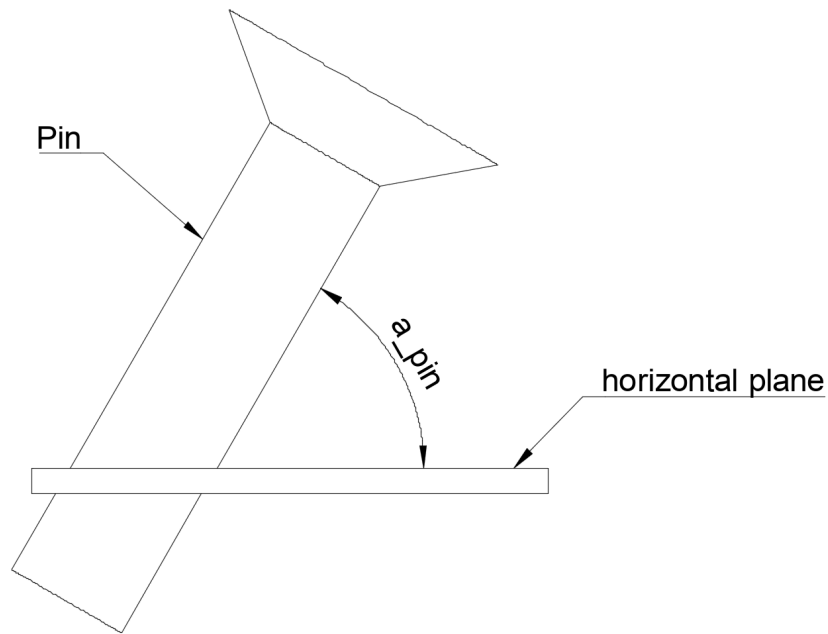


Figure 3.6: Illustration of the angle of the pin (a_{pin}) in relation to the horizontal plane for the angled tests.

3.1.2 Mold for sunken tests

The molds used for the sunken tests were based on the mold base with inserts designed for the sunken tests. These inserts are shown in figure 3.7 and the dimensions of the inserts are shown in table 3.2. The vent hole designed used in these inserts are inspired by the *star shaped* vent hole design.

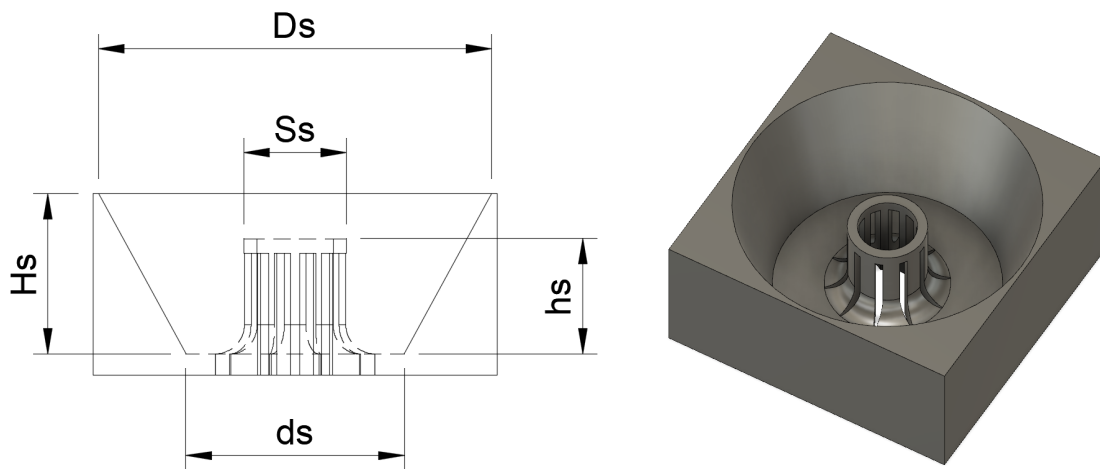


Figure 3.7: Illustration of the mold inserts used for the sunken tests.

Table 3.2: Table with information about the different sunken inserts. A visualisation of the parameters are shown in figure 3.7. Note that the dimensions are based of the CAD model and may be slightly different for the 3D printed models.

	$D_s[mm]$	$S_s[mm]$	$H_s[mm]$	$h_s[mm]$	$d_s[mm]$
Small insert	43	14	22	15.8	30
Medium insert	48	14	22	15.8	35
Large insert	53	14	22	15.8	40

3.1.3 Mold for rib tests

The mold used for the rib tests were developed based on the general mold and vent hole design, and are shown in figure 3.8. The mold shape is identical to the general mold design, but the vent holes had to be positioned so that the ribs could go across the width of the mold. The design and dimensions of the individual went hole arms are similar to the arm design showed in figure 3.3, but placed on a line instead of a circle. The number of ribs tested at once was changed to 5, instead of 6 for the pin tests. This was done to allow for enough space between the ribs, while still keeping the rib design similar to the pins, as discussed in section 3.3.

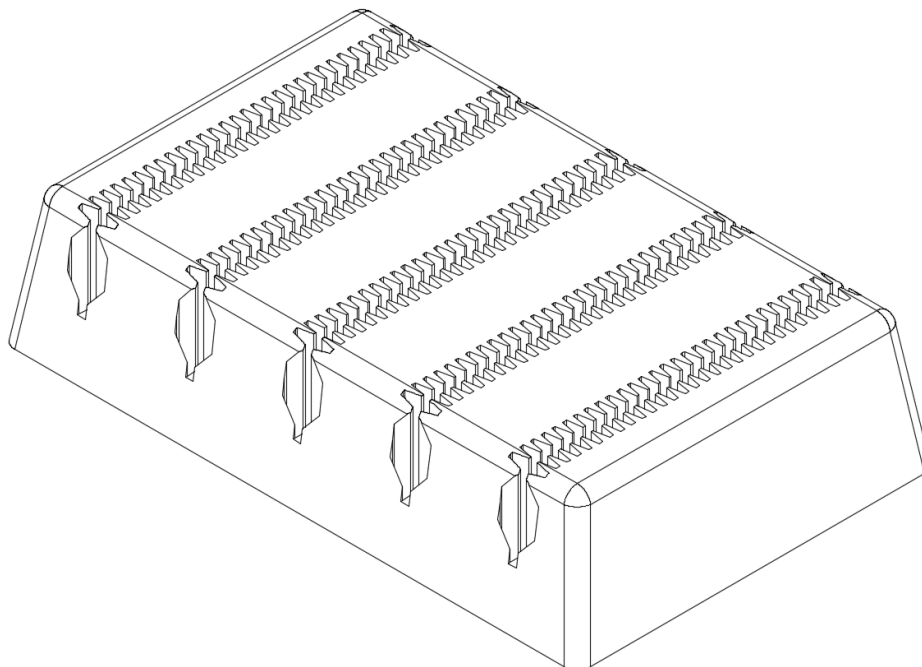


Figure 3.8: Illustration of the mold used for the rib tests.

3.2 Pins

The general pin designs were developed using the guidelines from *A Vacuum Forming Guide* [23]. The guidelines were used in an opposite way of how they were intended, trying to make sure that the pins stayed in the vacuum formed part after vacuum forming. The pins were designed as large nail-like shapes so that the polymer sheet, used for vacuum forming, could form around the head of the pins. This is shown in figure 1.1. Three main pinhead designs were developed. All of the designs had some design specific and some common parameters, as shown in figure 3.9. The common parameters are the height from the base of the mold to the top of the head, h , the diameter of the pin, S , and the diameter of the head D . A set of dimensions were chosen for the first qualitative tests, discussed in section 4.2. These dimensions are shown in table 3.3. The dimensions used for the quantitative tests are shown in table 3.4.

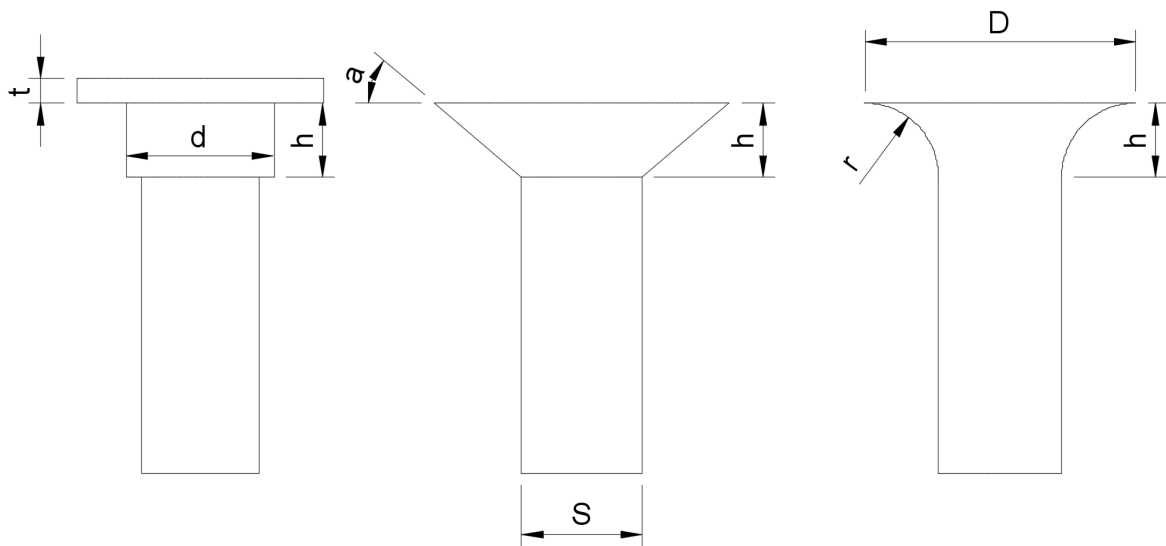


Figure 3.9: Dimensions of the *nail-like* design (left), straight slope design (middle) and the curved design (right)

The first pinhead design was based on the illustrations from *A Vacuum Forming Guide* [23], shown in figure 3.10, with a straight slope and the angle of the slope a as the additional parameter. This was also the first and only design to be tested with the different vent holes on the mold. The second pinhead design was based around a more classical nail design, with a flat head raised from the mold by a thicker section of the pin, which had a diameter larger than the 10mm holes in the mold. Additional parameters for the *nail-like* design were the thickness of the head t and the diameter of the thicker section of the pin d . The last design had a similar shape to the straight slope design, but with a curve instead of a straight slope. The additional parameter for the curved design was the radius r of the curve.

Table 3.3: Table with dimensions of the pin designs tested in the qualitative test.

	D <i>mm</i>	S <i>mm</i>	h <i>mm</i>	t <i>mm</i>	a	r <i>mm</i>
Straight angle design	24	9.80	6	–	40.2°	–
Nail-like design	24	9.80	6	2	–	6
Convex design	24	9.80	6	–	–	–

Table 3.4: Table with dimensions for the pins used in the quantitative tests. Note that the dimensions are based of the CAD model and may be slightly different for the 3D printed models.

	D [<i>mm</i>]	h [<i>mm</i>]	a	S [<i>mm</i>]
Small pin	20	6	49.6°	9.80
Medium pin	24	6	40.2°	9.80
Medium bolt	24	6	40.2°	4
Large pin	28	6	33.4°	9.80

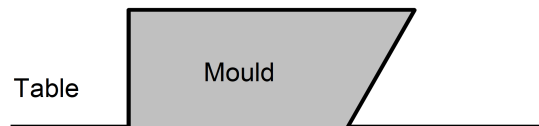


Figure 3.10: Undercut illustrated by Formech [23]



Figure 3.11: Image of the *medium bolt pin*.

3.3 Ribs

The process developed in this thesis has the potential to be used in many different cases. The ribs are an example of this. These ribs were developed with a cross sections based on the initial straight slope pin design, as shown in figure 3.9. The additional parameters, as seen in figure 3.12, were made so that the ribs would fit the standard mold design, similar to the mold shown in figure 3.4. The profile of the pinhead is also present at the bottom end of the rib, which has a shape similar to the straight slope pinheads, but without the curvature.

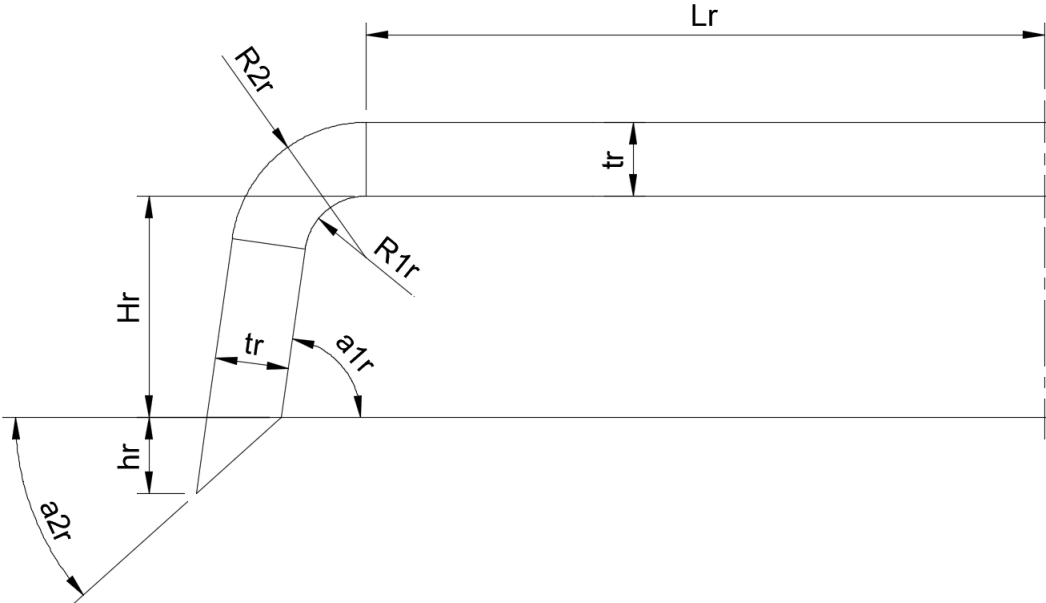


Figure 3.12: Illustration of the rib design with dimensions.

Table 3.5: Table of rib dimensions tested. Note that the dimensions are based of the CAD model and may be slightly different for the 3D printed models.

	$L_r[mm]$	$t_r[mm]$	$R_{1r}[mm]$	$R_{2r}[mm]$	$H_r[mm]$	$h_r[mm]$	a_{1r}	a_{2r}
Rib test 1-5	55.25	6	5	11	18	6.2	82°	41.8°

3.4 The jigs

Two jigs were used for testing the attachments created. The first jig was made of pre-cut metal pieces welded together, and can be seen in figure 3.13. The metal jig was made, trying to get a proper grip at the flat, vacuum formed part of the attachments. This part was therefore clamped between two metal sheets connected by two bolts. The jig manufactured was however not symmetrical in any direction, and it was hard to center the test pieces in the tensile testing machine. This jig was therefore only used for initial testing to see if it was possible to test the strength of the attachments in a tensile testing machine. The measurements of the jig are not given, since it is difficult to measure the jig. The tests where the metal jig was used are also not used to draw any conclusions.

A new 3D-printed jig was manufactured to solve the problems of the poorly constructed metal jig. This jig was designed in a similar way to the metal jig, but with a circular instead of a rectangular design. The number of bolts used for attaching the bottom and top part of the jig together also increased from 2 to 4. This made it easier to center the test pieces and allowed for more even clamping of the vacuum formed sheets. Additional centering tools were also printed to further facilitate easy centering of the test pieces, which are shown in figure 3.16 and table 3.7. The 3D-printed jig and its measurements are shown in figure 3.14 and 3.15, and additional information about the top plate is shown in table 3.6. The printer settings used are shown in table 3.10.

It is reasonable to assume that a metal jig will be more rigid than a 3D-printed jig because of the materials used. The 3D-printed jig did however show to be more than adequate to test the attachments. This can be seen in section 4 where the jig withstood tests where the pins broke, without showing any signs of deformations on the jig. This is also further discussed in section 5.

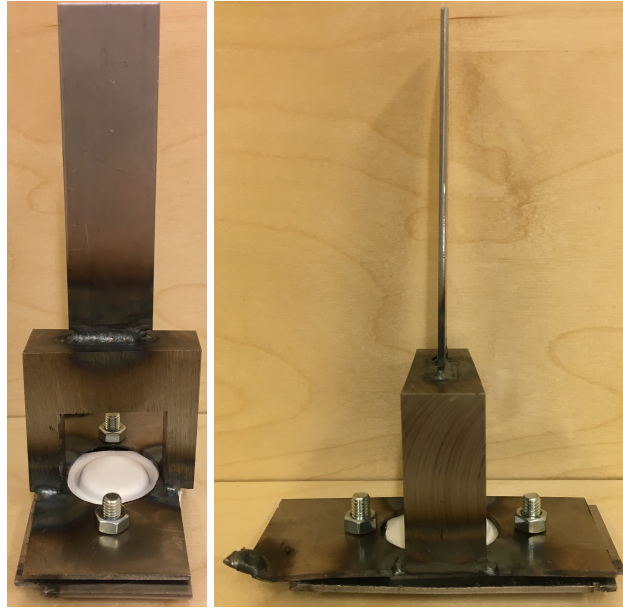


Figure 3.13: Welded test jig setup

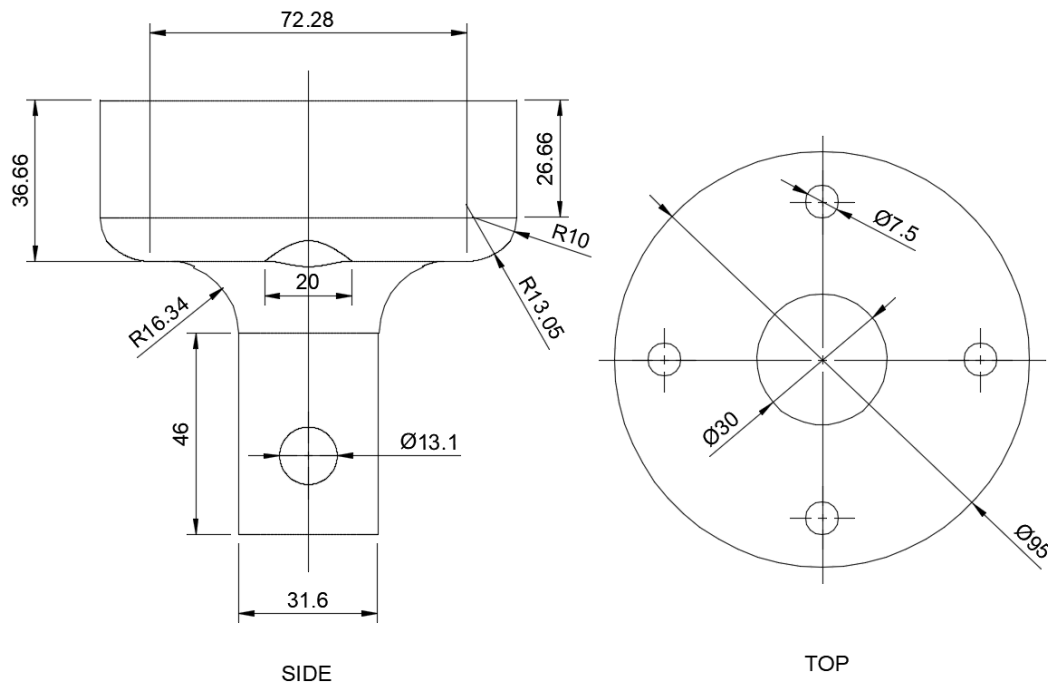


Figure 3.14: Drawing of the bottom 3D-printed jig with dimensions. All dimensions are in millimeters.

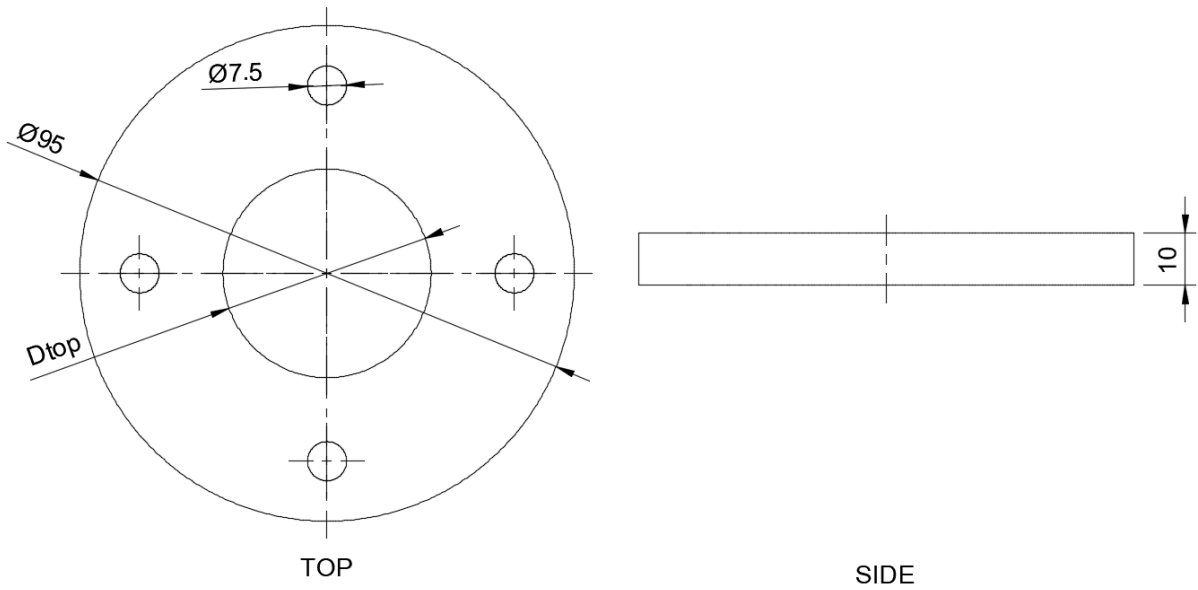


Figure 3.15: Drawing, with dimensions, of the top plate of the 3D-printed jig. All dimensions are in millimeters.

Table 3.6: Table of the dimensions of the top plates used in the 3D-printed test jigs. Note that the dimensions are based of the CAD model and may be slightly different for the 3D printed models.

	$D_{top}[mm]$
Small top plate	36
Medium top plate	40
Large top plate	44

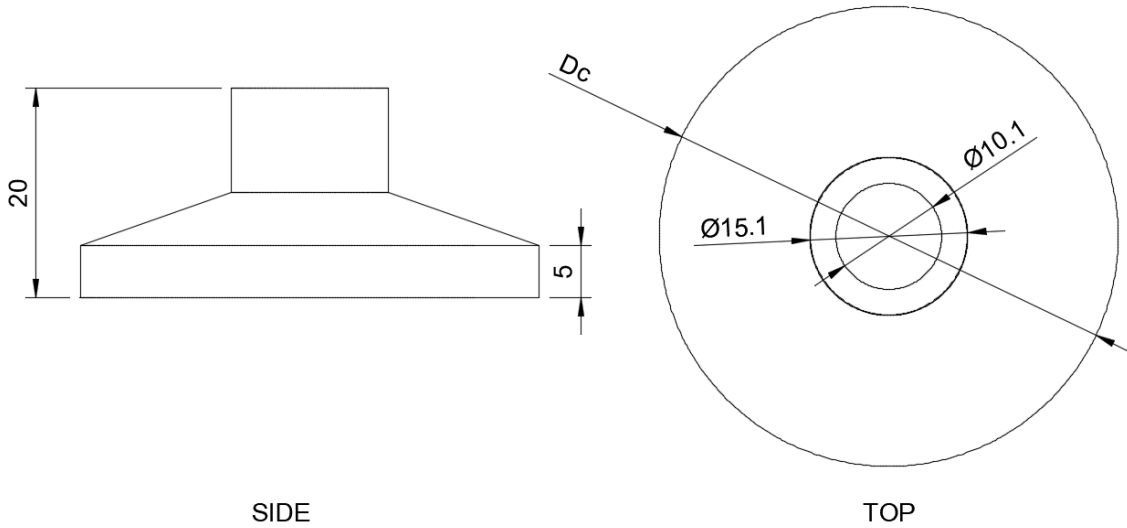


Figure 3.16: Drawing of the centering tool used for centering the test pieces in the 3D-printed jig. All measurements are in *mm*.

Table 3.7: Table of the dimensions of the centering tool used for centering the test pieces in the 3D-printed jig. Note that the dimensions are based of the CAD model and may be slightly different for the 3D printed models.

	$D_c[mm]$
Small centering tool	35.9
Medium centering tool	39.9
Large centering tool	43.9

3.5 Software

The prototypes were developed in the CAD software Autodesk Fusion 360, and prepared for 3D printing with the use of software for slicing the 3D-modeled parts into layers. The first molds were prepared using the Prusa Control software. After issues with the top layers of the mold deforming, the slicer software was changed to Slic3r Prusa Edition (PE) which have a lot more perimeters that can be manipulated compared to the Prusa Control software. The Slic3r PE was therefore used through the rest of the thesis. Prints where the *prusa control* printer settings are used, as shown in table 3.9 and 3.11, are the only ones where the Prusa Control software is used. Slic3r PE is used for the all other printer settings.

3.6 3D printer

The manufacture of pins and molds was done with FDM 3D printers. FDM is the chosen AM technology for this thesis, as this is probably the AM technology most people have access to [56]. This is further discussed in section 2. The details of the printers used are shown in table 3.8. Both printers used in this thesis are made by Prusa, which were the printers available at NTNU's additive prototyping workshops. The *Original Prusa i3 MK3* is known for offering high value and quality at a relatively reasonable price [35], which is probably why these printers were the choice for NTNU's additive prototyping workshops.

Table 3.8: Table with details about the printers and general settings used, according to the *Prusa 3D Printing handbook* for the *mk2* and *mk3* printers [43] [44]

Printer	Filament material	Filament diameter [mm]	Number of extruders	Nozzle diameter [mm]	Nozzle temperature °C	Bed temperature °C
Original Prusa i3 MK2S	PLA	1.75	1	0.4	215	60
Original Prusa i3 MK3	PLA	1.75	1	0.4	210	60

Different filament colours were used based on what was available at the time of printing, and the bed was cleaned before each print with propan-2-ol. The mold, regardless of slicer software, was printed upside-down, allowing it to be printed without support structures. The same method was used for the pins printed upright, as seen in table 4.8. These pins were printed with the head of the pins at the build plate, to assure good adhesion of the part to the printer bed. The pins printed sideways was printed with a combination of manually drawn support structures and automatically generated support structures, created by the Slic3r PE software. The bottom part of the jig was also printed sideways to ensure the best possible strength of the jig [33], which is further discussed in section 2. Details of the support structures for the pins and the jig are shown in figure 3.17 and 3.18 respectively.

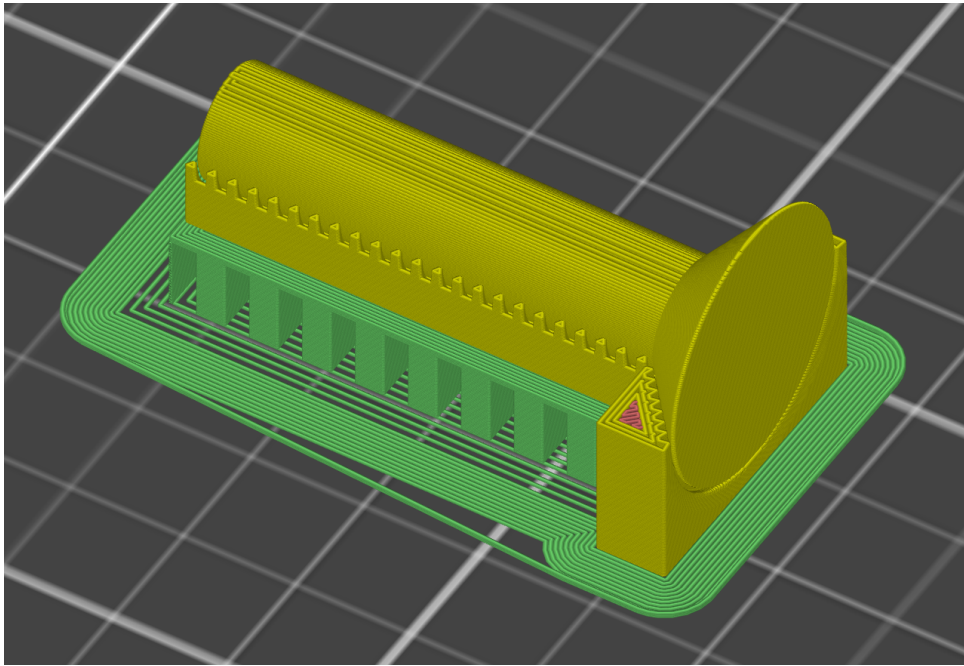


Figure 3.17: Illustration of manually drawn (yellow) and automatically generated (green) support structure for the sideways printed pins. Not that the pin is also colored yellow.

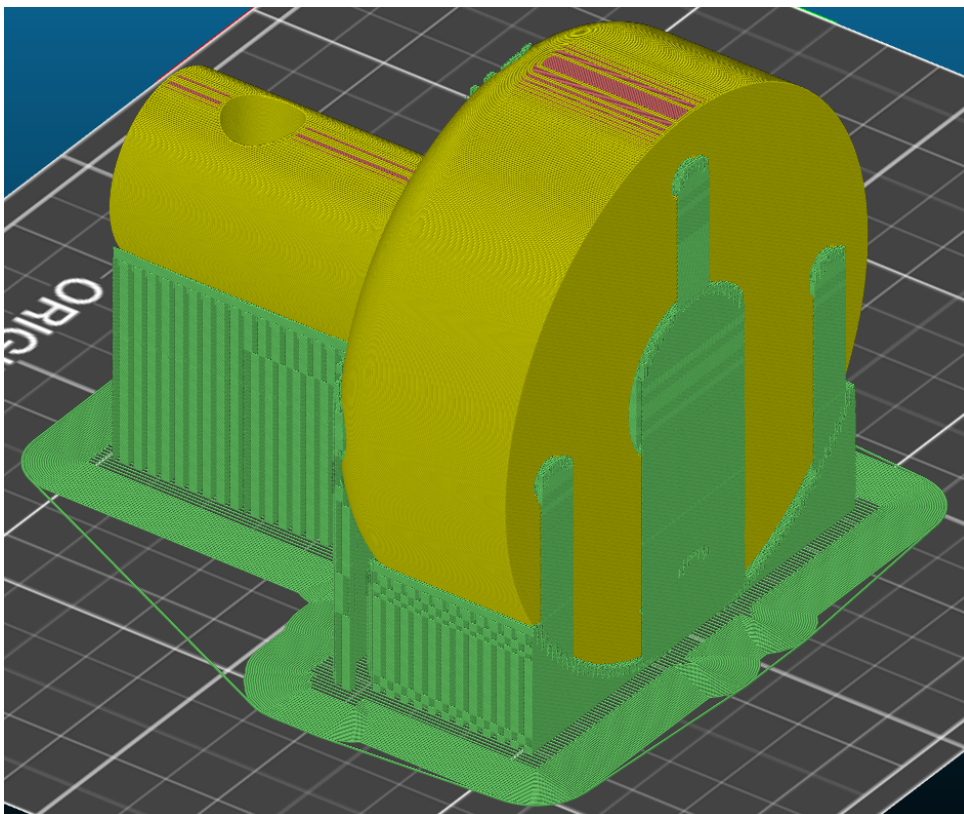


Figure 3.18: Illustration of the automatically generated (green) support structure for the bottom part of the jig.

Table 3.9: Printer parameters for the molds.

Slicer software	Layer height [mm]	Infill	Number of layer at the top of the mold
Prusa control	0.3	10%	— ²
Slic3r PE	0.2	10%	8

Table 3.10: Printer parameters for the jig.

	Slicer software	Printer used	Print orientation	Layer height [mm]	Infill
Bottom part	Slic3r PE	Prusa i3 MK3	sideways	0.15	100%
Top plate	Slic3r PE	Prusa i3 MK3	upright	0.15	100%
Centering tool	Slic3r PE	Prusa i3 MK3	upright	0.2	10%

Table 3.11: Printer parameters for pins.

Printer setting	Slicer software	Printer used	Layer height [mm]	Infill	Perimeters	Complete individual objects ³
prusa control	Prusa Control	Prusa i3 MK2S	0.3	70%	— ⁴	NO
sideways print	Slic3r PE	Prusa i3 MK3	0.15	100%	3	YES
upright print	Slic3r PE	Prusa i3 MK3	0.2	100%	15	YES

3.7 Vacuum forming

The vacuum forming machine used in this thesis was a Formech 686, with HIPS polymer sheets of 2mm thickness. The Formech 686 machine comes with the possibility of using a maximum sheet size of 686mm x 660mm with reducing windows available for smaller sheet sizes [22]. The molds were designed to fit in one of the smaller reducing window available for the machine, which has a 300mm x 300mm window. The sheet was clamped between a seal and the metal of the reducing window, before heated by the heating mechanism of the Formech 686 machine. The HIPS sheets were heated to approximately 150°C, as recommended by Formech [23]. The temperature was measured on the surface of the sheet with a hand held infrared thermometer.

²The prusa control software does not give information about number of perimeters

³If individual pins are printed

⁴The prusa control software does not give information about number of perimeters



Figure 3.19: Formech 686 vacuum forming machine [22]

3.8 Test setup

All of the tests were first inspected visually, before and after separating the attachment from the mold. The pins appearing to have a good attachment to the vacuum formed part were, after visual inspection, touched and pulled in various ways to see if they were possible to pull out with human force. All tests were also rated using the rating system showed in table 3.12. This is further discussed under section 4.2. Later, a design was chosen for further testing in a tensile testing machine shown under section 4.3.

Table 3.12: Description of the rating system used for qualitative testing

Rating	Description
1	The pin falls out by itself or it is easily pulled out
2	The pin can either be pulled out by human force or is hard to pull out, but seems insecure
3	The pin can not be pulled out by human force

The tensile testing was done using an MTS Criterion Model 42 tensile testing machine, as shown in figure 3.20. The first tests were done with the metal jig discussed in section 3.4. To attach the metal jig and the test pieces to the machine, mechanical wedge grips were used. The top grips were designed for circular specimens, with a diameter of 10-14mm, and the bottom grips were designed for flat specimens. The pin-part of the attachments were attached to the circular top grips, while the metal jig was attached to the flat bottom grips, as shown in figure 3.21. A similar method was used for the 3D-printed jig, as shown in figure 3.21. This jig was designed to fit the same mount where the grips are mounted. The bottom grip was therefore not necessary, and the jig was mounted directly in the machine while the pins were attached to the top grips. The settings for the tensile testing are shown in table 3.13.

Table 3.13: Tables with information about settings used for the tensile tests.

Setting	Value	Unit
Preload ⁵	4.000	N
Data Acquisition Rate	50.0	Hz
Test Speed	10.0	mm/min

⁵Preload is used to remove slack from the load string before data is collected [38]. This value is set so it does not interfere with important test data. [38]



Figure 3.20: MTS Criterion Model 42 (left) [40] and welded test jig attached to the machine (right)



Figure 3.21: Image of the metal jig (left) and the 3D-printed (right) jig attached to the machine.

3.8.1 Measurement of undercut (X_s)

The undercuts were measured by first splitting the test pieces in the middle by hand with a hacksaw, as shown in figure 3.22. Later one half of each test piece was photographed using a USB microscope. This was done with the use of a jig, where the test pieces was placed on the *specimen plate*, as shown in figure 3.22. The undercuts (X_s) were measured using the software *ImageJ*. An illustration of how the undercuts were measured is shown in figure 3.23.

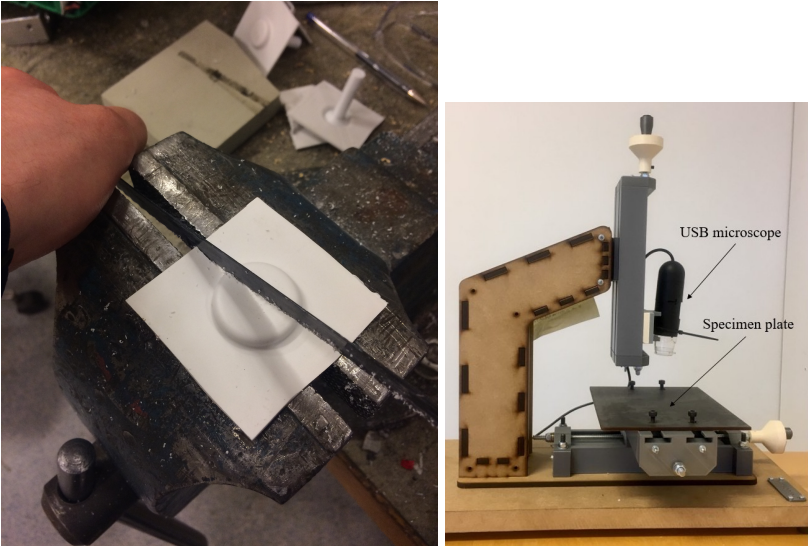


Figure 3.22: Images of spitting the test pieces (left) and the microscope used for measuring the undercuts (X_s) (right).

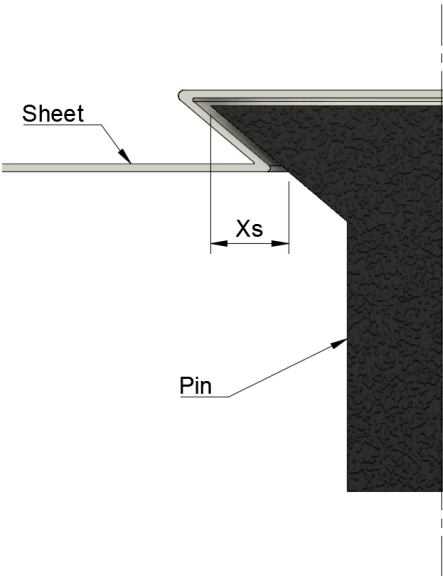


Figure 3.23: Illustration of the measurement of the overhang (X_s).

4 Work and Results

4.1 molds and air vents

The first test of the mold and the set of pin prototypes was done with the *medium pin* as shown in table 3.4. This test was done on the mold shown in figure 3.1 and table 3.1. The vent holes chosen for this test are based on the assumption that one of these vent holes would create sufficient attachment to be used for further testing. The *no venting* and *large gaps* vent holes were tested in a set of two each. This is because these vent holes are the extremes, where the *no venting* has no venting and the *large gaps* has the largest vent holes of the tests. To ensure rapid prototyping of vent holes it was therefore decided that it was most beneficial to test the extremes, so that if one of the extremes created the best attachments it would not be up to chance. The two other vent hole designs were more closely design according to the guidelines by Formech [23], and therefore more likely to create good attachments.

The *large gaps* and *star shaped* vent holes gave the best attachment results, which can be seen in table 4.1. One of the *large gaps* designs did however create a poor attachment. The *star shaped* vent hole was chosen for further testing since it is more closely designed according to the guidelines by Formech [23], and the attachment seemed secure. Further testing of the pins, discussed in the quantitative tests section, shows that it is possible to create good attachments with the vent hole design chosen *star shaped*. These tests also show results that are more than adequate for comparing the effect of pin designs. Further testing is however necessary to give an extensive understanding of how the vent hole designs affect the results.

Table 4.1: Table with results form the first vent hole test.

Vent hole type	Attachment	Possible to pull out	Attachment rated (1-3) ⁶
Star shaped	YES	NO	3
Large gaps (No. 1)	YES	NO	3
Large gaps (No. 2)	YES	YES	2
No venting (No. 1)	NO	Not applicable	Not applicable
No venting (No. 2)	NO	Not applicable	Not applicable
Circular venting	NO	Not applicable	Not applicable

The 3D-printed molds showed deformation after the first vacuum forming test. The solid top layers of the mold were most visibly affected, showing the internal infill structure of the mold. This is shown in figure 4.1 and 4.2. The deformation resulted in higher height, Δh , from the deformed base of the mold to the very top of the mold. This, consequently, resulted in a higher effective height, $h + \Delta h$, from the mold to the top of the pinhead, as shown in figure 4.3. Tests done on these molds showed that the height difference was large enough to impact the test results. This effect became evident when comparing the tests form the deformed mold to the improved mold, having 8 solid layer at the top of the mold.

The 3D-printer slicer settings for the molds were therefore changed, as mentioned in section 3, printing 8 solid layers at the top face of the mold. The mold with these properties showed significantly less deformation after vacuum forming, as shown in figure 4.1.

⁶See table 3.12 for information about the rating system.

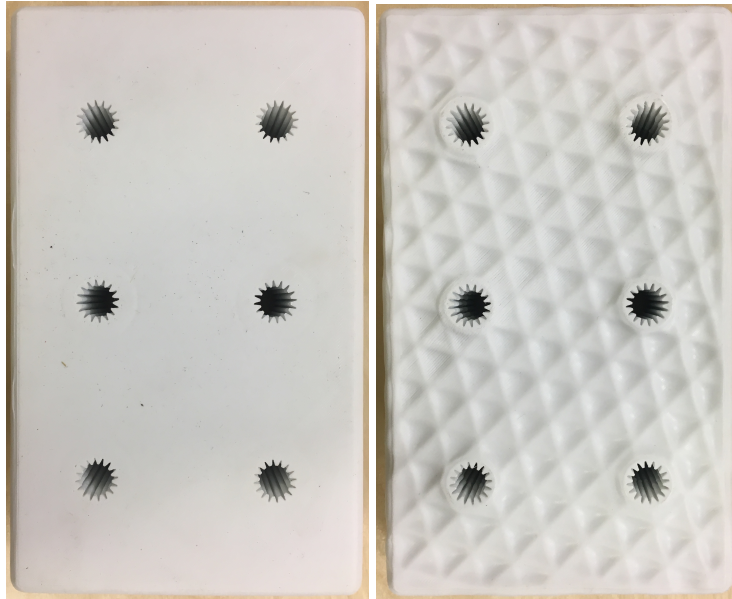


Figure 4.1: Mold with 8 solid top layers (left) and original mold (right), both after one test

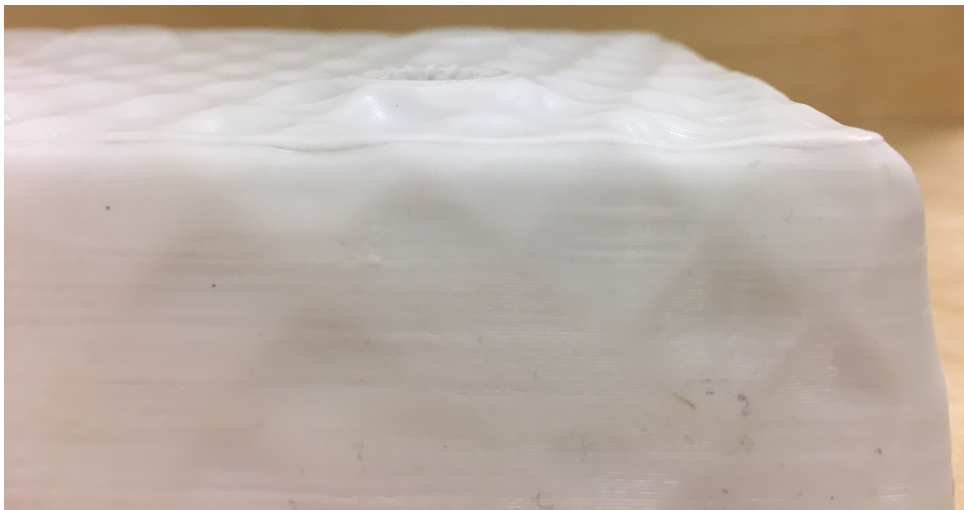


Figure 4.2: Image of the increased height caused by the deformation.

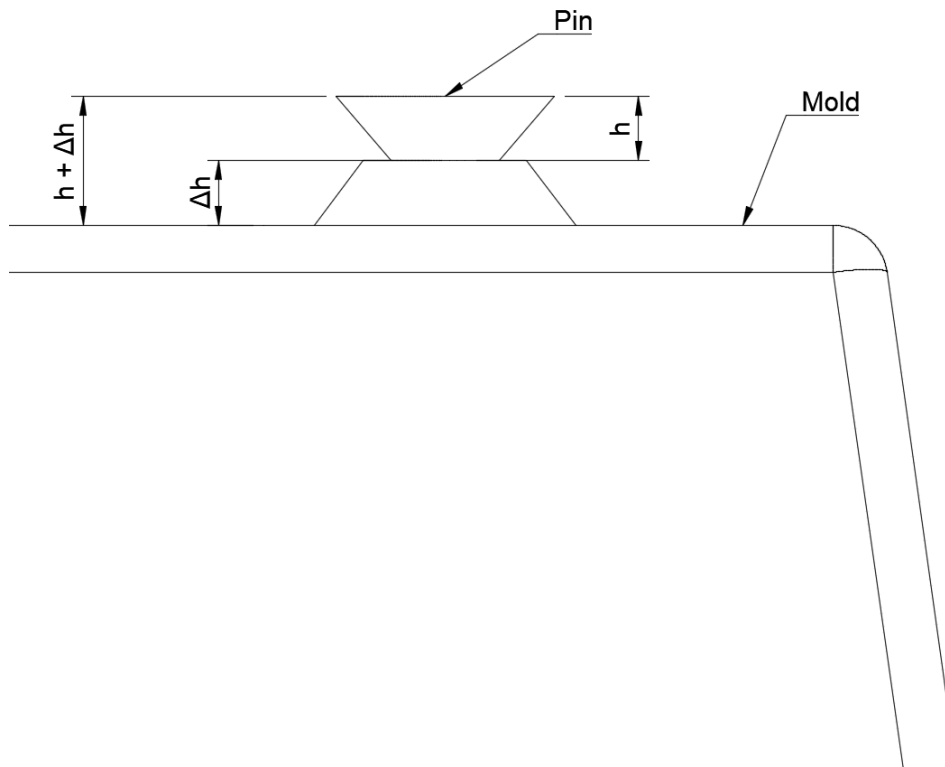


Figure 4.3: Illustration of the increased height, $h + \Delta h$, caused by the deformation.

4.2 Qualitative Testing of Attachment

Testing of the different pin designs showed that the *straight angle* design provided the best attachment at the lowest height, h . The dimensions of each pin design are shown in table 3.3. The *nail-like* design also showed good attachment, but greater protrusion of the pin on the vacuum formed side of the prototype, as shown in figure 4.6. The *convex* design showed the worst result with most of the pins showing signs of deformation at the edges of the pinheads, as shown in figure 4.5. This resulted in bad attachment to the vacuum formed part. A general trend for all the pin designs was that better attachment was achieved at greater heights, h . Both the *nail-like* design and the *straight angle* design showed good attachment at $h = 6\text{mm}$, but heights of 8mm or higher did however show a tendency to be more flexible when shear forces were applied by human force. The thickness t of the *nail-like* designs were printed at 2mm, to avoid large deformation of the head, which resulted in a greater protrusion of the pinhead on the vacuum formed side. This is shown in figure 4.6. Testing the relationship between the size of the vent hole diameter and the head diameter D showed that the pinheads with similar or greater diameter D than vent hole diameter had the best attachment results. The *straight angle* pins that showed the best attachment, shown in table 3.3, were designed so that they had a larger diameter than the vent holes, with a diameter of 15mm, as shown in figure 4.4. A summary of the qualitative pin design tests is shown in table 4.2.

Table 4.2: Table comparing the general trends shown through testing the different pin designs.

Pin design	Attachment	Possible to pull out	Best attachment height h [mm] ⁷	Attachment rated (1-3) ⁸	Comment
Straight slope	YES	NO	6	3	Generally easy to create good attachments with low protrusion. Does exhibit some deformation on the pinhead.
Curved	NO	–	–	1	Difficult to create good attachment. Shows a lot of deformation on the pinhead.
Nail-like	YES	NO	8	2	Generally easy to create good attachments, but at the expense of larger protrusions. Has the least amount of deformation.

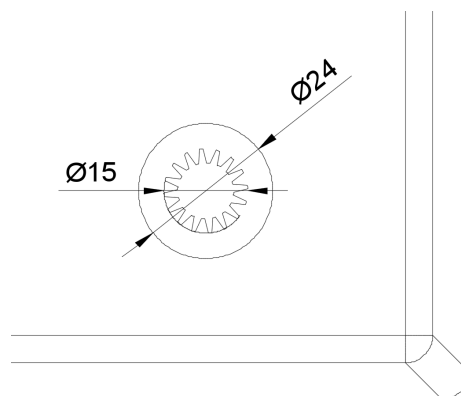


Figure 4.4: Diameter of the best pinhead (24mm) compared to the star shaped vent hole (15mm).

⁷The best attachment height is the height where good attachment is achieved with the lowest protrusion.

⁸See table 3.12 for information about the rating system.

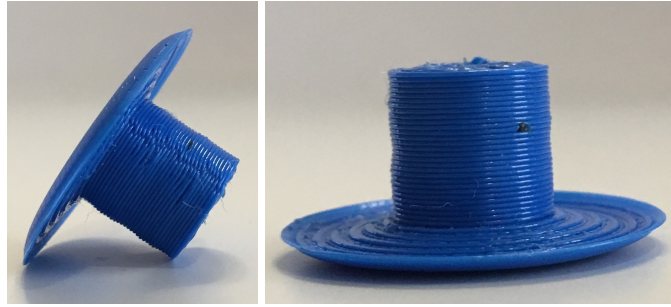


Figure 4.5: Deformation of the curved pinhead design after vacuum forming.



Figure 4.6: Protrusion of pinhead

4.2.1 Angled attachments

Further testing was also done on attachments at different angles. The angles tested are shown in table 4.3 and a picture of the mold used for the angled tests are shown in figure 3.5. All pins in this test was placed in the middle of the surface of the pins respective angle. The results of the test are shown in table 4.4 and figure 4.7.

Table 4.3: Table of angles tested.

	Angle
Angled test 1	90°
Angled test 2	0°
Angled test 3	45°
Angled test 4	30°
Angled test 5	-20°

Table 4.4: Table of results from angled pin tests.

	Attachment?	Possible to pull out?	Attachments rated (1-3) ⁹
Angled test 1	Yes	No	3
Angled test 2	Yes	Yes	1
Angled test 3	Yes	No	3
Angled test 4	Yes	No	3
Angled test 5	Yes	Yes	1

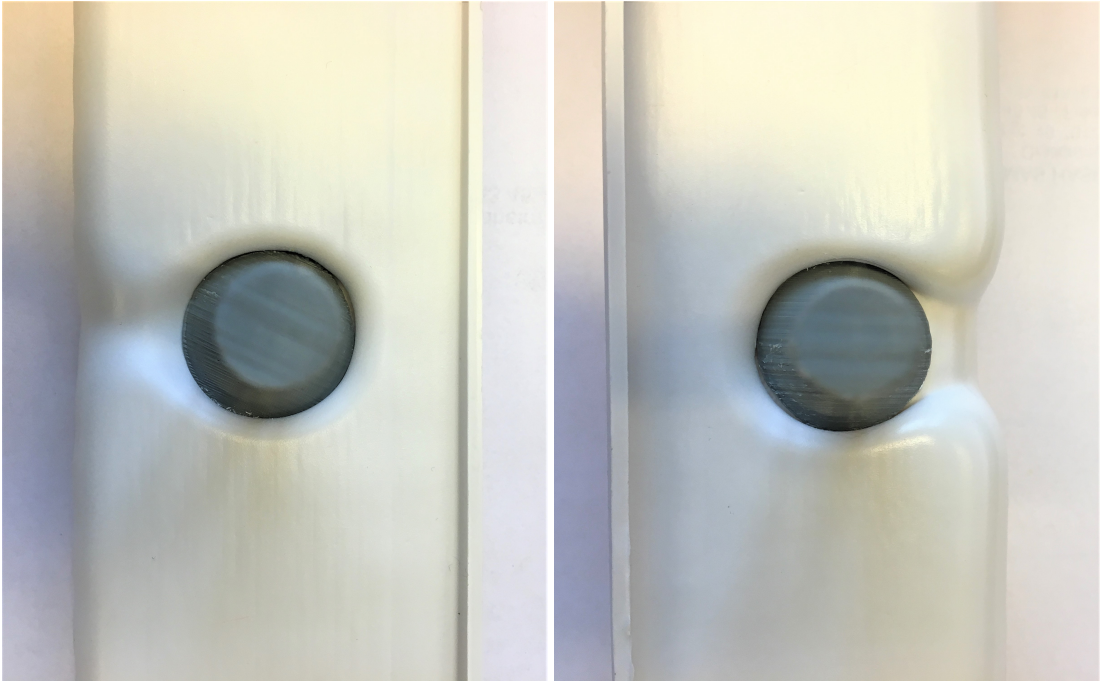


Figure 4.7: Pictures of the attachment of *angle pin 2* (left) and *angle pin 5* (right)

4.2.2 Sunken attachments

Testing was also done on sunken attachments trying to eliminate protrusion of the pins. The results of these tests are shown in table 4.6. The pins and corresponding mold inserts tested are shown in table 4.5 and illustrations of the mold insert are shown in figure 3.7. The results from these tests were somewhat different than the results observed in the other tests. An image of the test results can be seen in 4.8, where large shapes, similar to air-bubbles, can be observed where the vacuum formed sheet has formed around the pins.

⁹See table 3.12 for information about the rating system.

Table 4.5: Table of sunken attachment tests.

	Pin type	Print orientation	Printer settings	Mold insert ¹⁰
Sunk test 1	medium	sideways	sideways print	small insert
Sunk test 2	medium	sideways	sideways print	small insert
Sunk test 3	medium	sideways	sideways print	medium insert
Sunk test 4	medium	sideways	sideways print	medium insert
Sunk test 5	medium	sideways	sideways print	large insert
Sunk test 6	medium	sideways	sideways print	large insert
Sunk test 7	medium	sideways	sideways print	small insert
Sunk test 8	medium	sideways	sideways print	small insert
Sunk test 9	medium	sideways	sideways print	medium insert
Sunk test 10	medium	sideways	sideways print	medium insert
Sunk test 11	medium	sideways	sideways print	large insert
Sunk test 12	medium	sideways	sideways print	large insert

¹⁰Details for mold inserts can be found in table 3.2.

Table 4.6: Table of results from angled pin tests.

	Attachment?	Possible to pull out?	Attachments rated (1-3) ¹¹
Sunk test 1	Yes	Yes	2
Sunk test 2	Yes	Yes	2
Sunk test 3	Yes	No	2
Sunk test 4	Yes	No	3
Sunk test 5	Yes	No	2
Sunk test 6	Yes	No	2
Sunk test 7	Yes	Yes	2
Sunk test 8	Yes	Yes	2
Sunk test 9	Yes	No	3
Sunk test 10	Yes	No	3
Sunk test 11	Yes	No	3
Sunk test 12	Yes	No	3

¹¹See table 3.12 for information about the rating system.

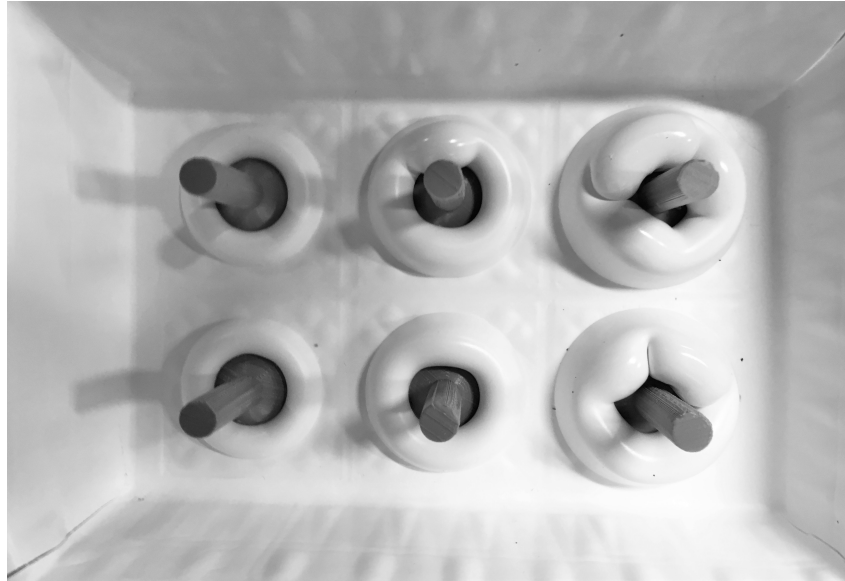


Figure 4.8: Image of the test results of *sunk test* 7 (bottom left), 8 (upper left), 9 (bottom middle), 10 (upper middle), 11 (bottom right) and 12 (upper right). Notice the large shapes, similar to air-bubbles, formed around the pins.

4.2.3 Ribs

The last qualitative tests were done on a rib design. The detail of the ribs tested are shown in table 3.5 and a picture of the mold used are shown in figure 3.8. The results of this test are shown in table 4.7 and figure 4.10. A comparison between a mold with no ribs and a mold with ribs are shown in figure 4.9.

	Attachment?	Possible to pull out?	Attachments rated (1-3) ¹²
Rib test 1-5	Yes	No	3

Table 4.7: Table of results from rib tests.

¹²See table 3.12 for information about the rating system.

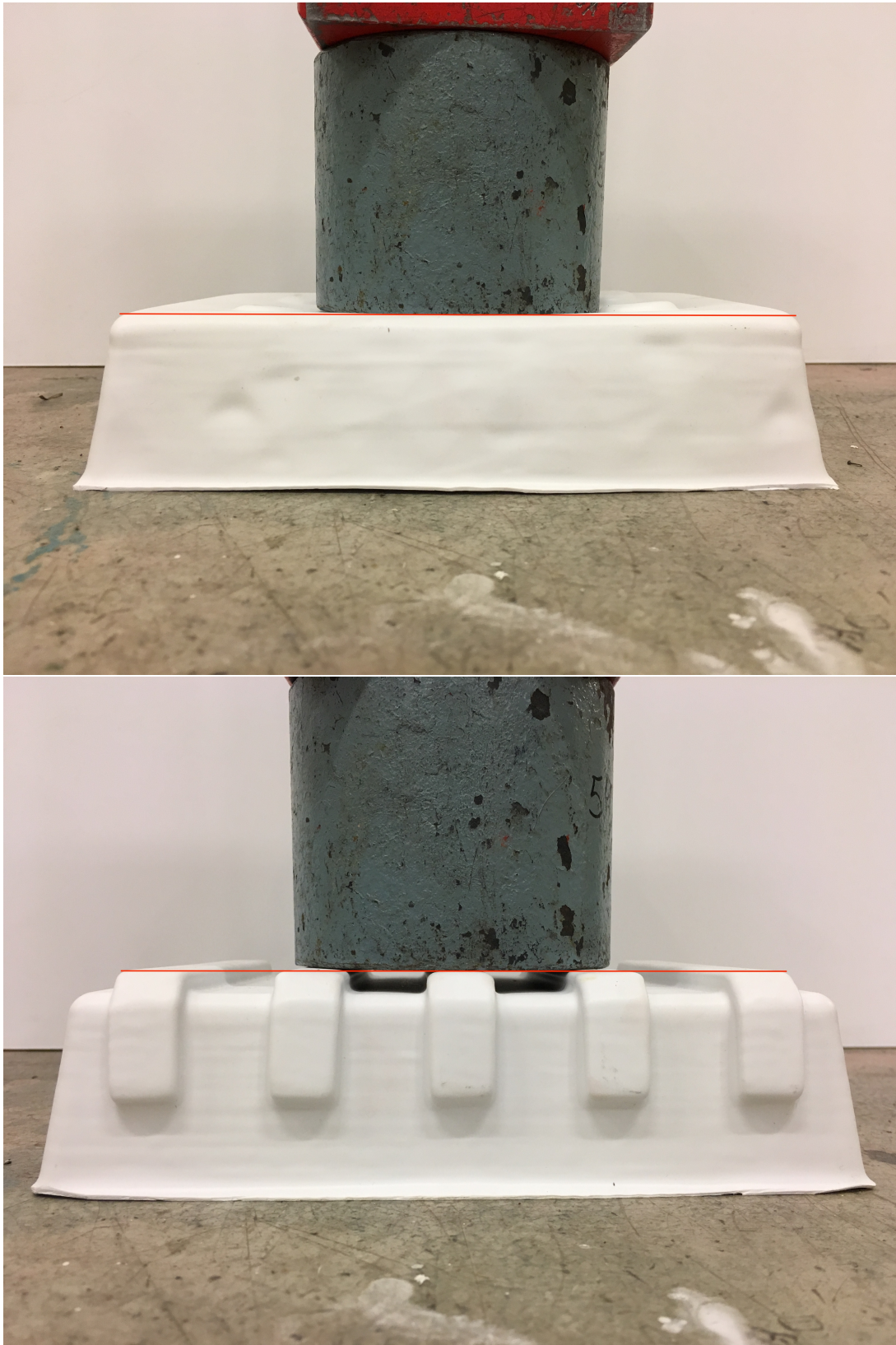


Figure 4.9: Pictures of a comparison between mold with no ribs (top) and a mold with ribs (bottom). Notice how the weight (grey) goes below the red line in the top image and stay at the red line in the bottom image. This was tested with a 22,4kg weight.



Figure 4.10: Pictures of test results from the rib tests.

4.3 Quantitative Testing of attachment

Further testing of the *straight angle* design was done to get a better understanding of how the different parameters, shown in figure 3.3, affect the attachment. The qualitative tests showed that increasing the height, h , could create better attachments. It was however difficult to say how the diameter, D , would affect the quality of the attachments from the qualitative tests. It was therefore decided that the diameter, D , of the pinhead was the most important parameter to test. To isolate this parameter it was decided that the height, h , would remain constant. This meant that the angle, a , would change as the diameter D , changed. The details of each test performed are shown in table 4.8 and the dimensions of each pin tested is are shown in table

3.4.

Table 4.8: Table with details of each tests. More detailed information about pin type, printer settings, top plates and jig type can be found in table 3.4 and 3.11, 3.11, 3.6 and figures 3.13, 3.14 and 3.15.

	Pin type	Print orientation	Printer settings	Jig type	Top plate dimensions
test 1	medium	upright	prusa control	metal	— ¹³
test 2	medium	upright	prusa control	metal	— ¹³
test 3	medium bolt	upright	prusa control	3D-printed	small
test 4	medium	sideways	sideways print	3D-printed	small
test 5	small	sideways	sideways print	3D-printed	small
test 6	medium	sideways	sideways print	3D-printed	small
test 7	large	sideways	sideways print	3D-printed	small
test 8	small	upright	upright print	3D-printed	medium
test 9	medium	upright	upright print	3D-printed	medium
test 10	large	upright	upright print	3D-printed	medium
test 11	small	upright	upright print	3D-printed	medium
test 12	medium	upright	upright print	3D-printed	medium
test 13	large	upright	upright print	3D-printed	medium
test 14	medium	upright	upright print	3D-printed	small
test 15	medium	upright	upright print	3D-printed	small
test 16	medium	upright	upright print	3D-printed	medium
test 17	medium	upright	upright print	3D-printed	medium
test 18	small	upright	upright print	3D-printed	small
test 19	medium	upright	upright print	3D-printed	medium
test 20	large	upright	upright print	3D-printed	large

The first quantitative tests of the pins were done on two *straight angle* pins as shown in figure

¹³Tests with the metal jig only had one top plate used.

3.3, and the details of the pins tested are shown as *test 1* and 2 in table 4.8. Failure happened, in both test, at the transition between the pinhead and the narrowest part of the pin, as shown in figure 4.11. No signs of detachment between the pinhead and the vacuum formed part was present, after visual inspection of the test pieces.



Figure 4.11: Point of failure on the transition between the pinhead and the narrowest part of the pin

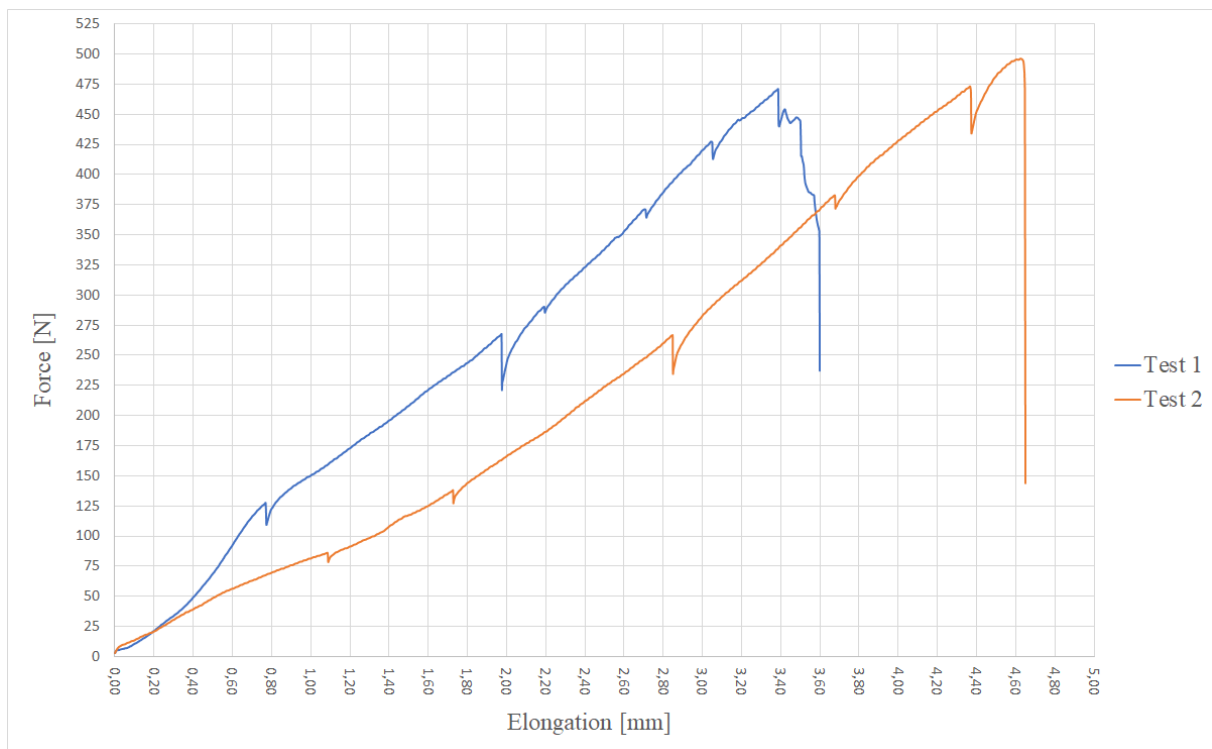


Figure 4.12: Graph of test results for the *test 1* and 2 pins.

Further testing was done to try to get information about the attachment between the vacuum formed sheets and the 3D-print, and not only the quality of the 3D-print. These tests were done with the *medium bolt* pins, and the details of the test setup is shown in table 4.8 as *test 3*. These test did however show similar results to the first test, where the prints broke instead of detachment, as can be seen in figure 4.13.

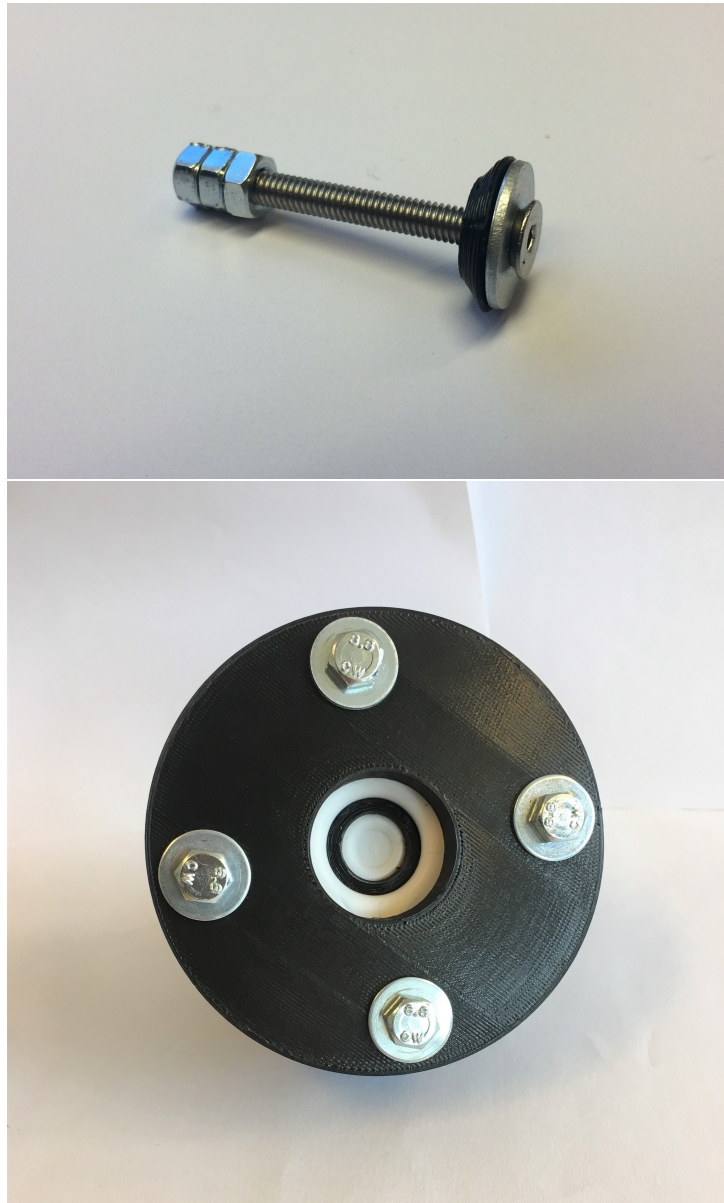


Figure 4.13: Point of failure on the transition between the skim and the pinhead

Another test was performed after changing the print orientation of the pin, which showed promising results. The pin in this test was printed sideways with support material as shown in figure 3.17. The details of this test are also shown in table 4.8 as *test 4*. This test showed that it was possible to pull the pins out from the attachment between the vacuum formed sheet without breaking the pins, as shown in figure 4.14. The results from this test are shown in table 4.10.

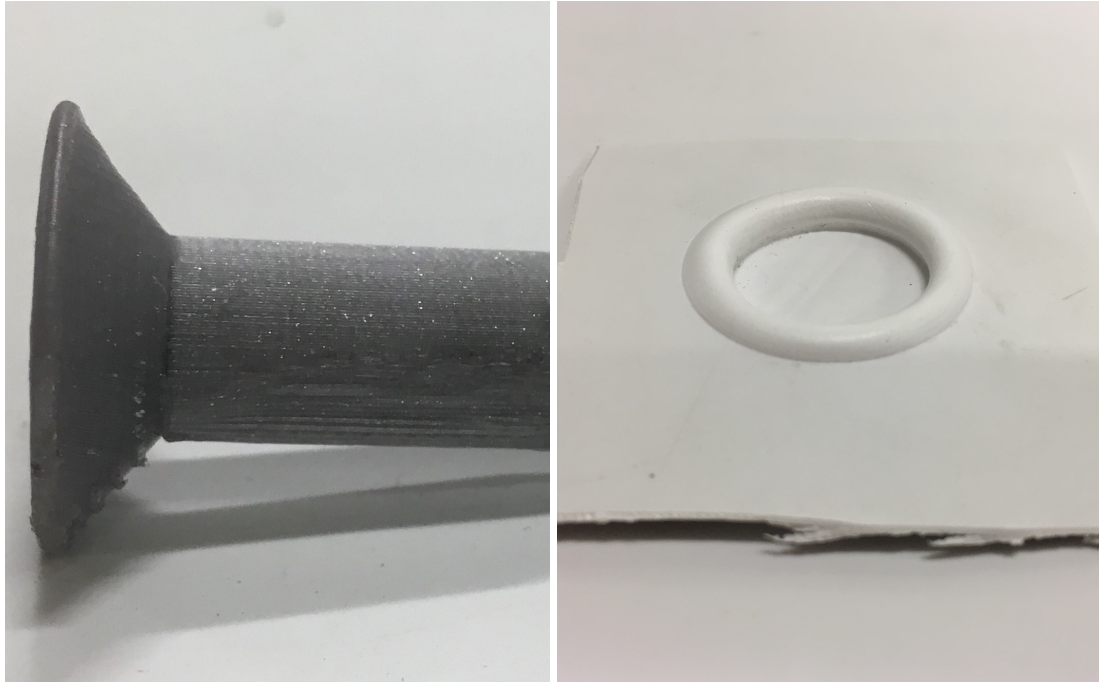


Figure 4.14: Pin and vacuum formed part after detachment. The deformed stem of the tap is caused by the grips on the test jig.

Several more tests were therefore performed on the sideways pins, which are described in table 4.8 as *test 5*, *test 6* and *test 7*. *Test 5* detached similar to *test 4* but at a lower max force, as can be seen in table 4.10. *Test 6* and *test 7* did detach as the previous two tests, but after inspection of the pins it was evident that pinheads were damaged, as shown in figure 4.15.

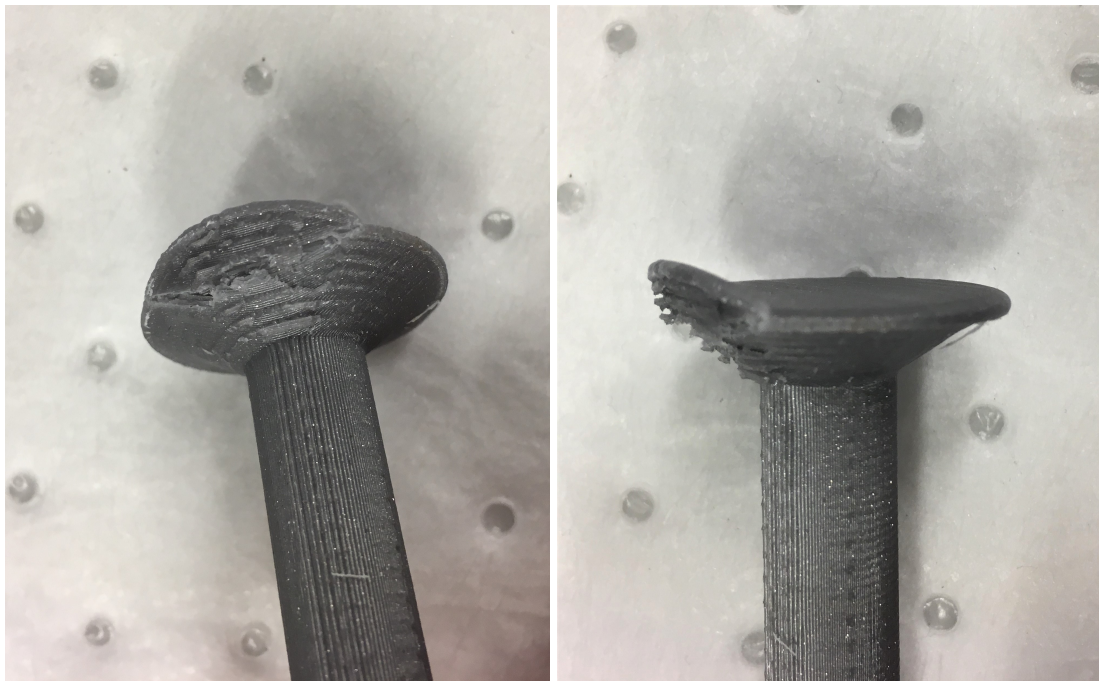


Figure 4.15: Image of the broken pinhead from *test 6*

The printing orientation was changed to upright position again, because of the problems with the sideways prints. Several more tests were performed. The details of these tests are shown in table 4.8 as *test 8* to *17*. *Test 8* to *10* was done to give an indication of how these pins performed. It was difficult to know if these tests gave a good representation of how the attachment performed. Another set of identical tests, *test 11* to *13*, were therefore performed. Both of these sets tests showed similar results, which are shown in figure 4.19. Further testing, *test 14* to *17*, was done to get a better understanding of the results. In these tests the pins were identical, but the top plate of the jig changed. The results of these tests showed that the top plate had a significant effect on the test results. This can be seen in the images of the broken pins, as shown in figure 4.16 and the test results shown in figure 4.20. Figure 4.20 shows the two broken pins as *test 14* and *15* and two pins detaching as *test 16* and *17*.

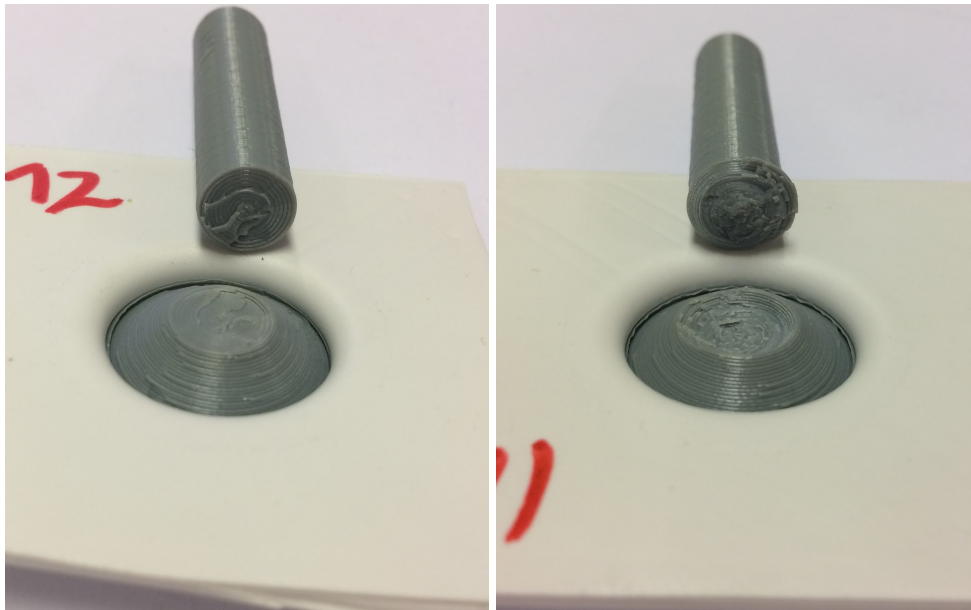


Figure 4.16: Image of broken pin from *test 14* and *test 15* (the numbers in the images are not relevant).

The last quantitative tests were done as *test 18* to *20*, shown in table 4.8. These tests were done on three different pins with top plates according to the size of the pins. In one single vacuum forming process a two identical sets of three different pin sizes were manufactured. The first set was tensile tested. The other set was sectioned into two parts to investigate how well the vacuum forming sheets formed around the pins. The results from the tests can be seen in figure 4.21 and 4.17 and table 4.9.

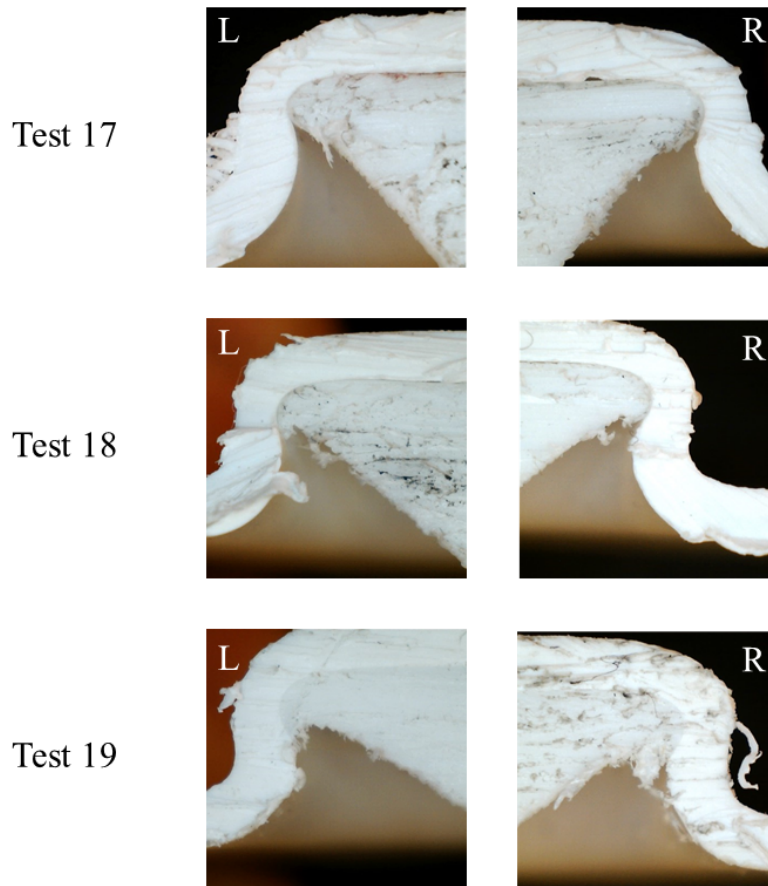


Figure 4.17: Image of the sections of *test 18* (top) *19* (middle) and *20* (bottom). The outer white shape is the vacuum formed sheet while the inner white rectangular shape is the pinhead.

Table 4.9: Results from the overhang measurements.

	X_s [mm]
Test 18 Left	0.242
Test 18 Right	0.333
Test 19 Left	0.165
Test 19 Right	0.526
Test 20 Left	0.583
Test 20 Right	0.563

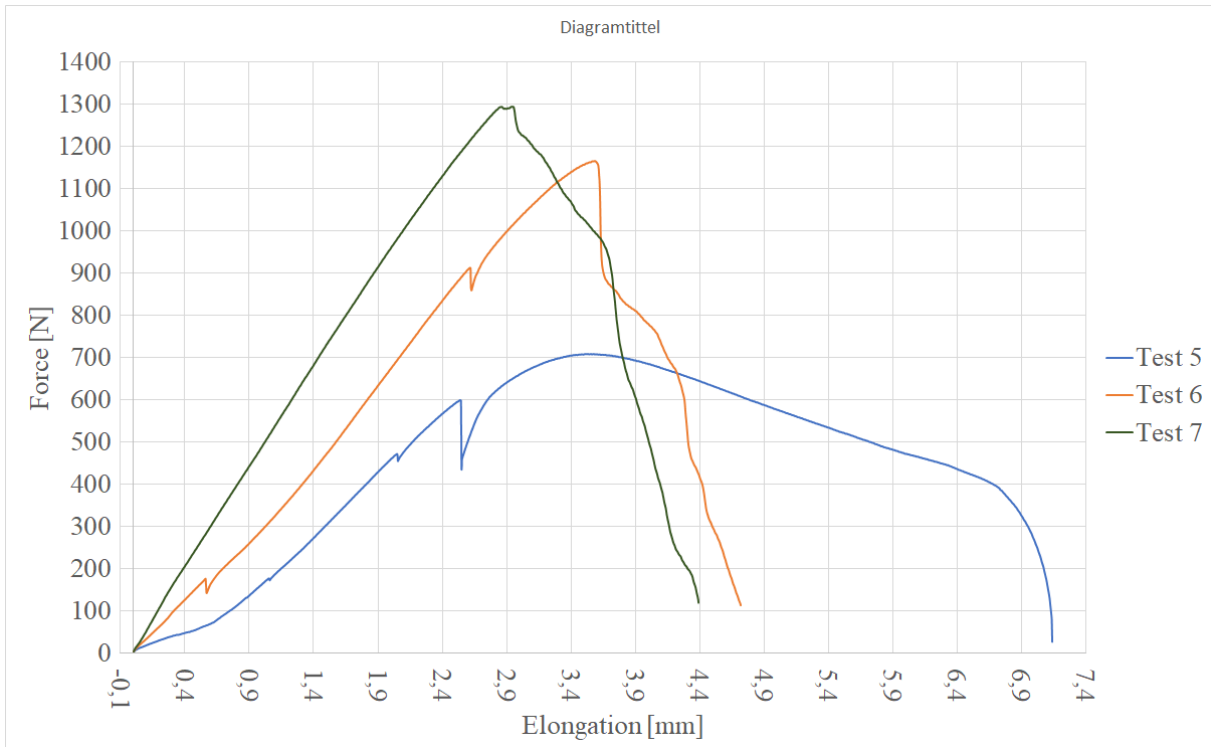


Figure 4.18: Graph of test results for the *test 5, 6 and 7* pins.

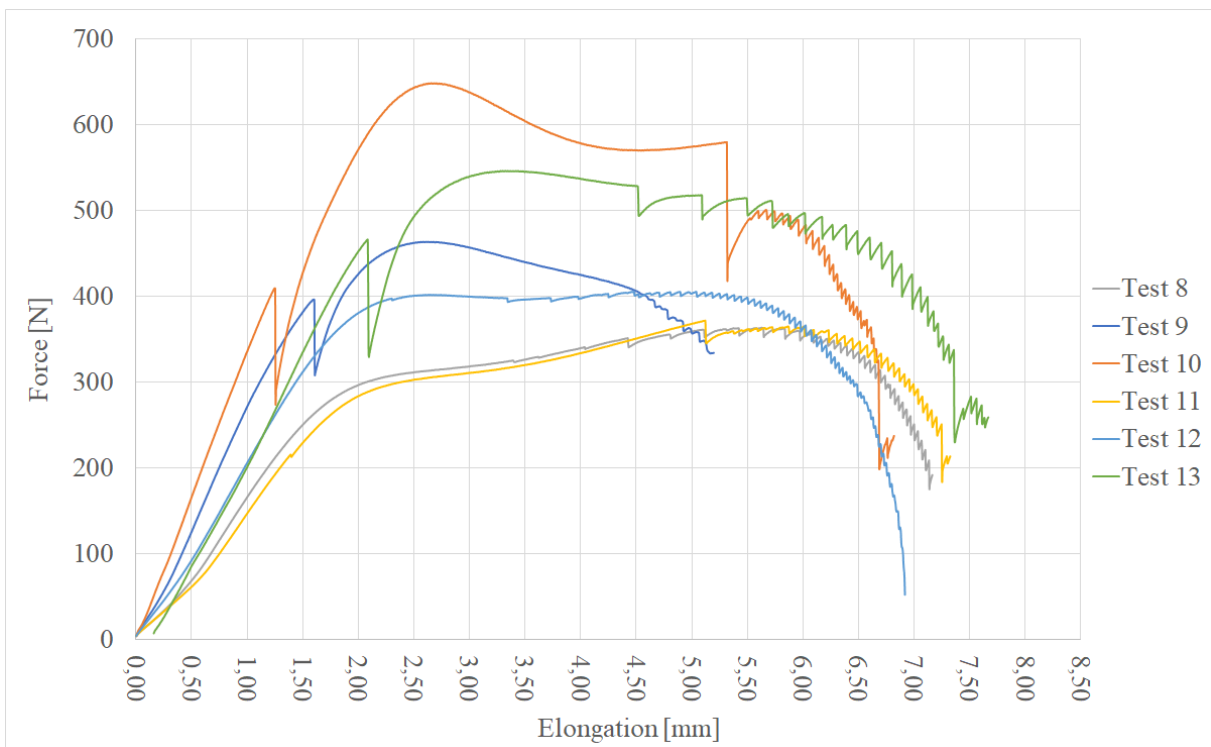


Figure 4.19: Graph of test results for the *test 8 to 13* pins.

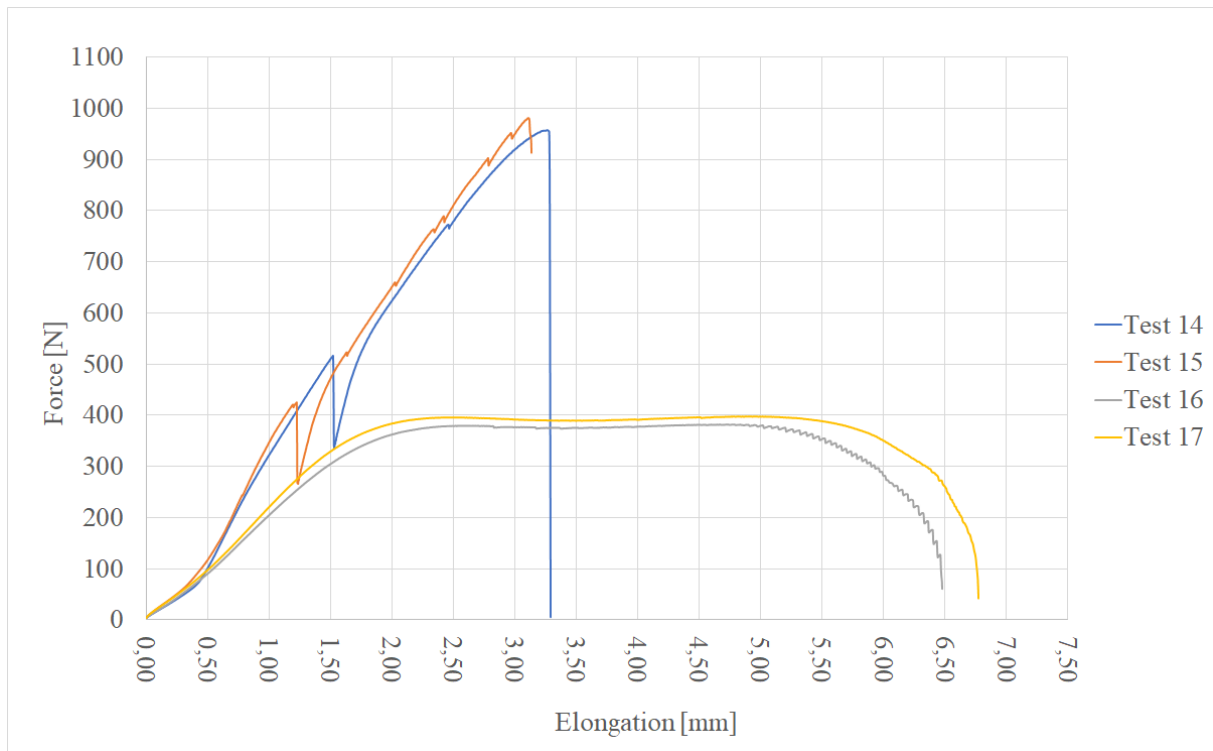


Figure 4.20: Graph of test results for the *test 14* to *17* pins.

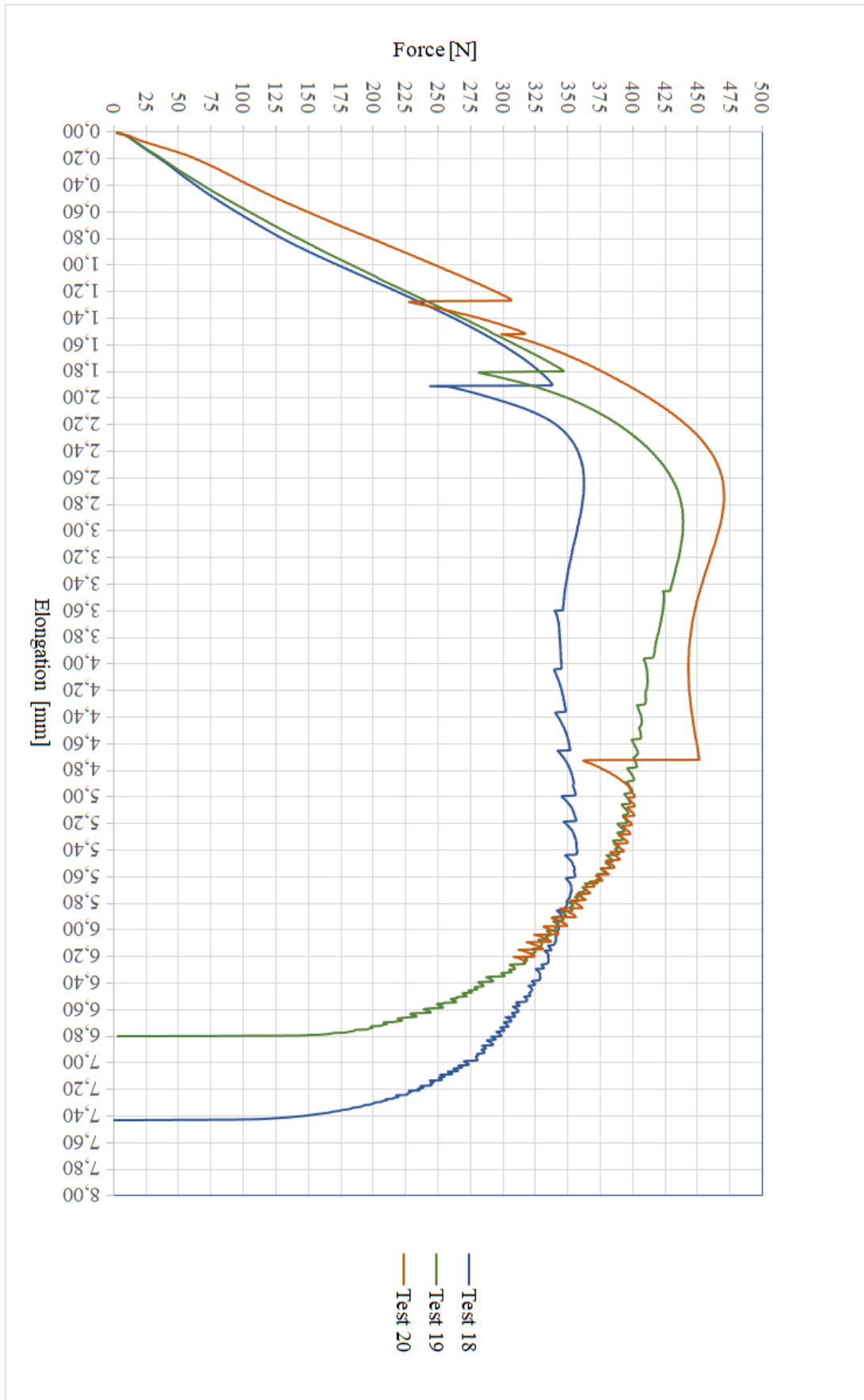


Figure 4.21: Graph of test results for the *test 18* to *20* pins.

Table 4.10: Results from the quantitative tests.

	Max force (<i>N</i>)	Elongation at max force (<i>mm</i>)
Test 1	471.42	3.38
Test 2	496.49	4.62
Test 4	1289.55	1.80
Test 5	707.80	3.53
Test 6	1164.44	3.58
Test 7	1293.25	2.94
Test 8	363.09	5.62
Test 9	463.27	2.63
Test 10	648.12	2.65
Test 11	371.55	5.12
Test 12	405.01	4.47
Test 13	545.78	3.34
Test 14	957.12	3.26
Test 15	980.40	3.11
Test 16	382.75	4.78
Test 17	397.68	4.92
Test 18	362.53	2.67
Test 19	439.21	2.93
Test 20	470.41	2.73

5 Discussion

5.1 Set-based approach

The set-based approach allowed for large sets of results at a rapid phase, while minimizing repetition of processes, something that might be more present in a point-based approach. The vent holes were developed using the set-based approach. This resulted in only one test necessary to decide on a vent hole design with sufficient qualities to be used for further testing. All pin designs were also tested using this method where sets, consisting of six similar designs with different properties, were tested simultaneously. The set-based approach did however require more time to prepare before testing. The molds were only produced in low quantities, with relatively large intervals compared to the pins. The manufacture of molds was therefore not affected as much by the possible disadvantages of the set-based approach. Because of the design of the 3D-printers, printing a set of six pins will take approximately six times longer than a single pin. Which was measured in actual printing time after preparation. This means that simple ideas, where one test might give the necessary information to make a decision, take longer time to test if a strictly set-based approach is used. Although most of the test were done by following a set-based approach, some of the tests deviated from this approach to allow for rapid testing of single ideas.

5.2 mold and vent hole design

The design of the mold and the vent holes were decided quite early in the process, with limited testing of different designs. The results of the tests with the initial mold design, similar in shape to figure 3.4, did not show any complications during vacuum forming. The mold shape was also able to create good attachments. The shape of the mold might vary largely in real world use. It would therefore be too time consuming to test many different mold shapes in this thesis, trying to simulate a real world use. The initial mold design was therefore chosen as a sufficient enough platform to use for further testing. Further investigation is however necessary to get

an extensive understanding of how the mold shape might affect the attachments. It's worth noting that some other mold designs were tested to facilitate different pin configurations. This is further discussed in section 5.5.1 and 5.5.2.

The vent holes were tested in set-based manner, with a set of four designs tested in one vacuum forming operation. The first test showed that the *large gap* design had good attachment, but only in one of the two holes tested. The *star shaped* design did only have one hole tested, but showed no apparent disadvantages. Further testing of the star shaped design showed that it was able to create repeatable and good attachment with the *straight slope* pin design. This was considered sufficient and the *star shaped* design was therefore chosen for further testing. The *large gap* design was not tested further, since one of the two pins did not attach. It is important to recognize that the vent hole design is an important factor of the process considering the varying results in the first test. The time available in this thesis did however not allow for further testing of the vent holes. Other designs can therefore not be excluded as a similar or better alternative to the *star shaped* design. Further investigation is needed to get a better understanding of how the vent hole design affects the attachment.

To test the different vent hole designs, a pin design and its parameters were chosen. The design tested was the straight slope pin design, as shown in figure 3.9. Testing the vent holes with the straight slope pin design showed good results, as mention above. This does however not give an indication of how other combinations of vent hole and pin designs would perform. Such information would require further testing, which was decided to be too time consuming given the time available for this thesis. It was therefore decided that it was sufficient to only test the straight slope pin design with the different vent hole designs to fulfill the objectives in this thesis.

The placement of the pins in the mold was also a parameter tested in the first test. One of the two pins tested with the *large gap* design did not create proper attachment, which might have been caused by the difference in placement. Later tests, with the *star shaped* design, did however not show this effect. It was therefore decided that the effect of the placement of the pins was relatively small compared to other factors. Further investigation is however needed to give a proper understanding of how the placement of the pins on the mold might affect the results.

5.3 FDM

The FDM process had a lot of impact on the test results in this thesis and include many factors that are considered important the process. These factors include the FDM process and material, which are further discussed in this section.

5.3.1 Process

As opposed to the vacuum forming process, the FDM process has a lot of parameters that can be manipulated while still having the accuracy of a automated process. A large portion of the

work in this thesis was done trying to find the best parameters to use for printing the pins and molds. The first issue encountered was the deformation of the molds during the first vacuum forming tests. This was solved by adding more top layers to the mold. With more top layers, the top of the mold became more rigid making it harder for the vacuum forces to deform the mold. The added top layers also possibly allowed the top of the mold to absorb more heat before it reached temperatures close or above T_g , as further discussed in section 2.4.3 and 5.3.2.

The second issue observed concerned the strength of the pins. *Test 1* and *Test 2* showed that the pins were weaker than the attachment, resulting in a test of the quality of the 3D print instead of the attachments. This could also have been caused by the dimensions of the jig, as discussed section 5.6.1. A stronger pin proved to be necessary anyway, and different parameters were modified trying to get a better result. In *test 3* a bolt with a washer was used, as seen in figure 3.11. The part of the pinhead that was in contact with the vacuum formed part was still printed. This made sure that the effects of vacuum forming PLA was still present. The design did however not strengthen the pin enough to be stronger than the attachment, which was probably caused by the washer concentrating all the stress on the transition between the washer and the print. This is further substantiated by the point of failure, shown in figure 4.13.

The two first tests were printed in upright position, as described in section 3.6. This did not seem to be strong enough for testing the attachment. It was therefore decided to print the pins sideways, as shown in figure 3.17. This was done because a print is significantly stronger along the layer than across [33], as discussed in section 2.4.3. Printing the pins sideways did however create some complications. The geometry of the pins required support structures to be printed in this orientation. Automatically generating support structures in the Slic3r PE software resulted in non-circular pinheads, similar to what is shown in figure 5.1. The non-circular pinheads was still present after adjusting the available parameters to optimize the results. Support structures were therefore drawn manually in the CAD software, which resulted in more circular pinheads. The process was however time consuming and highly dependant on a printer that was well calibrated, which complicated the process. Some of the pins printed sideways also broke at the edge of the pinhead, as shown in figure 4.15. This happened both when separating the pin from the support material and during testing of pins. The point of fracture, for all the pins, was at the supported side of the head, meaning the part of the head that was closest to the printer bed. This was probably a result of errors in the print caused by printing the support material. Another possible cause is increased stress, introduced when removing the support material.

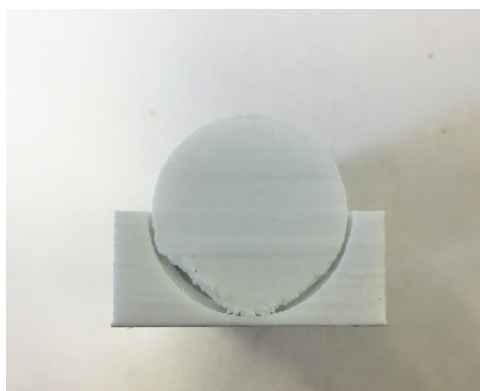


Figure 5.1: Picture of non-circular pinheads printed sideways.

The first upright pins were printed with the standard settings for the slicer software, only adjusting layer height and infill percentage. There are however a lot of other parameters that can be adjusted. One of these parameters are counter number or external perimeters. Increasing the number of external perimeters will possibly make a stronger part [39], as discussed in section 2.4.3. This will however increase the printing time as well. It was therefore decided to try printing the pins in upright position. This was done with a large enough number of external parameters so that the transition between the pinhead and the narrowest part of the pin was only constructed using external perimeters. Fracture happened at this part of the pin in the previous tests, as shown in *test 1* and *2*. This created a much stronger part, which can be seen by comparing *test 1* and *2* with *test 14* and *15* in table 4.10. It was later discovered that the pins probably did not have to be as strong as first assumed, which is further discussed in section 5.6.1. The printing time of the stronger upright pins was however relatively short, and shorter than the sideways printed pins. The increased strength of these pins would also limit uncertainties caused by the print in the tensile tests. It was therefore decided to use these pins for the final tests, *test 18* to *20*, that would be used for comparison between pin sizes.

5.3.2 Material

Using an entry level FDM 3D-printer, with PLA filament, resulted in some complications. PLA has a glass transition temperature of 45-60°C [20], which means that the 3D-printed parts will be weakened and start to more easily deform at these temperatures [27]. The vacuum formed sheets of HIPS needed to be heated to around 150°C [23] before vacuum forming. The 3D-printed molds would therefore come in contact with the vacuum formed sheet at this temperature, increasing the temperature of the surface of the 3D-printed parts above 45-60°C. This, in combination with the forces on the pins caused by the vacuum, possibly resulted in parts of the 3D printing molds and pins being deformed after vacuum forming.

The pins with the convex shape were the ones that showed the most deformation. This was probably a result of the thin section at the edges of the heads, shown in figure 5.2. The flat head designs showed the least amount of deformation, which probably is a result of the thicker section t of the head, as shown in figure 3.9. The straight slope design showed some deformation, especially with small angles a . Visual inspection indicated that deformation was present on all the straight slope designed pins. The effect of the deformation did however not prevent the pins from creating good attachments. The results shown in figure 4.17 indicate that deformation of the pinheads might even increase the quality of the attachments to a certain degree. Looking at figure 4.17 it is evident that *test 20* exhibits larger deformation of the pinhead compared to the other test. *Test 20* was also the pin showing the best results in the tensile tests. The deformation of the pinhead might allow the vacuum formed sheet to form more closely to the pinhead, since the deformation happens during the vacuum forming process. The less deformed pins might not allow for the same contact to the vacuum formed sheet. Deformation can however also be a factor that affects the attachments in a negative way, as shown in the curved pin tests described in table 4.2. It's important to note that the curved pins did show greater deformation than *test 20*, as can be seen comparing figure 4.5 and figure 4.17. The deformed shape of the curved pin is somewhat unrecognizable compared to the original shape shown in figure 3.9. This seem to indicate that deformation can help create good attachments if the general shape of the pinhead

is preserved after forming. The curved shape might also have deformed to the degree that it covered the vent hole. This might have resulted in poor venting and therefore poor attachment.

Further testing could be done on materials that does not exhibit deformation when vacuum formed. These results could be compared to the pins made from PLA to get a better understanding of how the deformation affects the results. The curved pinhead shapes might for example create better attachments if the deformation is negligible. This is because the convex shape might allow for greater undercuts with low protrusion, creating low profile attachment points. The effect of the size of the undercut will be further discussed in section 5.6. The comparison of materials is however beyond the scope of this thesis. PLA has, as discussed in section 2.4, many benefits compared to other common materials used in FDM. It was therefore a natural choice to use PLA as a basis for developing the process discussed in this thesis.



Figure 5.2: Picture of thin section of convex pinhead

5.4 Vacuum forming

5.4.1 Process

The vacuum forming process was done using a Formech 686 machine which has few automatic controls. This meant that most of the vacuum forming was done adjusting the available parameters manually. The only automatic function used was the application of vacuum right after the mold tool had been pushed as far as possible into the heated sheet. The sheet was first heated, and the temperature was then measured using a hand held infrared thermometer. This might have introduced some errors depending on the accuracy of the thermometer. It was also difficult to reach exactly 150°C and the vacuum forming process was continued if the temperature measurement was $150\pm 3^{\circ}\text{C}$. The mold was then pushed into the heated sheet and vacuum was applied. The Vacuum was applied until it looked like the sheet could not form any closer to the mold, which varied some for each vacuum forming operation. This might have contributed to some sheets being less closely formed to the mold than others. Larger deformations might also have occurred when the vacuum was applied for too long. Air from a fan was then applied to the outside of the mold before the vacuum was turned of. This air was used to cool down the part. The air was applied until the temperature of the part felt close to body temperature. This was just measured by touching the mold. After the air was turned of, the part and the mold tool were removed from the machine. Then the part was separated from the mold tool. Separating

the part from the mold tool before the part was cooled below the glass transition temperature (T_g) for HIPS, might have resulted in a more largely deformed part compared to a part that was cooled to room temperature [23] [27]. This could in turn affect the test results.

The vacuum forming process used in this thesis is therefore rather unpredictable, although the machine used is of professional quality. It is assumed that the vacuum forming process is one of the largest causes of unpredictability in the tests performed in this thesis. It was therefore decided that several tests of each parameter, beyond tests to confirm unexpected results, was too time consuming and would require a more controllable vacuum forming process. The vacuum forming process is, because of this, considered a possible important factor impacting the product development process developed in this thesis. Further investigation is necessary to get an extensive understanding of its impact on the results.

5.4.2 Material

The material tested for the vacuum forming process was only 2mm thick HIPS sheets. Although good results were achievable with the HIPS sheets, it is not necessary transferable to other materials or sheet thicknesses. HIPS is one of the most commonly used materials for vacuum forming and was a natural choice for indicative testing to see if the process would work or not [23]. The time available for this thesis did not allow for testing of different sheet thicknesses and materials. Further investigation into this subject is therefore necessary to give an extensive understanding of how this affects the attachments.

5.5 Qualitative tests

Qualitative tests were done in the initial phases of this thesis to give a general overview of the process. More scientific testing, like tensile testing, usually requires more resources and may therefore limit rapid prototyping in the early stages of the process development process. All qualitative tests are subject to subjective bias, which should be taken into account when assessing the test result. To limit the subjective bias a rating system was developed, see table 3.12, where a set of three ratings are described. The ratings are subjective in the difference in the strength of the tester, and the interpretation of how secure an attachment seems. It can however be considered a tool for comparison, since the tester is the same for each test, which somewhat limits the variation in tests. All qualitative tests were done by visual inspection, touching, pulling and bending on the test pieces.

The results of the first qualitative tests showed that the straight angle designs gave the best results, and proved that the process worked. This was also the design used for further testing. It was however evident that the design of the pins had a great impact on the results. This makes the pin design one of the important factors impacting the process. It is important to note that each tap design was tested by its own, which means that the error in the vacuum forming process might have influenced the results, as discussed in section 5.4. There was also only a limited, but similar, amount of dimensions tested for each pin design, as can be seen in table 3.3. This

does not exclude the possibility of the other parameters or designs yielding better result than the design chosen for further testing. Other factors like the material chosen was also a significant factor, as further discussed in section 5.3.2. The objective of this thesis was however not to find the absolute best pin design, and the straight angle design was assumed to be sufficient for further development of the process.

Further testing of the straight angle pins showed that certain dimensions yielded the best attachment results, while minimizing protrusion, shown as *Medium pin* in table 3.4. These dimensions were used as a starting point for the subsequent qualitative and the quantitative tests.

5.5.1 Angled tests

One perimeter that was not tested in the initial tests was the angle of the placement of the pin in relation to the horizontal plane of the vacuum forming machine, as seen in figure 3.6. Real world use of the process would probably involve some kind of angled attachments. Tests on angled attachments was therefore performed. These tests showed that the pins performed well on angles closest to 90° to the horizontal plane, as can be seen in table 4.4. 0° performed quite bad which would probably limit the use of the process in a significant way for real world use. Products like suitcases, where attachment are necessary to facilitate hinges between the two parts of the suitcase, could be difficult to make. These products would probably require additional operations to get the wanted attachment points. -20° performed similarly to 0° and would not create sufficient attachment if used. This shows that the angle of the attachment is an important factor impacting the process.

The issues with the tests at 0° and -20° may have been caused by the lack of venting because of the position of the vent holes in the mold, as shown in figure 5.3. The printed quality of the 0° and -20° vent holes were also of lesser quality than the other vent holes, as shown in figure 5.4. The degradation in quality did however not seem to be significant enough to limit venting. This was based visual inspection of the vent holes. It is however important to note that negative angles are difficult to produce when vacuum forming, as this would create undercuts which complicates the process of removing the mold from the vacuum formed part [23].

The investigation into the effect of angled pins is not sufficient to give an extensive overview of how the perimeter affects the attachments. Only one test with one pin type was performed, which does not eliminate errors in the vacuum forming process, as discussed in section 5.4. Different pin designs and parameters might also yield better results. Further investigation is therefore necessary before the use of 0° or negative angles are disregarded for real world use.



Figure 5.3: Picture of the placement of vent holes on the inside of the angled mold. Notice that all the vent holes, except 0° and -20° , are pointed downwards (or out if the image) when the mold is placed right side up.

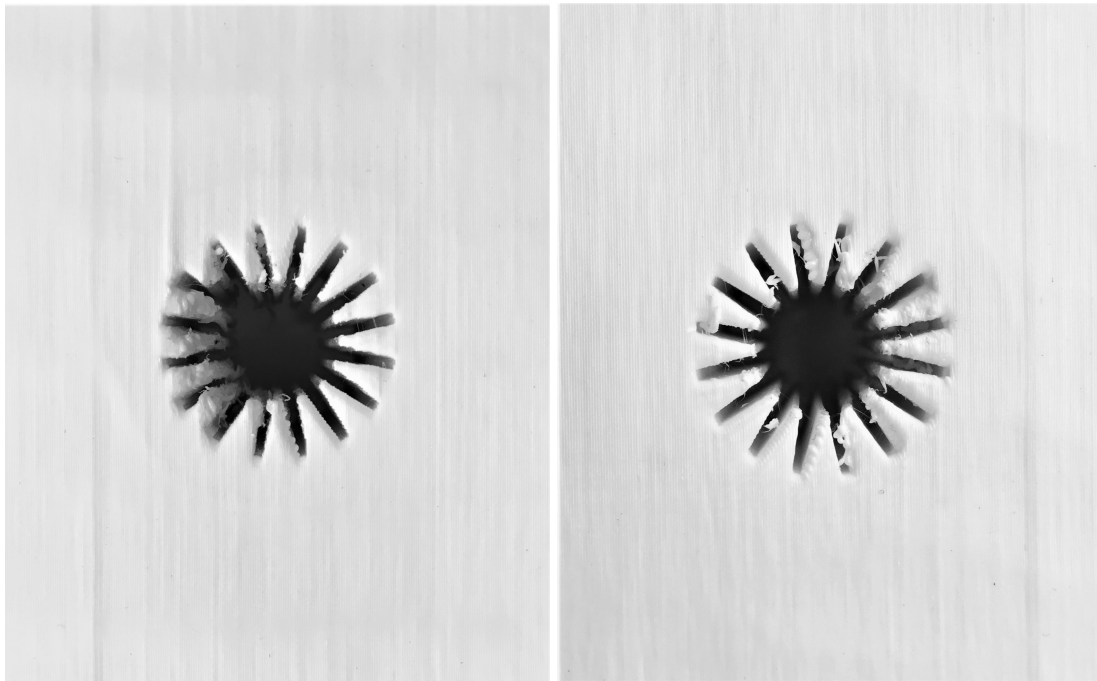


Figure 5.4: Picture of the lesser quality of the 0° (left) and -20° (right) vent holes. Notice the poor quality of the left side of the 0° vent hole.

5.5.2 Sunken tests

Another factor that might affect the real world use of this process is the protrusion of the attachment on the vacuum formed surfaces. Tests of molds where the pins could sit flush with the mold surface was performed, trying to minimize protrusion. Two similar tests were performed. The first test showed large uneven shapes, like air-bubbles, on the inside of the molds, as shown in figure 4.8. This had not been experienced in previous tests. These large uneven shapes resulted in very thin sections of the vacuum formed sheet around the pins, as shown in figure 5.5. These thin areas led to a less secure attachment, with more play than attachment without these large uneven shapes. The rating of 2 was therefore given to some of the attachments, even though it was not possible to pull the pins out by human force.

The second test was performed to understand if the shapes were caused by the variation in the vacuum forming process, as discussed in section 5.4. Similar results were shown in both tests. This led to the conclusion that the large shapes were caused by the shape of the mold inserts. This is also shown in the lack of large uneven shapes in *sunk test 7* and *8* in figure 4.8, which have the smallest D_s parameter, described in figure 3.7. The parameter h_s might also have an effect, since the shapes extend far below the height h of the pinhead, as shown in figure 5.6. A smaller h_s would therefore probably limit the the space the vacuum formed sheet has to move in. This might stop the large uneven shapes from forming. Further testing is therefore necessary to give a extensive understanding of these attachments.

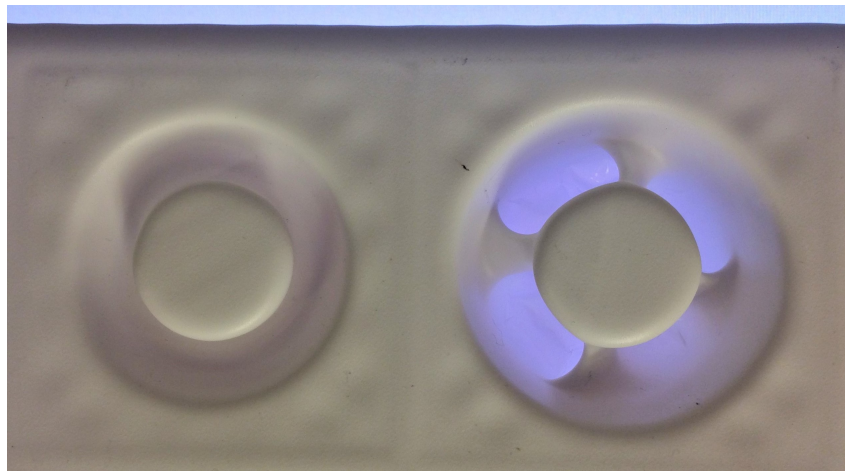


Figure 5.5: Images of the thin sections of the sunken tests. Notice how much more light is let through from *sunk test 3* compared to *sunk test 2*.

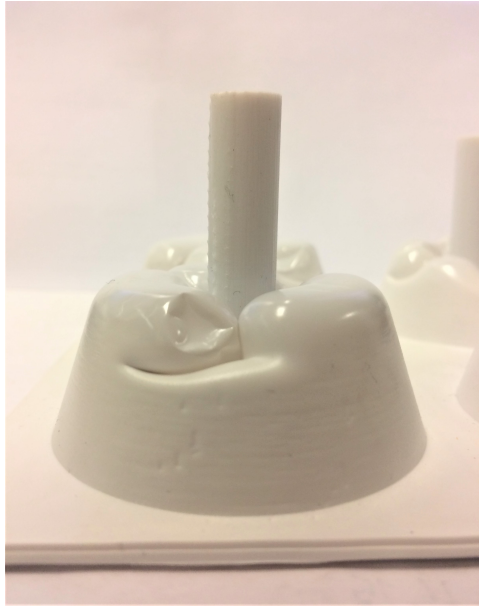


Figure 5.6: Image of large uneven shapes, similar to air bubbles.

5.5.3 Ribs

The ribs tested in this thesis are based on the *straight slope* pin design, as shown in figure 3.9. From this, it is reasonable to assume that the ribs would perform similar to the *straight slope* pins. The qualitative tests indicate that the ribs did create good attachments, similar to the results observed from the pin tests. As a proof-of-concept test it was therefore decided not necessary to perform more tests on the ribs. Further testing on the attachment and different rib designs is necessary to get a better understanding of how good the rib attachments perform. The design of the ribs and the mold might also be changed to incorporate sunken attachments. This was however not investigated in this thesis because of the limited time available.

As shown in figure 4.9, the ribs create a substantial increase in structural integrity compared to parts made without ribs. This is however at the expense of the ribs protruding on the outside of the mold and less room on the inside of the mold, as seen in figure 4.10 and 5.7. As discussed, protrusion on the outside can probably be solved with using the sunken attachment method. This will further decrease room on the inside, as can be seen in figure 5.6. Since the ribs extend on the inside of the part with the parameter h_r , as shown in figure 3.12, minimizing this parameter will increase the room inside the mold. This can however decrease the structural integrity of the part.

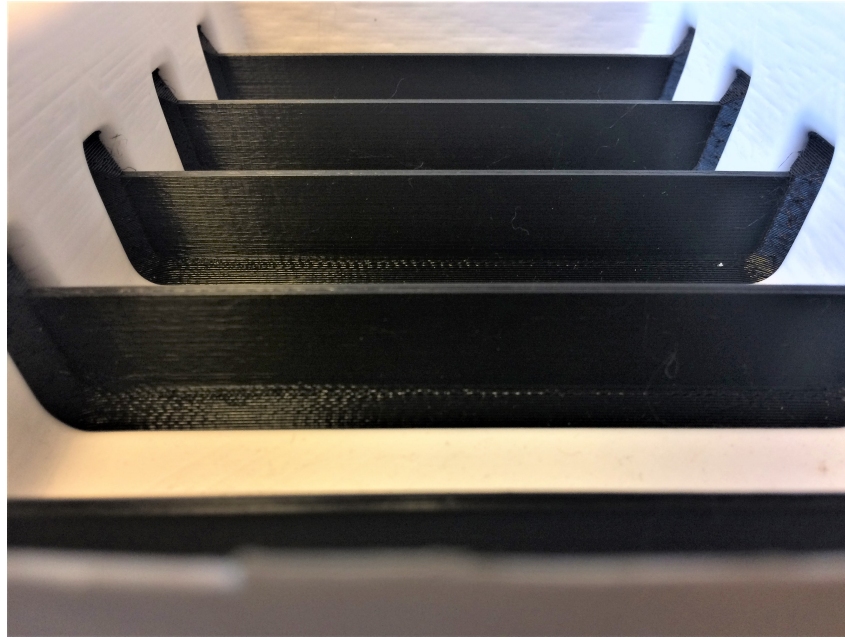


Figure 5.7: Image of the inside of the vacuum formed ribs.

5.6 Quantitative tests

Further testing, to give a better understanding of how well the selected design would perform, was done by tensile testing. The test jigs and specimens used in the tensile tests does not follow any standards for tensile tests. The manufacturing standard of the jigs are also not of a quality that ensure proper tolerances required for repeatable tests if a new and similar jig was manufactured. These tests are therefore only used for comparison between different attachments tested on the same jig. The figures obtained from these tests can therefore not be used for calculating how strong the attachments actually are, and can only be used as an indication and for comparing the test results in this thesis.

5.6.1 Jig setup

Trying to attach the vacuum formed part in the jig, while not affecting the attachment between the pin and the vacuum formed part as well as securing the vacuum formed part well enough so that it would not slip in the jig under testing, was a complicated task. The possible slippage of the vacuum formed part, in the jig, might have contributed to causing some errors in the tests.

The first jig manufactured was made of metal and are shown in figure 3.13. This jig was hard to control, with stiff parts creating little or no contact and friction against the vacuum formed sheet. The placement of the bolts, attaching the two parts of the jig and clamping the vacuum sheets, also created an uneven attachment of the test pieces. This could have led to errors in the tests. The jig was also hard to modify to allow for different pin-sizes and designs. This resulted in a new design which solved most of these problems.

Tests were later done to see if a 3D-printed jig would stand up to the forces in the tensile test, which it did. This jig is shown in figure 3.14. It is difficult to say how much stronger the 3D-printed jig is compared to the 3D-printed pins and vacuum formed attachments. The tests, where the 3D-printed jig was used, did however show that the jig could withstand up to almost 1.3KN as shown in *test 7* in table 4.10. After this test there was no apparent signs of damage or issues with the jig. The new 3D-printed jig also used 3D-printed top plates. These top plates were somewhat flexible, see figure 5.8, allowing for possibly better clamping of the vacuum formed sheets.

The first tests were done with one top plate, the *small top plate*, as shown in table 3.6. It was later discovered that the top plate has a large impact on the test results, as can be seen in *test 13* to *16* in section 4.3. It may seem from these tests that the top plate of the jig acts as a barrier, stopping the test piece from detaching if the hole, D_{top} , is not large enough. This is probably caused by the vacuum formed part of the attachment deforming in a way that needs extra space around the pinhead, which can be seen in figure 4.14. This may also have been the cause of the pins in *test 1, 2, 14* and *15* breaking instead of detaching. It was therefore decided that the difference between the diameter, D_{top} , of the top plate hole and the diameter, D , of the pinhead had to be constant to get comparable results between different pin sizes. This difference also had to be large enough so that the pins would not break instead of detaching. Only the last three tests, *test 18* to *20*, used specific top plates for each pin size. This makes these test results the only results that can be used for comparison of the different pin sizes.

The tests performed in this thesis are assumed to test the greatest loads the attachments designed are capable of withstanding. This is because the top plate of the jig concentrates most of the force around the attachments. This can be seen in the tests where small top plates and medium or large pins are used. These tests either break or exhibit the largest forces. A larger difference in top plate diameters, D_{top} , to pin head diameters, D , are therefore assumed to show results with lower forces. An attachment on a real world prototype or product would probably only have the rigidity of the vacuum formed sheet preventing it from moving if load is applied. The vacuum formed sheets are significantly more flexible than the top plates of the jig. This makes it reasonable to assume that an attachment would withstand lower loads in real world use compared to the tests performed in this thesis.

Most of the tests show sudden drops in force before reaching max force, as can be seen in the graphs in section 5.6. These drops in force might be caused by the vacuum formed sheet slipping in the jig. It is unlikely that the lack of strength in the 3D-printed jig is the cause of the drops in force. This is because both the metal jig and the 3D-printed jig shows similar types of drop in force.

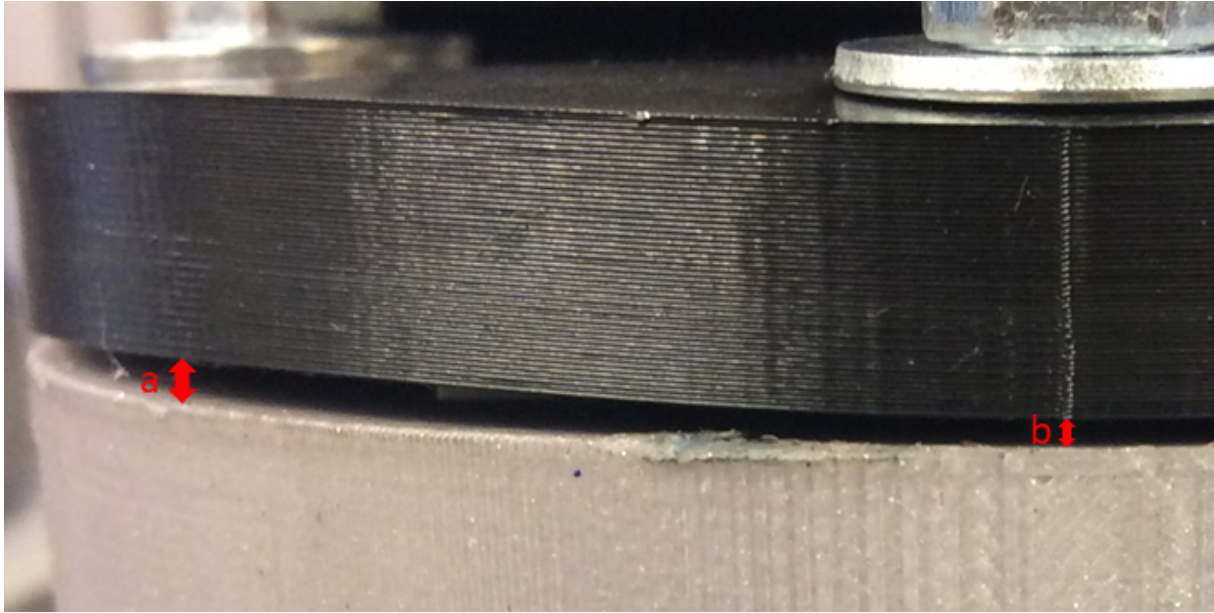


Figure 5.8: Image of the flexible top plate of the 3D-printed jig. Notice the difference in the gap between *a* and *b*.

5.6.2 Test setup and settings

The details of the test setup are described in section 3.8. The grips used for the tests were standard grips supplied with the tensile test machine. The bottom part of the jig was attached with a bolt going through the 3D printed jig, as shown in figure 3.21. This removes the possibility of this end of the jig slipping because of poor attachment or friction. This part of the jig could be subject to deformation. Considering the grater dimensions of the jig compared to the attachments this is rather unlikely. No signs of deformations was present after visual inspection, as seen in figure 5.9. The top part of the test setup could however be subject to slippage and deformation caused by poor attachment. The grips used for attaching the pins to the machine, as shown in figure 3.8, where mechanically gripping the pins with a jagged surface, as shown in figure 5.10. Each pin was made sure to be properly attached, confirming the attachment by pushing on the lever actuating the grips. The attachment of the pins could however be one of the factors causing the sudden drops in force showed in almost all test graphs in section 5.6.

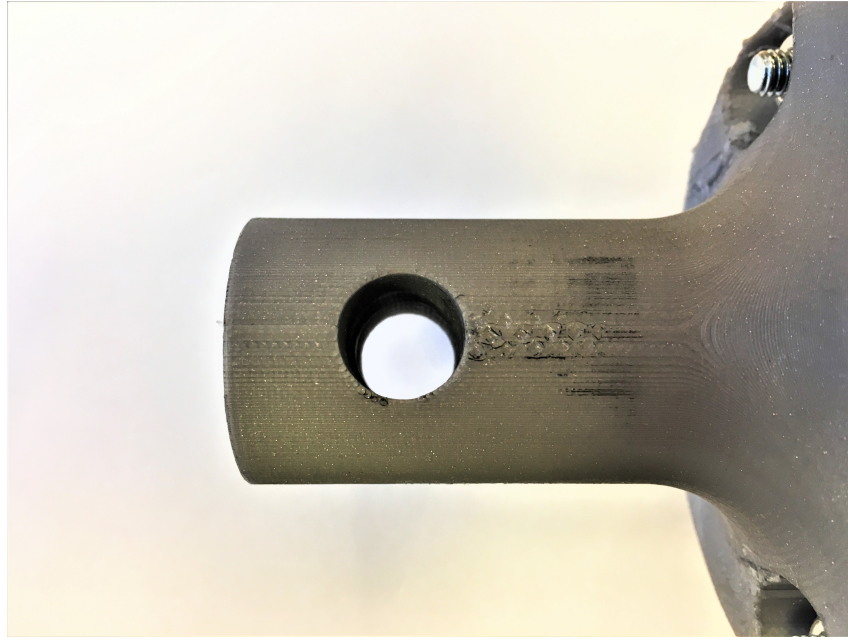


Figure 5.9: Image of the part of the 3D print jig attached to the bottom part of the jig. Notice the lack of deformation at the hole where the bolt attaching the jig to the machine was attached.

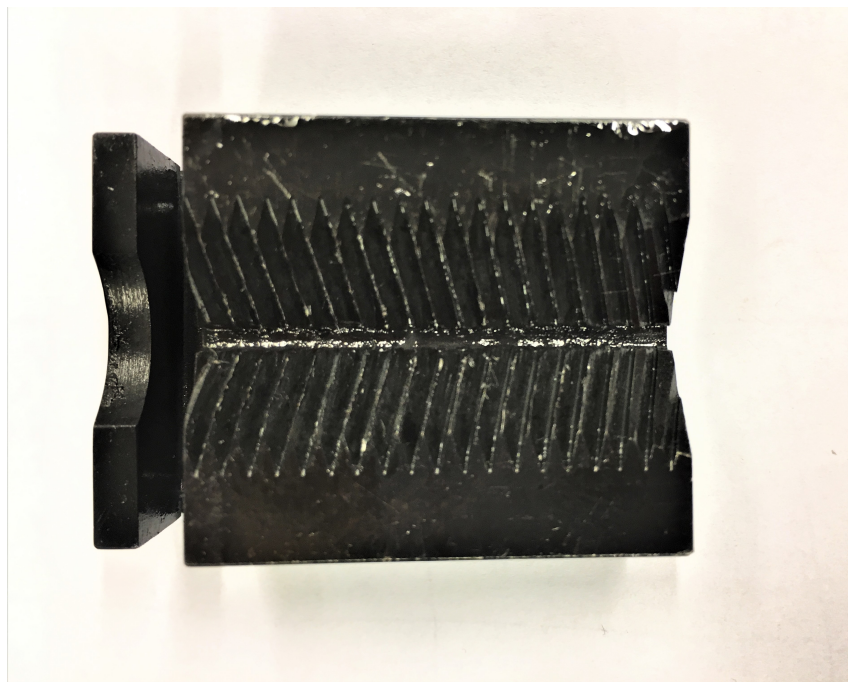


Figure 5.10: Image of one of the sides of the grip used to grip the pins in the test machine.

The settings used for the tests were used to simulate a relative rapid pull out of the pins from the attachments. The tests are only used for comparison in between themselves and no standards were used. It was therefore decided that the test speed used was sufficient as long as identical test speed was used for all the test. The test speed chosen at 10 mm/min was also relatively rapid compared to the tensile testing standards for polymers, ASTM D638 [5], which suggests

a test speed of 5 mm/min. Looking at the ASTM D638 standard there are however suggested test speeds ranging from 1 mm/min to 500 mm/min depending on the specimen dimensions, the material type and the test conditions. This means that the test speed chosen for the tests in this thesis are in the range of recommended tests. The tests performed in this thesis are also not tests of the tensile properties of the attachments, but rather a test used for comparison between attachments. This makes it difficult to find a standard to follow, especially considering the geometry of the test specimens.

5.6.3 Results

The only quantitative tests that can be used for comparison between dimensions of pin heads are, as mentioned, *test 18* to *20*. The other tests were used to drive the research in this thesis forward and to allow for test results with as few uncertainties as possible given the time available. The qualitative testing revealed that it was important to have a pinhead diameter, D , similar or larger than the vent hole diameter, as shown in figure 4.4. It was however not investigated how the relationship between the vent hole diameter and the pinhead diameter affects the attachment quality beyond this. This relationship might however be an important factor to the process. All the quantitative tests pieces were made with 15mm vent hole diameter, not changing the vent holes in relation to the pinhead diameter. This is probably one of the most relevant uncertainties in the quantitative tests, and should be taken into account when assessing the results. A smaller vent hole diameter, still allowing for good airflow, might create a larger X_s , as shown in figure 3.23. This can probably be one of the factors that made *test 20* exhibit larger overhang, X_s , than the other tests, since this was the pin with the largest diameter, D , tested. There are however other factors that may have contributed to the results shown in *test 18* to *20*, as discussed in section 5.3.2.

Sudden drops in force before reaching max force can be observed in a large amount of the test graphs. These graphs are shown in section 5.6. The drops in force might be caused by the vacuum formed sheet slipping in the jig, as discussed in section 5.6.1. The drops in force could possibly also be caused by small fractures in the pins. However, no signs of fracture was present after visually inspecting the pins from *test 18* to *20*. The section of the pins in figure 4.17 does however exhibit large deformations at the outer edges of the pinheads. This is especially visible in *test 20* if the shape of the pinhead is compared to the CAD drawing in figure 3.23. It is possible that the deformation may have created weaker parts of the pins in the transition between the pin and the vacuum formed sheet. These weaker parts may be the cause of the drops in force when force is applied and these parts of the pinhead break.

Test 5, *10* and *13* show that the attachments created in this thesis are capable of withstanding forces up to around 700N, as shown in 4.10. *Test 4* showed that the attachment were able to withstand close to 1300N. It was however difficult to repeat the test results shown for *test 4*. The results of *test 4* are therefore considered not representative of the quality of the attachments. The other tests that show greater max force than *test 5*, *10* and *13* are tests where the pin broke. This is not considered tests of the whole attachment and will therefore not be representative of the quality of the attachments. It is important to note that the results discussed in this section are highly dependant on the top plate used for testing, as discussed in section 5.6.1.

Test 18 to 20 did show that the larger the diameter, D , of the pinhead, the better attachment. One of the factors observed is that a large the diameter, D , creates a larger overhang, which means a larger value of X_s . It is therefore reasonable to assume that the overhang, X_s , is one of the main factors impacting the process and should be maximized if good attachments are necessary. The value of X_s is however also highly dependant on other important factors like the material used for the pins and vent hole and pin design. These factors are further discussed earlier in the discussion section.

The measured values of the X_s , shown in table 4.9 generally show consistent results with the statement above. *Test 19 Left* does however diverge from the other results having a significantly lower X_s than all the other measurements. This is probably caused by some error, which is further substantiated by comparing the measurements of X_s for the left side to the right side of *test 19*. The right side of *test 19* follow the trend observed from the other test, with increasing X_s as the diameter, D , gets larger. Comparing the measured X_s of left and right side for *test 18* and *20* also shows that the similarity of measured X_s within each test is significantly larger than what is shown in *test 19*. Some possible errors causing the results shown in *test 19* might be errors in the FDM or vacuum forming process. It is however reasonable to assume that the error in measurement was introduced when splitting the test pieces and measuring the value of X_s . This is because it was difficult to find a repeatable way of splitting and measuring the test pieces without making a specialized jig for each of the operations, eliminating all possible errors. The other results of *test 18 to 20* does however seem reasonable although more tests are required to get a complete understanding of the process.

6 Use and Proposed guidelines

The tests performed in this thesis were used to see if the prototyping process developed could work. As the tests showed good results, it is possible that the process can be used in the development and production of products. This thesis has only focused on testing the attachment between the vacuum formed sheets and the 3D printed parts. Further investigation and development of the actual use of the concept is therefore necessary. The intended use of this process are primarily in prototypes and products where there is a need for large surfaces combined with rigid structures like ribs or connection points. This is something that might be difficult to achieve with the use of only 3D printing or vacuum forming. Examples of this is particularly present in injection moulded products, which is relatively costly production method [23]. Some examples of this are show in in figure 6.1.



Figure 6.1: Images of injection molded car bumper (left) [19] and Tool Storage Box (right) [14].

6.1 Guidelines

Some design guidelines for producing 3D print and vacuum forming hybrids were developed to allow for easier application to prototypes, products and further development of the process. These guidelines are based on the results given from the tests performed in this thesis. Further investigation into the topic is needed to get a complete set of guidelines. These guidelines are therefore only intended to be used as starting points for further testing and development. It is also important to consider the limited testing of materials in this thesis, which might impact the results significantly. The guidelines developed are:

- Ensure even distribution of venting by minimizing airflow obstruction close to the 3D printed part that should be encapsulated by the vacuum formed sheet.
- Large undercuts of the 3D printed parts are preferable.
- The 3D printed parts should completely cover vent holes when observed from straight above the vent holes to ensure good encapsulation by the vacuum formed sheet.
- Greater heights from surface of mold to the top of the undercut generates better encapsulation of the 3D printed part, but can lower the shear strength of the attachment.
- Avoid low angles of attachment orientation. Attachments below 30° to the horizontal plane are possible but attachments between 30° and 90° are recommended.
- The elimination of protrusion on the opposite side of the 3D printed part of the vacuum formed sheet is possible. It is however important to ensure good venting and space around the 3D printed part to allow for good encapsulation by the vacuum formed sheet.
- Controlled deformation of the 3D printed parts can ensure better attachment by allowing the vacuum formed sheet to form more closely around the part. This can for example be achieved with thin sections of the 3D printed part, made to intentionally deform.

7 Conclusion and further work

This thesis has investigated the possibilities of expanding the use of the tools, 3D printing and vacuum forming, by combining them into 3D print and vacuum forming hybrids. A set-based, process development approach was used to give a good overview of the possibilities in a short span of time. The findings in this thesis show that it is possible to create 3D print and vacuum forming hybrids that can be used for prototyping and possibly production of parts. Several parameters were identified, tested and compared. The tests and comparisons shows that the attachment between the 3D printed parts and the vacuum formed sheets are capable of withstanding forces higher than what the 3D prints can withstand in certain conditions. This means that in certain conditions the attachments manufactured using the process developed in this thesis are comparable to other common forms of pre-existing attachment methods, like adhesive bonding, mechanical fastening or welding [2]. This is because the attachment method is not the weakest part of the system. It is however important to note that the strength of the attachment is highly dependant on the use and test setup. It can therefore be considered irrelevant to discuss any precise description of the strength of the attachment, and each situation should be assessed individually. This thesis does however present results that identify certain parameters that may be manipulated to generally improve the attachments manufactured using the process developed in this thesis. These parameters are condensed into general guidelines that can be applied to the production of prototypes, products and help further development of the process.

Several variations of attachments were also tested qualitatively to be able to develop a rapid, low cost product development process. These variations include angular orientation of attachments, structural attachments like ribs and attachments that are designed to minimize impacting the design of the product, like sunken attachments. The results from these tests show that the process is flexible to a certain degree, although limited in some ways compared to common pre-existing attachment methods. This is particularly evident in the limited range of angular orientation where the process is able to create a proper attachment. This means that the best results are achieved with the attachment oriented in the range of 30° to 90° to the horizontal plane. These tests are however only qualitative and further testing is necessary to get an extensive understanding of the flexibility of the process. It is therefore important to consider the

cost of possibly needing to redesign a product or prototype to allow for the use of this process and compare it to other alternatives. The financial cost of using this process is however possibly quite low because of the low investment cost of equipment required to use this process [26] [16]. This, combined with the elimination of additional steps after vacuum forming compared to other common joining methods, makes the process developed in this thesis a viable alternative to common pre-existing attachment methods.

Further work is required to get a complete understanding of the properties and use of the process developed in this thesis. Factors like the material used in the FDM process and sheet material used in the vacuum forming process needs further research. Only one type of material was used in both these processes which may limit the results. It is also worth looking into replacing the FDM process with other 3D printing processes, which might yield different and better results. This might however increase the cost of the process because of the low investment cost of using the FDM process [26]. Different sheet material thicknesses might also yield different results and therefore also requires further testing.

Only a limited set of 3D printed geometries for the attachments were tested, which means that further research into geometries and parameters of the geometries are necessary for a better understanding of the process. This is also true for the geometries of molds and vent holes on the molds. Better understanding of these factors might also yield a better overview of different usage cases for the process.

BIBLIOGRAPHY

- [1] Basic Injection Molding Design Guidelines. 2015. <https://8tbae6putd20uxilwag7pt3m-wpengine.netdna-ssl.com/wp-content/uploads/2015/01/Design-Guidelines.pdf>, visited 2018-05-28.
- [2] Joining of polymers and polymer-metal hybrid structures: Recent developments and trends. *Polymer Engineering & Science*, 49(8):1461–1476, aug 2009.
- [3] A Review of Additive Manufacturing. *ISRN Mechanical Engineering*, 2012(1):1–10, 2012.
- [4] AS OM BE Plast. Plast produksjon i små serier. Technical report, 2017.
- [5] ASTM D 638 -02a. Standard test method for tensile properties of plastics. *ASTM D 638 -02a*, 08:46–58, 2003.
- [6] O. Avinc and A. Khoddami. Overview of Poly(lactic acid) (PLA) Fibre. *Fibre Chemistry*, (6):391–401, nov. 2009. <http://link.springer.com/10.1007/s10692-010-9213-z>, visited 2018-05-28.
- [7] P. Azimi, D. Zhao, C. Pouzet, N. E. Crain, and B. Stephens. Emissions of Ultrafine Particles and Volatile Organic Compounds from Commercially Available Desktop Three-Dimensional Printers with Multiple Filaments. *Environmental Science and Technology*, 50(3):1260–1268, 2016.
- [8] K. Bates-Green and T. Howie. Materials for 3D Printing by Fused Deposition. 2017.
- [9] M. Behzadnasab and A. A. Yousefi. Effects of 3D printer nozzle head temperature on the physical and mechanical properties of PLA based product. (December):3–5, 2016.
- [10] M. Burns. The StL Format Standard Data Format for Fabbers, 1989.
- [11] P. Cain. Selecting the optimal shell and infill parameters for FDM 3D Printing — 3D Hubs, 2018.
- [12] D. Chakravorty. 3D Printing Support Structures All You Need To Know in 2018 — All3DP, 2018.
- [13] D. Chakravorty. STL File Format (3D Printing) - Simply Explained — All3DP, 2018.

-
- [14] Cromwell Group (Holdings) Ltd. ken5931600k_6.jpg (854854), 2019.
- [15] M. A. Cuiffo, J. Snyder, A. M. Elliott, N. Romero, S. Kannan, and G. P. Halada. Impact of the Fused Deposition (FDM) Printing Process on Polylactic Acid (PLA) Chemistry and Structure. *Applied Sciences*, 7(6):579, 2017.
- [16] Dr. Crash. Make a Good, Cheap, Upgradeable Sheet Plastic Vacuum Former: 11 Steps (with Pictures).
- [17] C. W. Elverum and T. Welo. On the use of directional and incremental prototyping in the development of high novelty products: Two case studies in the automotive industry. *Journal of Engineering and Technology Management*, 38(C):71–88, oct 2015.
- [18] C. W. Elverum, T. Welo, and S. Tronvoll. Prototyping in New Product Development: Strategy Considerations. *Procedia CIRP*, 50:117–122, 2016.
- [19] A. Engineering and I. Production. by Douglass Post. (December):4–7, 2014.
- [20] S. Farah, D. G. Anderson, and R. Langer. Physical and mechanical properties of PLA, and their functions in widespread applications A comprehensive review. *Advanced Drug Delivery Reviews*, 107:367–392, 2016.
- [21] D. Farbman and C. McCoy. Materials Testing of 3D Printed ABS and PLA Samples to Guide Mechanical Design. *Volume 2: Materials; Biomanufacturing; Properties, Applications and Systems; Sustainable Manufacturing*, (June 2016):V002T01A015, 2016.
- [22] Formech International Limited. Formech 686 — Floor standing vacuum forming machine. 2018. <http://formech.com/product/686/>, visited 2018-05-28.
- [23] Formech International Ltd. A Vacuum Forming Guide. 2010. <http://isites.harvard.edu/fs/docs/icb.topic907894.files/FormechVacuumGuide.pdf>, visited 2018-05-28.
- [24] M. Ghobadnam, P. Mosaddegh, M. Rezaei Rejani, H. Amirabadi, and A. Ghaei. Numerical and experimental analysis of HIPS sheets in thermoforming process. *International Journal of Advanced Manufacturing Technology*, 76(5-8):1079–1089, 2014.
- [25] S. Ghosh and W. Seering. Set-Based Thinking in the Engineering Design Community and Beyond. In *Volume 7: 2nd Biennial International Conference on Dynamics for Design; 26th International Conference on Design Theory and Methodology*. ASME, aug. 2014. <http://proceedings.asmedigitalcollection.asme.org/proceeding.aspx?doi=10.1115/DETC2014-35597>, visited 2018-05-28.
- [26] I. Gibson, D. Rosen, and B. Stucker. *Additive Technologies Manufacturing 3D Printing, Rapid Prototyping, and Direct Digital Manufacturing*. Springer, New York, 2 edition, 2015.
- [27] J. W. Gooch, editor. *Glass transition*, pages 460–460. Springer New York, New York, NY, 2007.
- [28] M. P. Groover. *Principles of Modern Manufacturing Materials Processes and Systems*. 5th edition, 2013.
-

-
- [29] D.-P. (Hrsg.). Fused Deposition Modeling. (July), 2011.
- [30] S. Junk, J. Sämann-Sun, and M. Niederhofer. Application of 3D Printing for the Rapid Tooling of Thermoforming Moulds. In *Proceedings of the 36th International MATADOR*, 2010.
- [31] O. S. Karlsen. Agile Product Development : Prototyping and testing of mobile flood protection systems. 2017.
- [32] C. Kriesi, J. Blindheim, Ø. Bjelland, and M. Steinert. Creating Dynamic Requirements through Iteratively Prototyping Critical Functionalities. *Procedia CIRP*, 50:790–795, 2016.
- [33] V. E. Kuznetsov, A. N. Solonin, O. D. Urzhumtsev, R. Schilling, and A. G. Tavitov. Strength of PLA components fabricated with fused deposition technology using a desktop 3D printer as a function of geometrical parameters of the process. *Polymers*, 10(3), 2018.
- [34] J. Y. Lee, J. An, and C. K. Chua. Fundamentals and applications of 3D printing for novel materials. *Applied Materials Today*, 7:120–133, 2017.
- [35] A. Locker. 16 Best 3D Printers of Fall 2018 — All3DP, 2018.
- [36] L. Macarrão and P. C. Kaminski. Vacuum Forming Process: Parts Manufactured with Simplicity. nov. 2007. <http://papers.sae.org/2007-01-2705/>, visited 2018-05-28.
- [37] Mad River Outfitters. LineKurv Stripping Basket. 2015. <http://www.madriveroutfitters.com/p-11461-linekurv-stripping-basket.aspx>, visited 2018-05-28.
- [38] E. Mangano. Preloading, and How It Affects Your Mechanical Test - Instron, 2015.
- [39] S. B. Mishra, R. Malik, and S. S. Mahapatra. Effect of External Perimeter on Flexural Strength of FDM Build Parts. *Arabian Journal for Science and Engineering*, 42(11):4587–4595, nov 2017.
- [40] MTS Systems Corporation. MTS Criterion® Series 40 Electromechanical Universal Test Systems. 2018. https://www.mts.com/cs/groups/public/documents/library/mts_{_}006225.pdf, visited 2018-05-28.
- [41] S. Ore and A. Stori. plast Store norske leksikon, 2018.
- [42] Oxford University Press. tessellate — Definition of tessellate in English by Oxford Dictionaries, 2018.
- [43] J. Prusa. 3D Printing handbook.User manual for 3D printers :Original Prusa i3 MK2 kit 1.75mm. 2016. https://www.prusa3d.com/downloads/manual/prusa3d_{_}manual_{_}175_{_}en.pdf, visited 2018-05-28.
- [44] J. Prusa. 3D Printing handbook.User manual for 3D printers :Original Prusa i3 MK2 kit 1.75mm, 2016.

-
- [45] B. Rankouhi, S. Javadpour, F. Delfanian, and T. Letcher. Failure Analysis and Mechanical Characterization of 3D Printed ABS With Respect to Layer Thickness and Orientation. *Journal of Failure Analysis and Prevention*, 16(3):467–481, 2016.
- [46] B. Redwood. Additive Manufacturing Technologies: An Overview — 3D Hubs, 2018.
- [47] Robinson Plc. Robinson Packaging — Custom Injection Moulded Plastic. 2018. <http://robinsonpackaging.com/plastics/injection-moulding/>, visited 2018-05-28.
- [48] B. Sabart and J. Gangel. Application Guide: Thermoforming, 2015.
- [49] G. S. Services. Plastic Injection Moulding. 2014. <http://www.globalsourcings.com.au/products-services/plastic-mouldingmachining-forming/plastic-injection-moulding/>, visited 2018-05-28.
- [50] P. G. Smith. *Flexible Product Development: Bring Agility for Changing Markets*. John Wiley & Sons, 2007.
- [51] P. G. Smith. *Flexible Product Development: Bring Agility for Changing Markets*. John Wiley & Sons, 2007.
- [52] Stratasys. Abs-M30 Propierties. pages 2–3, 2015.
- [53] Stratasys. FDM Thermoforming, 2017.
- [54] I. Stratasys Direct. Injection Molding Design Guidelines. 2015.
- [55] K. T. Ulrich and S. D. Eppinger. *Product Design and Development Product Design and Development*, volume 4th. 2012.
- [56] A. B. Varotsis. Introduction to FDM 3D printing — 3D Hubs, 2018.
- [57] N. Volpato, J. A. Foggiatto, and D. C. Schwarz. The influence of support base on FDM accuracy in *Z. Rapid Prototyping Journal*, 20(3):182–191, 2014.
- [58] D. I. Wimpenny, P. M. Pandey, and J. L. Kumar. *Advances in 3D Printing & Additive Manufacturing Technologies*, volume 21. Springer Singapore, Singapore, 2017.
- [59] M. Zuza. Everything about nozzles with a different diameter - Prusa Printers, 2018.

Appendix



Detaljert Risikoreport

ID	28144	Status	Dato
Risikoområde	Risikovurdering: Helse, miljø og sikkerhet (HMS)	Opprettet	21.02.2018
Opprettet av	Jonathan Hermansen	Vurdering startet	21.02.2018
Ansvarlig	Jonathan Hermansen	Tiltak besluttet	
		Avsluttet	

Risikovurdering:
Labarbeid flomvernssystem

Gyldig i perioden:

-

Sted:

Institutt for maskinteknikk og produksjon

Mål / hensikt

[Ingen registreringer]

Bakgrunn

[Ingen registreringer]

Beskrivelse og avgrensninger

Forutsetninger, antakelser og forenklinger

[Ingen registreringer]

Vedlegg

[Ingen registreringer]

Referanser

[Ingen registreringer]

ok.
CWW W. Elvén

Jonathan Hermansen

Norges teknisk-naturvitenskapelige
universitet (NTNU)

Unntatt offentlighet jf. Offentlighetsloven § 14

Utskriftsdato:

27.02.2018

Utskrift foretatt av:

Jonathan Hermansen

Side:

1/12



Oppsummering, resultat og endelig vurdering

I oppsummeringen presenteres en oversikt over farer og uønskede hendelser, samt resultat for det enkelte konsekvensområdet.

Farekilde: Båndsag

Uønsket hendelse: Skade på hender

Konsekvensområde: Helse

Risiko før tiltak: Risiko etter tiltak:

Uønsket hendelse: Skade på øyne

Konsekvensområde: Helse

Risiko før tiltak: Risiko etter tiltak:

Farekilde: Slipemaskin

Uønsket hendelse: Skade på hud

Konsekvensområde: Helse

Risiko før tiltak: Risiko etter tiltak:

Uønsket hendelse: Skade øyne

Konsekvensområde: Helse

Risiko før tiltak: Risiko etter tiltak:

Farekilde: Sammenføyningsmidler

Uønsket hendelse: Skade på hud

Konsekvensområde: Helse

Risiko før tiltak: Risiko etter tiltak:

Uønsket hendelse: Skade på øyet

Konsekvensområde: Helse

Risiko før tiltak: Risiko etter tiltak:

Farekilde: 3D-printer

Uønsket hendelse: Brannskader

Konsekvensområde: Helse

Risiko før tiltak: Risiko etter tiltak:

Materielle verdier

Risiko før tiltak: Risiko etter tiltak:



Endelig vurdering

Norges teknisk-naturvitenskapelige universitet (NTNU)
Unntatt offentlighet jf. Offentlighetsloven § 14

Utskriftsdato:
27.02.2018

Utskrift foretatt av:
Jonathan Hermansen

Side:
3/12



Involverte enheter og personer

En risikovurdering kan gjelde for en, eller flere enheter i organisasjonen. Denne oversikten presenterer involverte enheter og personell for gjeldende risikovurdering.

Enhet /-er risikovurderingen omfatter

- NTNU
- Institutt for maskinteknikk og produksjon

Deltakere

Jonathan Hermansen

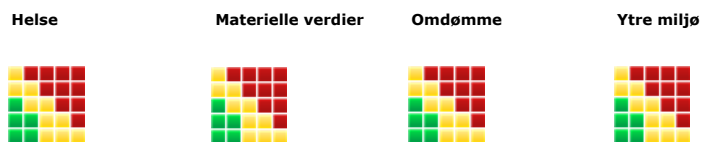
Lesere

[Ingen registreringer]

Andre involverte/interessenter

[Ingen registreringer]

Følgende akseptkriterier er besluttet for risikoområdet Risikovurdering: Helse, miljø og sikkerhet (HMS):





Oversikt over eksisterende, relevante tiltak som er hensyntatt i risikovurderingen

I tabellen under presenteres eksisterende tiltak som er hensyntatt ved vurdering av sannsynlighet og konsekvens for aktuelle uønskede hendelser.

Farekilde	Uønsket hendelse	Tiltak hensyntatt ved vurdering
Båndsag	Skade på hender	Bruke hansker
	Skade på hender	Opplæring
	Skade på øyne	Bruke værnebriller
Slipemaskin	Skade på hud	Bruke hansker
	Skade på hud	Opplæring
	Skade øyne	Bruke værnebriller
Sammenføyningsmidler	Skade på hud	Bruke hansker
	Skade på øyet	Bruke hansker
3D-printer	Brannskader	Sjekke printer jevnlig
	Brannskader	Opplæring

Eksisterende og relevante tiltak med beskrivelse:

Sjekke printer jevnlig

Ha kontroll på om alt fungerer som det skal

Bruke hansker

Beskytte utsatt hud

Bruke værnebriller

Hindre at fremmedlegemer kommer inn i øyene

Opplæring

Hindre feil bruk av utstyr



Risikoanalyse med vurdering av sannsynlighet og konsekvens

I denne delen av rapporten presenteres detaljer dokumentasjon av de farer, uønskede hendelser og årsaker som er vurdert. Innledningsvis oppsummeres farer med tilhørende uønskede hendelser som er tatt med i vurderingen.

Følgende farer og uønskede hendelser er vurdert i denne risikovurderingen:

- **Båndsag**
 - Skade på hender
 - Skade på øyne
- **Slipemaskin**
 - Skade på hud
 - Skade øyne
- **Sammenføyingsmidler**
 - Skade på hud
 - Skade på øyet
- **3D-printer**
 - Brannskader



Detaljert oversikt over farekilder og uønskede hendelser:

Farekilde: Båndsag

Uønsket hendelse: Skade på hender

Hender kommer i kontakt med sagblad

Sannsynlighet for hendelsen (felles for alle konsekvensområder): **Lite sannsynlig (2)**

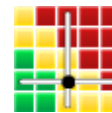
Kommentar:
[Ingen registreringer]

Konsekvensområde: Helse

Vurdert konsekvens: **Stor (3)**

Kommentar: [Ingen registreringer]

Risiko:



Uønsket hendelse: Skade på øyne

spån fra sag kan komme i øyet

Sannsynlighet for hendelsen (felles for alle konsekvensområder): **Lite sannsynlig (2)**

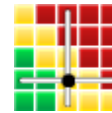
Kommentar:
[Ingen registreringer]

Konsekvensområde: Helse

Vurdert konsekvens: **Stor (3)**

Kommentar: [Ingen registreringer]

Risiko:





Førekilde: Slipemaskin

Uønsket hendelse: Skade på hud

Hud kan komme i kontakt med slipebånd

Sannsynlighet for hendelsen (felles for alle konsekvensområder): **Sannsynlig (3)**

Kommentar:

[Ingen registreringer]

Konsekvensområde: HelseVurdert konsekvens: **Middels (2)**

Kommentar: [Ingen registreringer]

Risiko:**Uønsket hendelse: Skade øyne**

Rester fra sliping kan sprute opp i øyet

Sannsynlighet for hendelsen (felles for alle konsekvensområder): **Svært lite sannsynlig (1)**

Kommentar:

[Ingen registreringer]

Konsekvensområde: HelseVurdert konsekvens: **Stor (3)**

Kommentar: [Ingen registreringer]

Risiko:



Førekilde: Sammenføyningsmidler

Uønsket hendelse: Skade på hud

Hud kan komme i kontakt med sammenføyningsmidler som kan skade huden

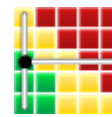
Sannsynlighet for hendelsen (felles for alle konsekvensområder): **Sannsynlig (3)**

Kommentar:
[Ingen registreringer]

Konsekvensområde: Helse

Vurdert konsekvens: **Liten (1)**

Kommentar: [Ingen registreringer]

Risiko:**Uønsket hendelse: Skade på øyet**

Rester av sammenføyningsmidler kan være i gjenn på hendene og dermed komme i kontakt med øyet

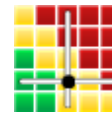
Sannsynlighet for hendelsen (felles for alle konsekvensområder): **Lite sannsynlig (2)**

Kommentar:
[Ingen registreringer]

Konsekvensområde: Helse

Vurdert konsekvens: **Stor (3)**

Kommentar: [Ingen registreringer]

Risiko:



Farekilde: 3D-printer

Uønsket hendelse: Brannskader

Printeren har varmelementer som kan ta fyr om printeren ikke brukes riktig

Sannsynlighet for hendelsen (felles for alle konsekvensområder): **Lite sannsynlig (2)**

Kommentar:
[Ingen registreringer]

Konsekvensområde: Helse

Vurdert konsekvens: **Middels (2)**

Kommentar: [Ingen registreringer]

Risiko:



Konsekvensområde: Materielle verdier

Vurdert konsekvens: **Middels (2)**

Kommentar: [Ingen registreringer]

Risiko:





Oversikt over besluttede risikoreducerende tiltak:

Under presenteres en oversikt over risikoreducerende tiltak som skal bidra til å reduseres sannsynlighet og/eller konsekvens for uønskede hendelser.

Detaljert oversikt over besluttede risikoreducerende tiltak med beskrivelse:



Detaljert oversikt over vurdert risiko for hver farekilde/uønsket hendelse før og etter besluttede tiltak

